Freeway Travel Time Estimation Using Existing Fixed Traffic Sensors (Phase 2)

Prepared By
Yao-Jan Wu, Assistant Professor, Ph.D., P.E. and Shu Yang, Graduate Research Assistant
Department of Civil Engineering and Engineering Mechanics, University of Arizona

Zhaozheng Yin, Assistant Professor and Wenchao Jiang, Graduate Research Assistant
Department of Computer Science, Missouri University of Science and Technology

Final Report Prepared for Missouri Department of Transportation
August 2015 Project TR201407 Report cmr 16-002

FREEWAY TRAVEL TIME ESTIMATION USING EXISTING FIXED TRAFFIC SENSORS – PHASE 2

2013 - 2015

Submission Date:

March, 31st, 2015

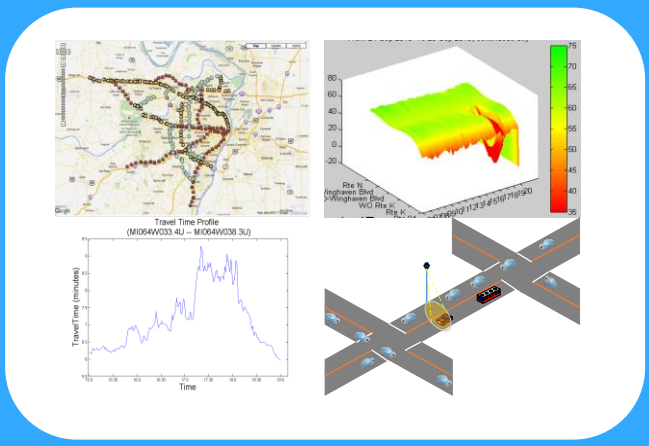

THE UNIVERSITY OF ARIZONA

MoDOT

MISSOURI S&T
University of Science & Technology

Final Report

Project Number TR201407

Freeway Travel Time Estimation using Existing Fixed Traffic Sensors (Phase 2)

– A Computer-Vision-Based Vehicle Matching Approach

Prepared for

Missouri Department of Transportation

By

Yao-Jan Wu
Assistant Professor, PhD, P.E.
Department of Civil Engineering and Engineering Mechanics
University of Arizona

Zhaozheng Yin
Assistant Professor
Department of Computer Science
Missouri University of Science and Technology

Shu Yang
Graduate Research Assistant
Department of Civil Engineering and Engineering Mechanics
University of Arizona

Wenchao Jiang
Graduate Research Assistant
Department of Computer Science
Missouri University of Science and Technology

March 2015

1. REPORT NO.	2. GOVERNMENT ACCESSION NO.	3. RECIPIENT'S CATALOG NO.
cmr 16-002		

4. TITLE AND SUBTITLE	5. REPORT DATE
Freeway Travel Time Estimation Using Existing Fixed Traffic Sensors – Phase 2	March 2015
	6. PERFORMING ORGANIZATION CODE
7. AUTHOR(S)	8. PERFORMING ORGANIZATION REPORT NO.
Yao-Jan Wu, Zhaozheng Yin, Shu Yang and Wenchao Jiang	
9. PERFORMING ORGANIZATION NAME AND ADDRESS	10. WORK UNIT NO.
Missouri Department of Transportation Organizational Results PO BOX 270, JEFFERSON CITY MO 65102	11. CONTRACT OR GRANT NO. TR201407
12. SPONSORING AGENCY NAME AND ADDRESS	13. TYPE OF REPORT AND PERIOD COVERED
Missouri Department of Transportation Research, Development and Technology P.O. Box 270 Jefferson City, MO 65102	Final Report 14. SPONSORING AGENCY CODE

15. SUPPLEMENTARY NOTES

The investigation was conducted in cooperation with the Mid-America Transportation Consortium (MATC) – USDOT University Transportation Center (UTC).

16. ABSTRACT

Travel time, one of the most important freeway performance metrics, can be easily estimated using the data collected from fixed traffic sensors, avoiding the need to install additional travel time data collectors. This project is aimed at fully utilizing the data gathered by existing fixed sensors to estimate point-to-point freeway network travel time in the MoDOT St. Louis District. The objectives of the project were achieved by accomplishing three major tasks: 1) A new travel time estimation model was developed and its ability to outperformed two traditional models, the instantaneous and time-slice models, demonstrated using real-world data. 2) The verification of the proposed model relies on the ground truth travel time. Collecting ground truth travel time is both time-consuming and challenging, so a novel Vehicle Re-identification (VRI) method was developed to facilitate the ground truth data collection process with satisfactory results. 3) A point-to-point network travel time estimation prototype system was also developed. In addition to the primary module of travel time estimation, both data assurance report production and traffic volume report production were modularized. The prototype system was then applied to four case studies measuring: freeway corridor performance (both with and without a turning junction), the impact of severe weather events on traffic volume, and travel time reliability. The prototype system clearly demonstrated its capability and efficiency through these case studies. Because of its high design flexibility, the system is confidently expected to support additional case studies with minimal system revision and tune-up.

17. KEY WORDS	18. DISTRIBUTION STATEMENT
Travel time estimation, traffic sensors, data collection, data quality control, computer vision.	No restrictions. This document is available to the public through the National Technical Information Service, Springfield, VA 22616

19. SECURITY CLASSIF. (of this report)	20. SECURITY CLASSIF. (of this page)	21. NO. OF PAGES	22. PRICE
None	None		

Table of Contents

List of Figures

List of Tables

Acknowledgements

The authors are thankful for the assistance provided by MoDOT staff members Tom Blair, Greg Owens and Davar Divanbeigi for coordination. Special thanks go to MoDOT GGTECH team, and Transcore staff Rick Zygowicz and Tiffany Rando for data support and coordinating video recording. The authors also wish to acknowledge the contributions of Chengchuan An, Kiet Dao and Haohan Li for the traffic data collection.

Disclaimer

The content of this report reflect the views of the authors, who are responsible for the facts and the accuracy of the information presented herein. This document is disseminated under the sponsorship of the Missouri Department of Transportation, in the interest of information exchange. The U.S. Government assumes no liability for the contents or use thereof.

Executive Summary

Travel time is a key performance measure for transportation systems. In the Greater St. Louis area, data are collected from the fixed traffic sensors located along the major freeways and arterials by Gateway Guide, the Transportation Management Center (TMC) managed by MoDOT. Travel time can be easily estimated using the existing fixed traffic sensors without the need to install additional travel time data collectors. The primary goal of this research is to expand the functionality of the system developed in Phase I to cover all the major freeways in St. Louis, MO.

In order to accomplish this goal, a travel time estimation prototype system was designed to efficiently and effectively provide network travel time analytics information for the MoDOT staff at Gateway Guide as follows:

1. An innovative travel time estimation model was proposed.
2. A feasibility study on estimating travel times along freeway corridors with a junction was also conducted.
3. A novel Vehicle Re-identification (VRI) algorithm was proposed to facilitate ground truth travel time data collection from existing surveillance traffic cameras.
4. A point-to-point network travel time estimation prototype system was developed.

The first step in this process was to conduct a comprehensive literature review that focused on: 1) investigating existing travel time estimation methods for freeway links and segments; 2) investigating existing methods of point-to-point network travel time estimation; and 3) investigating computer-vision-based methods for travel time data collection. Three major findings were identified in the literature review:

1. Existing travel time estimation methods for fixed sensors may not be capable of estimating travel time accurately in congested conditions. A new method is needed.
2. Few studies have focused on travel time estimation methods for freeway corridors with turning junctions.
3. Most vehicle matching algorithms rely on high-resolution video images, but only low-resolution video images would be available for this project. A novel vision-based vehicle

matching method was therefore required to facilitate the ground truth travel time collection procedure.

At the beginning of the project, multiple data sources were identified. Travel time estimation was based on the data collected from over 450 fixed Remote Traffic Microwave Sensors (RTMS) on major freeways in the St. Louis District. The digitized traffic videos, the second data source, were recorded using the surveillance video feed provided by the TMC. The recorded video was used to collect ground truth travel time data for model calibration and verification. The third data source consisted of the freeway geometry information obtained from Google Earth using the measuring tool.

A computer-vision-based Vehicle Re-identification (VRI) method was developed to facilitate ground truth data collection. This process was challenging because only low-resolution videos are captured by the existing traffic surveillance cameras. One of the major contributions of this work includes setting up a complete vehicle detection and feature extraction system capable of dealing with poor quality vehicle images. To collect ground truth travel time, Support Vector Machine (SVM) and linear programming techniques were adopted to solve the vehicle matching problem. The approach was tested for two cases, achieving re-identification F-scores of around 68% and 57%. The results are satisfying because the method would be able to provide sufficient samples for travel time verification.

An innovative travel time estimation method based on a car-following model was proposed in this project. The conventional travel time estimation models (i.e. the instantaneous model, and the time slice model) both suffer from difficulties in estimating accurate travel time in heavily congested traffic conditions. Our verification results demonstrate that the proposed model is indeed able to estimate travel times accurately even in congested conditions. Our findings provide mathematical evidence that confirms that the proposed travel time estimation model outperforms the other two conventional methods.

Two case study scenarios were selected for model verification: freeway corridors with and without a turning junction. As expected, the results showed that it is fairly challenging to accurately estimate accurate travel times at a freeway junction because the variations in traffic

conditions cannot be easily captured by the upstream and downstream traffic sensors. In contrast, travel time estimation is fairly robust for freeway corridors with no turning junction.

Three modules were implemented in the prototype travel time estimation system: 1) travel time estimation, 2) data assurance report production, and 3) traffic volume report production. The proposed system also includes a user-friendly interface. To demonstrate the effectiveness and efficiency of the proposed system, it was applied to four specific cases and the following metrics evaluated: 1) performance on major routes, 2) performance for freeway corridors with a turning junction, 3) the impact of severe weather events on traffic volume, and 4) travel time reliability.

To further improve the accuracy of travel time estimation and assist MoDOT's freeway performance management, the research team made the following recommendations:

- Three potential solutions are presented that would improve the accuracy of travel time estimation at freeway junctions:
    - Install additional sensors at turning junctions
    - Use a different type of detector (one option would be Bluetooth detectors) to boost the data collection coverage
    - Utilize third party data (e.g. the HERE dataset)
- Traffic volume and vehicle classification information, both of which are already part of the traffic data, could be incorporated into the proposed travel time estimation model, thus helping to generate more accurate travel times.
- As currently formulated, the Vehicle Re-identification (VRI) algorithm suffers from a relatively low computing efficiency; implementing a high-performance computing language and alternative models could overcome this issue.
- The prototype system could easily be applied to more cases studies to demonstrate its capability and efficiency. The current prototype system is designed for research use, but it could be implemented in a web-based or standalone computer program to enhance its usability for traffic engineers and practitioners. In this case, the MoDOT staff would benefit by gaining access to various system modules, especially those for travel time estimation, data assurance report production and traffic volume report production, when called upon to generate timely reports after an incident has occurred.

Section 1 Introduction

1.1 Project Background

MAP-21, the federal Moving Ahead for Progress in the 21st Century Act, has transformed our national highway program by adopting a performance and outcome-based approach and is making strides toward the regular public reporting of performance data to improve the accountability of federal spending. A key part of this effort is the use of travel time as a performance measure for congestion and transportation system reliability. In the Greater St. Louis area, traffic data are collected from fixed traffic sensors located along the major freeways and arterials by Gateway Guide, the Transportation Management Center (TMC) operated by the Missouri Department of Transportation (MoDOT). The traffic flow data gathered by these sensors are fed into the TMC server in real-time, but are not yet fully utilized by MoDOT. Travel time, as an important freeway performance metric, can be easily estimated using these fixed traffic sensors without the need to install additional travel time data collectors. However, the process of estimation can be fairly tedious using traditional computing tools such as Excel and the staff at the TMC also have to deal with data requests from other agencies or institutes. As manual downloading takes MoDOT staff a considerable amount of time, it is clearly desirable to have an integrated database system to provide a portal that facilitates data access for other transportation agencies as well as providing an automatic travel time estimation and visualization tool for efficient traffic data analysis and travel time estimation.

In Phase 1 (2012 ~2013) (Wu et al, 2013), a new method to estimate travel time using existing fixed traffic sensors on I-64 was developed, its feasibility verified and a prototype system established. Phase 2 of the project was designed to expand the new method and system developed in Phase 1 to cover all the major freeways in the Greater St. Louis area, namely I-44, I-55, I-64, I-70, I-255, I-170 and I-270.

1.2 Research Objectives

The major goal of this research has been to expand the functionality of the system developed in Phase 1 to cover all the major freeways passing through St. Louis. A network travel time estimation system has therefore been developed for the St. Louis area. Specifically, this study focuses on the following research objectives:

- Develop an innovative and accurate travel time estimation model that fully utilizes the existing fixed sensor data
- Conduct a feasibility study of estimating travel time on freeway corridors with junctions using existing fixed traffic sensors
- Apply a computer vision based algorithm to facilitate the ground truth data collection process and increase its sample size
- Develop a prototype system that supports point-to-point network travel time estimation

Section 2 Literature Review

To achieve the project objectives, a comprehensive literature review was conducted focusing on the following areas: 1) investigating existing travel time estimation methods for freeway segments and corridors; 2) investigating existing methods of point-to-point network travel time estimation; and 3) investigating the use of computer vision based algorithms to collect freeway travel time data.

2.1 Freeway Travel Time Estimation

According to previous researchers, all the existing freeway travel time estimation methods can be categorized as either 1) direct measurement or 2) indirect measurement. The commonly used methods of direct measurement include the use of test vehicles, vehicle signature recognition, probe vehicles, Bluetooth-based methods and transportation-related surveys (ITE Manual, 2010). The travel time data collected from these methods is often referred to as "measured travel time". In contrast, the indirect measurement methods generally collect travel time data by estimating travel time using the existing traffic data collection infrastructure. The popularity of "estimating" travel time is a result of the growing deployment of fixed Intelligent Transportation Systems (ITS) sensors.

Speed information can be either directly measured from traffic sensors (e.g. dual loop and radar-based sensors) or estimated by volume and occupancy information (e.g. single loop sensors). Because of the ready availability of speed information, travel times can be easily estimated in an intuitive approach known as the "instantaneous travel time estimation model". This takes the mathematical form shown in Equation 2-1.

$$traveltime(i) = \frac{2 * l_i}{v(i_{up}, k) + v(i_{down}, k)} \qquad (2-1)$$

Where: i represents the freeway link index; l_i is the length of the link; k is a vehicle departure time; and $v(i_{up}, k)$ and $v(i_{down}, k)$ represent the speed information gathered by upstream and downstream traffic sensors, respectively, at time *k*. The underlying assumption of the instantaneous model is that there will be a linear change in speed as the vehicles moves from the upstream to the downstream sensor location. This model is classified as a time-independent

travel time estimation model because both the upstream and downstream speed are measured for the same departure time k. In Phase I (Wu et al, 2013), the travel times estimated by the instantaneous model were consistent with the ground truth travel times under free flow traffic conditions. However, a closer examination of the data revealed that the travel times tended to be underestimated under congested conditions. In order to overcome the "underestimation" issue, a time slice model (Li et al, 2006) has been proposed to transform the instantaneous model to a time-dependent model by incorporating vehicle speeds at the time of arrival at the next downstream link. However, Equation 2-1 is still applied to individual links. The dynamic time slice model (Cortés et al, 2002) is an enhanced version of the time slice model that utilizes a recursive formulation to estimate the arrival time. All three of these models, the instantaneous model, the time slice model and the dynamic slice model, use Equation 2-1 to calculate the travel times for individual links; their only difference lies in the arrival time at the downstream links. The speed at the downstream links would be accordingly changed with the arrival time.

In addition to the three speed-based models, vehicle-trajectory based models have been developed in order to further improve the travel time estimation accuracy. Coifman (2002) proposed a traffic-flow-based travel time estimation method using dual loop sensor data where the travel time can be estimated from the reconstructed vehicle trajectory. Ni and Wang (2008) summarized previous research regarding speed-based travel time estimation and proposed a new speed-based model where a speed surface was constructed as a function of space and time to infer vehicle trajectory, enabling the travel time to be calculated using the vehicle trajectory. Similarly, Sun et al (2008) investigated vehicle trajectories based on a piecewise truncated quadratic function to estimate freeway travel times.

2.2 Freeway Network Travel Time Estimation

The models introduced in Section 2.1 focus on point-to-point travel time estimation on individual freeways. A comprehensive literature review revealed few studies that focused specifically on point-to-point network travel time estimation that takes into account the junctions on freeways. However, the point-to-point network travel time with a junction can still be considered as a freeway corridor and the travel time estimated by using the traditional freeway travel time models.

2.3 Computer-Vision-Based Travel Time Data Collection

Computer-vision-based travel time data collection is generally accomplished by using vehicle re-identification (VRI) techniques that track vehicles as they travel through a transportation network using distributed sensors. A typical vehicle re-identification procedure consists of three stages: vehicle detection, feature extraction and vehicle matching. The accuracy of vehicle detection, the availability of features and the selection of matching algorithm all have important effects on the robustness of a VRI system.

Vision-based VRI is one of the most straightforward and intuitive techniques that can be used to re-identify the same vehicle as it moves between two sensors. This type of technique has been intensively researched due to the prevalence of surveillance cameras installed above traffic roads (Ozbay & Ergun, 2005; Wang et al, 2011; Jiang, 2013; Hou et al, 2009; Sumalee et al, 2012; Sun et al, 2004). Vehicles are easily re-identified by their plate number (Ozbay & Ergun, 2005), although Wang et al. (2011) took a different approach by extracting a color histogram, Histogram of Oriented Gradient (HOG), and aspect ratio as vehicle features in their study. Later, Jiang (2013) added Local Binary Pattern (LBP) to improve the accuracy. To deal with the constantly changing viewpoint, Hou et al. (2009) calibrated vehicles' poses by using 3D models of the vehicles.

Although these methods have achieved relatively good performances, they all rely on the availability of high-resolution cameras. When dealing with low-resolution cameras, Hou et al. (2009) was able to achieve only 54.75% re-identification precision in videos with a resolution of 764*563 pixels. Sun et al. (2004) attempted to mitigate these camera limitations by combining vision-based and induction loop sensor-based vehicle features to re-identify vehicles.

A variety of vehicle matching methods have been developed; their main differences lie in the way they define the probability of one vehicle being identical/different to another. Wang et al. (2011) directly incorporated the weighted sum of feature distances as the probability of a pair of vehicles being identical. Kamijo et al. (2005) took a different approach, performing dynamic programming on two video sequences of vehicles passing between upstream and downstream cameras to identify individual vehicles. However, this method required that the order of vehicles remains relatively unchanged. Tawfik et al. (2004) defined a threshold for each feature distance and used a decision tree cascade framework to determine whether two vehicles are identical,

while Sumalee et al. (2012) and Cetin et al. (2009) both used a Bayes-based probabilistic technique to fuse vehicle features for the re-identification decision.

There are two main drawbacks to all the previous vehicle matching methods: 1. The threshold and weight for each feature are usually manually determined; and 2. The vehicle pairs may not be linearly separable in the feature space, which is important because most of the previous work has depended on linear decision models.

The challenges related to vision-based vehicle re-identification can be summarized as follows:

1. In low-resolution camera images, a vehicle may be represented by a relatively small number of pixels. General visual features such as Histogram of Oriented Gradients (HOG) (Dalal & Triggs, 2005), Local Binary Patterns (LBP) (Guo et al, 2004), and Scale Invariant Feature Transforms (SIFT)(Lowe, 2004) will not work well since these local-statistics-based features tend to be inaccurate when there are insufficient pixels.

2. The lighting conditions under which the cameras operate may change considerably over time, which may cause the color of a pair of identical vehicles to appear different when viewed by upstream and downstream cameras.

3. The viewpoints inevitably vary between the upstream and downstream cameras, resulting in marked variations in the vehicle's texture.

The above challenges mean that the identification of reliable visual features for low-resolution vehicle images is vital. These features should be invariant to both illumination and viewpoint. Meanwhile, because of the limited information provided by low-resolution vehicle images, a more effective matching strategy is required to clearly classify identical/different vehicle identities.

Section 3 Data Collection

This section provides a brief summary of the data collection procedure utilized for this research. The data used in this project included: 1) traffic sensor data; 2) streaming videos from Surveillance Cameras, and 3) freeway geometry data.

3.1 Traffic Data

As of Dec. 15, 2014, over 450 Remote Traffic Microwave Sensors (RTMS) have been deployed on major freeways in St. Louis, MO. These are all managed by Gateway Guide, the Transportation Management Center (TMC) of MoDOT. Figure 3-1 shows the locations of the traffic sensors in the Greater St. Louis area. The traffic sensors collect lane-by-lane traffic information, including traffic volume, travel speed and occupancy[1] every 30 seconds. All the data, stored in an Extensible Markup Language (XML) file, is pushed to the data server at the University of Arizona in real time through File Transfer Protocol (FTP). A data sharing mechanism has been established to distribute the data to other MoDOT partners (including both the Missouri University of Science and Technology and the University of Missouri, Columbia) without incurring any additional costs.

Figure 3-2 shows an example of the traffic data set typically collected on I-70 EB and I-44 WB. The collected data attributes are (from left to right): date/time, detector ID, lane number and lane status, lane-by-lane volume, occupancy and speed, all at 30 second intervals.

[1] "Occupancy" is defined as "the percentage of time a traffic sensor is occupied by vehicles").

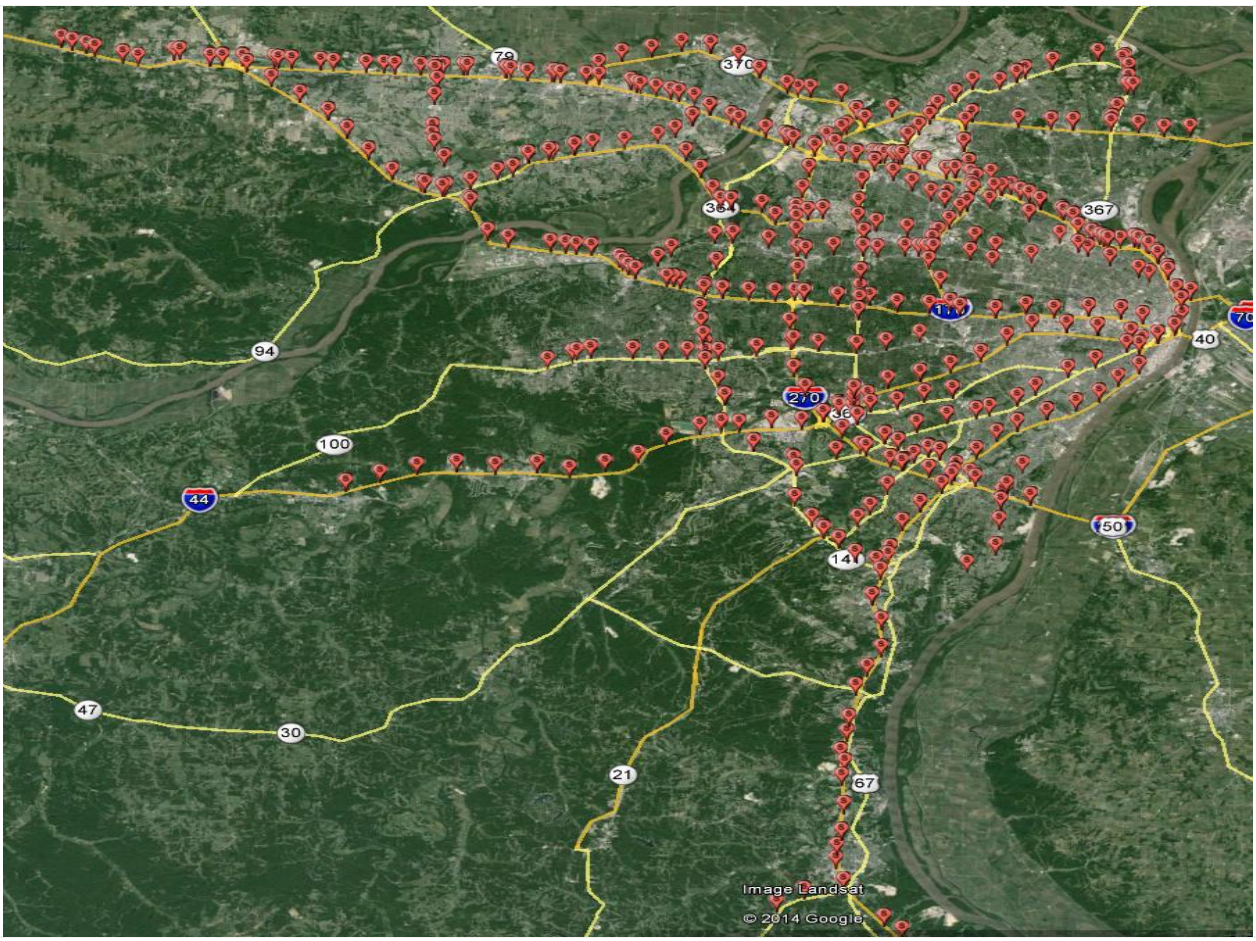

FIGURE 3-1 Traffic sensor locations in St. Louis, MO
(background image is from Google Earth)

Date_Time	DetectorID	Lane_Number_1	Lane_Status_1	Lane_Volume_1	Lane_Occupancy_1	Lane_Speed_1	Lane_Number_2	Lane_Status_2	Lane_Volume_2	Lane_Occupancy_2	Lane_Speed_2
2014-03-01 00:00:03.000	MI070E209.6D	1	OK	1	1	63	2	OK	2	3	63
2014-03-01 00:00:03.000	MI070E219.1E	1	OK	2	1	43	2	OK	0	0	0
2014-03-01 00:00:03.000	MI070E238.2E	1	OK	1	1	53	2	OK	2	1	54
2014-03-01 00:00:03.000	MI070E244.6F	1	OK	5	3	59	2	OK	5	2	60
2014-03-01 00:00:03.000	MI070E245.4F	1	OK	1	1	63	2	OK	9	6	65
2014-03-01 00:00:03.000	MI070E247.0F	1	OK	1	1	66	2	OK	0	0	0
2014-03-01 00:00:03.000	MI070E247.5F	1	OK	1	1	55	2	OK	0	0	0
2014-03-01 00:00:03.000	MI070E248.4F	1	OK	0	0	0	2	OK	1	1	71
2014-03-01 00:00:03.000	MI070E249.2F	1	Disabled	-1	-1	-1	2	Disabled	-1	-1	-1
2014-03-01 00:00:03.000	MI044W292.7D	1	OK	3	2	65	2	OK	3	1	63
2014-03-01 00:00:03.000	MI044W291.5D	1	OK	3	2	53	2	OK	2	1	57
2014-03-01 00:00:03.000	MI070W203.7D	1	OK	2	1	63	2	OK	2	1	70
2014-03-01 00:00:03.000	MI070W204.7D	1	OK	0	0	0	2	OK	1	1	67
2014-03-01 00:00:03.000	MI070W204.7E	1	OK	0	0	0	2	OK	0	0	0
2014-03-01 00:00:03.000	MI070W206.0D	1	OK	1	1	69	2	OK	4	2	65
2014-03-01 00:00:03.000	MI070W207.2D	1	OK	2	3	73	2	OK	3	4	64
2014-03-01 00:00:03.000	MI070W208.2D	1	OK	2	1	67	2	OK	1	1	60

FIGURE 3-2 Example traffic dataset collected in the SQL database

3.2 Streaming Video from Surveillance Cameras

The streaming video captured from surveillance cameras is used to verify the estimated travel time. Figure 3-3 demonstrates the camera network and examples illustrating the vehicle

matching process. Figure 3-3(b) shows the roughly 317 traffic surveillance cameras that can be accessed by the research team and their data recorded for our travel time verification task. As shown in Figures 3-3(a) and 3-3(c), by matching identical vehicles in images captured by pairs of cameras in upstream and downstream locations, the corresponding travel time from the matched vehicles can be calculated. In Phase 1 (Wu et al, 2013), this step was accomplished manually, but in this project, a computer-vision-based method was developed to process these videos more efficiently.

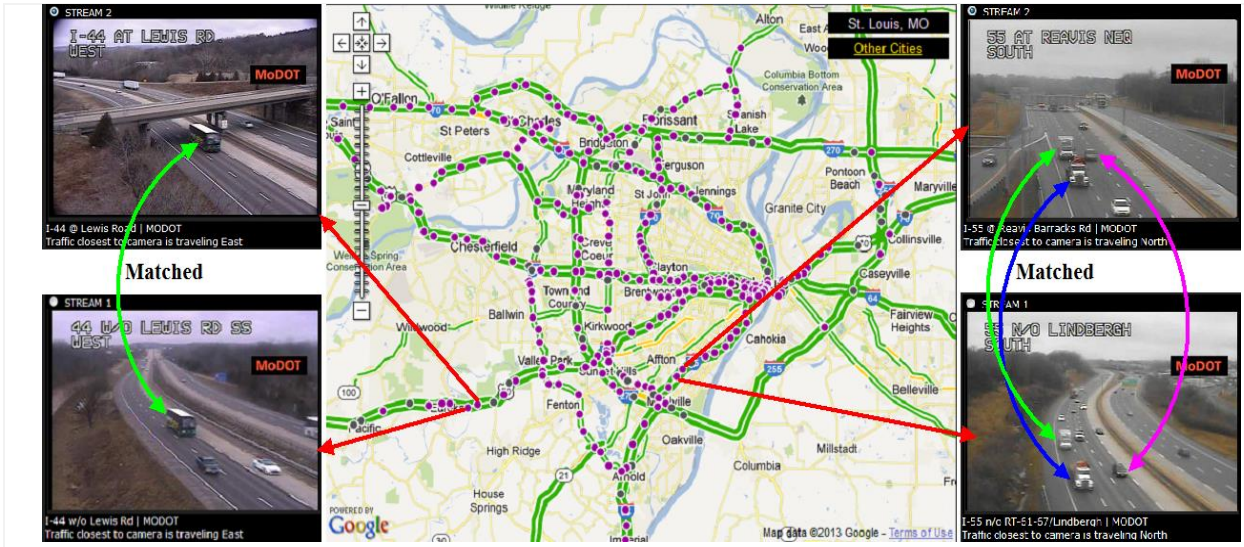

(a) **(b)** **(c)**

FIGURE 3-3 Study videos
(a) identical vehicles in images from two cameras on I-44; (b) the 317 cameras in the greater St Louis area; (c) identical vehicles in images from two cameras on I-55.

3.3 Freeway Geometry Data

In this project, freeway links, segments and corridors are defined as follows.

- Links: a freeway portion bounded by two consecutive traffic sensors.
- Segments: any combination of two or more consecutive links is regarded as a segment.
- Corridor: any combination of two or more consecutive segments is regarded as a corridor. Note that a corridor can consist of two segments connected by a turning junction.

Figure 3-4 depicts these definitions of Link, Segment and Corridor. Links AB, BC and CD are shown in Figure 3-4 (a), where three segments can also be found, namely Segments AC, BD and AD. AD can also be considered a corridor. Figure 3-4 (b) shows an example of a

freeway corridor. Even though the corridor is bounded by two Sensors, E and F, a turning junction is located between these two sensors on two different freeways.

Accurate length measurements for the freeway links, segments and corridors are essential for the travel time estimation calculation shown in Equation 2-1. This information could be acquired either through geographic information systems (GIS) such as Google Maps or Google Earth, or the built-in information from traffic sensors. Link lengths can be easily calculated as the difference between the mileage information for two consecutive traffic sensors, all of which are labeled according to their mile posts. However, when the link, for example, consists of a part of I-64, a part of I-170 and a part of the interchange between the two, the length of this type of link cannot be calculated using mileage information. In such cases, Google Earth provides a useful measuring tool to determine the distances between any two points on the freeway network.

(a) examples of freeway links, segments and corridors (b) example of freeway corridor

FIGURE 3-4 Measuring link length with Google Earth

Legend:

 and  represent the locations of traffic sensors

Section 4 Computer-Vision-Based Travel Time Collection

This section presents the computer-vision-based travel time collection algorithm. As shown in Figure 3-3, the ability to match vehicles shown by two cameras is a precondition for calculating the travel time and this relies heavily on robust Vehicle Re-identification (VRI) methods. VRI essentially resolves the following mathematical problem:

$$\text{Upstream Vehicle Set: } U = \{U_1, \dots, U_i, \dots, U_I, \mathrm{U}_\varphi\}$$

$$\text{Downstream Vehicle Set: } D = \{D_1, \dots, D_j, \dots, D_J, \mathrm{D}_\varphi\}$$

$$\text{Re-identification: } \{U_1, \dots, U_i, \dots, U_I, U_\varphi\} \leftrightarrow \{D_1, \dots, D_j, \dots, D_J, D_\varphi\}$$

where U_i and D_j are the i_{th} and j_{th} vehicle captured by upstream and downstream cameras within the same time interval, respectively, and U_φ and D_φ are special void objects, different from U_i or D_j, that can be used to map unmatched vehicles. Two different aspects of this re-identification problem are important.

First, it is a **classification** problem. A category must be assigned to each vehicle pair (U_i, D_j), namely either "U_i and D_j are identical" or "U_i and D_j are different". From another point of view, this is a **mapping** problem. For each upstream vehicle in the set U, we need to find the most identical and unique vehicle in D, the downstream set, and vice versa. Because some vehicles may be miss-detected in the downstream or exit before reaching the downstream camera, vehicles in U may not correspond to any mapped vehicle in D, so these vehicles are mapped to a void object D_φ. Similarly, vehicles in D having no matched vehicles in U are mapped to the void object U_φ. All mappings involving D_φ and U_φ can be many-to-one mapping; the remaining elements in sets U and D are all one-to-one mappings.

Based on this mathematical formulation, the VRI algorithm introduced here consists of three phases:

1. **Vehicle Detection**. Videos are recorded from upstream and downstream cameras simultaneously and vehicles are detected by Motion History Image (MHI) and Viola-Jones detectors. The detected vehicle images are preprocessed using segmentation and warping techniques.

2. **Feature Extraction**. Features including vehicle size, color and texture information are extracted from the vehicle images. A feature distance vector describing the similarity of each pair of vehicles is then obtained.

3. **Vehicle Matching**. The classification problem illustrated above is solved by a Support Vector Machine (SVM), while the mapping problem is regarded as a global optimization problem with some constraints and can be solved by linear programming.

In this project, there are roughly three steps involved in dealing with the vehicle matching problem. 1. Vehicle Detection: Vehicles are detected separately by two cameras. 2. Feature Extraction: Color, texture, size, and time constraints are considered as features describing every vehicles. 3. Feature matching: features are matched in SVM and linear programming frameworks to determine whether two vehicles are indeed identical.

4.1 Vehicle Detection

Detecting vehicles in each video frame is the initial critical step of a Vehicle Re-identification (VRI) system. This step is especially challenging when the lighting conditions and viewpoints vary among cameras. For each frame of a video such as the one shown in Figure 4-1 (a), the technique of Motion History Image (MHI) (Yin & Collins, 2009) is first adopted to detect image regions with moving pixels. The results of this process are shown in Figure 4-1 (b). The Viola-Jones vehicle detector (Torralba et al, 2004) is then applied to find the precise positions of the vehicles (Figure 4-1 c) within the regions of moving objects. To further locate the boundaries of the vehicles, segmentation is applied to separate the foreground (vehicles) from the surrounding background (Figure 4-1 f). Finally, the vehicle image is warped to the viewpoint directly facing the lanes (Figure 4-1 g), thus mitigating the problem of viewpoint differences between the upstream and downstream cameras. The same process is applied to both the upstream and downstream videos.

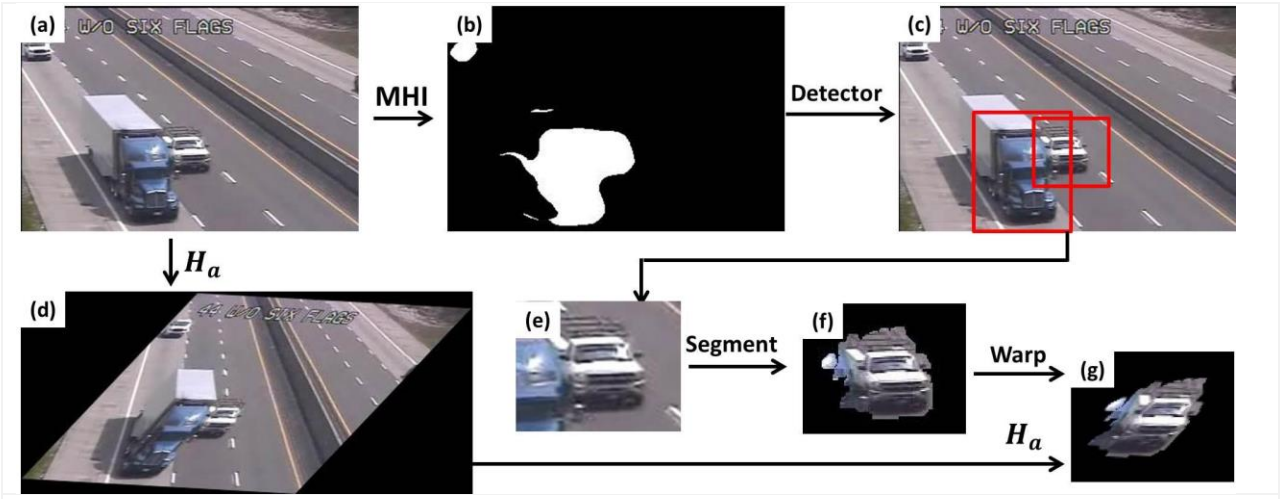

FIGURE 4-1 The flowchart for vehicle detection
(a) A frame in a video; (b) The moving object detection result for MHI; (c) Positions of vehicles detected by the Viola-Jones detector; (d) The warped image of (a); (e) One cropped vehicle image; (f) Vehicle image after eliminating the background; (g) The warped vehicle image.

Motion History Images (MHI) and the Viola-Jones detector perform complementary functions in the proposed algorithm to detect vehicles. Although MHI is an efficient way to find moving objects, as Figure 1b shows, it is difficult for MHI to determine whether the moving regions consists of one or two vehicles when two vehicles are adjacent to each other or one vehicle is moving with its own shadow. Thus, the Viola-Jones detector is applied to moving regions to determine the accurate positions of vehicles within the candidate regions without the need to also search in other impossible regions. In addition, MHI is more resistant to illumination changes than ordinary background subtractions such as the Gaussian Mixture Model (GMM) (Stauffer & Grimson, 1999). Figure 4-2 (a) shows a frame when the illumination is changing due to clouds moving across the sun. Figure 4-2 (b) shows the moving object detection result obtained using GMM, which is unsatisfactory because GMM updates the background at constant time intervals but the illumination level changes relatively rapidly and in an unpredictable way due to the intermittent cloud cover. MHI solves this problem by applying a forward and backward decaying background subtraction (Yin & Collins, 2009). Figure 4-2 (c) shows the results of the MHI moving object detection. The influence of the changing background illumination is removed and the moving objects are clearly detected.

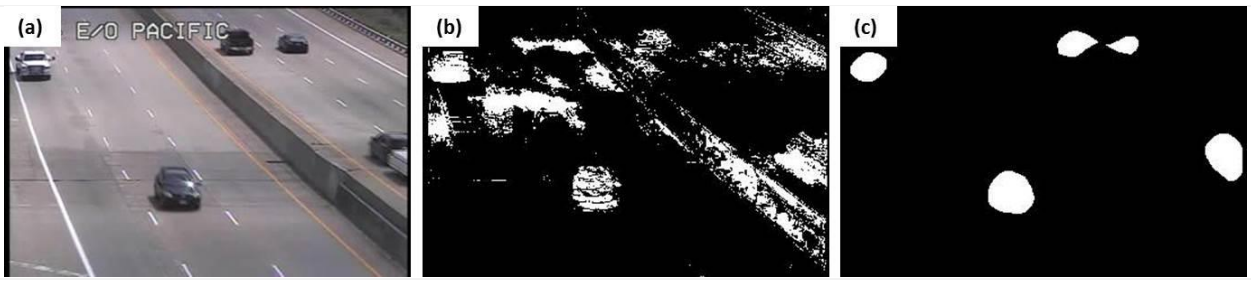

FIGURE 4-2 Advantage gained by using MHI
(a) Original image. (b) GMM detection results. (c) MHI detection results.

The detailed information that can be extracted from vehicle images is limited by the low camera resolution and the background surrounding the vehicles can worsen this problem because it adds noise to the feature extraction. Thus, removing the background from vehicle images is of great significance for extracting valuable features. Here, we consider pixels outside the boundary of a vehicle to be background while pixels within the boundary are part of the foreground image and adopt the Graph-Based Image Segmentation algorithm (Felzenszwalb & Huttenlocher, 2004) to rule out the background (Figure 4-1f).

To mitigate the problem of different viewpoints between upstream and downstream cameras, as shown in Figures 4-1 (a) & 4-1 (d), the original image is warped to the viewpoint directly facing the lanes by a homography matrix H_a using the warping method proposed by Kanhere et al. (2007). Once H_a is determined, it remains fixed because the camera is stationary. H_a is then applied to every detected vehicle image, as shown in Figure 4-1 (g), thus ensuring that every vehicle is viewed from the same viewpoint.

4.2 Feature Extraction

The vehicle image (template) is the raw vehicle feature. Other features, such as size, color and texture, can be extracted for vehicles. Let V_{U_i} and V_{D_j} denote the warped and background-eliminated vehicle images for vehicles U_i and D_j, respectively. For each vehicle in U, a feature set F_{U_i} can be formed to describe U_i. The corresponding feature set for downstream vehicles is denoted as F_{D_j}. Without loss of generality, only F_{U_i} is described in this section.

4.2.1 Size Feature

Because the viewpoints and resolutions of the upstream and downstream cameras are warped to be the same, this preprocessing implicitly normalizes vehicles between different cameras and

lanes, which simplifies their size comparison. The number of foreground pixels is a good way to estimate the size of U_i, which is denoted as S_{U_i}.

4.2.2 Color Feature

To fully extract the color information of a vehicle, we adopt two color models: original Hue (H)-Saturation (S)-Illumination (I) (HSI) histograms ($C_{U_i}^H$,$C_{U_i}^S$, $C_{U_i}^I$), and normalized hue histogram ($C_{U_i}^{NH}$).

For original HSI histograms, the three image channels are treated separately. Each channel is divided into 20 bins, thus U_i has three 20-bin histograms: $C_{U_i}^H$,$C_{U_i}^S$, $C_{U_i}^I$, corresponding to the H,S and I color channels, respectively. However, the original HSI histograms may vary in response to illumination changes. This problem can be mitigated if the illumination and saturation information is normalized. To achieve this, a 20-bin normalized hue histogram is added to extract the pure hue information of a vehicle image (Finlayson & Xu, 2002), denoted as $C_{U_i}^{NH}$.

Original HSI histograms are satisfactory when illumination condition is stable. Figure 4-3 shows an example of what happens when the illumination changes. Vehicles **a** and **b** are identical, while **c** is different. The original hue histograms of **a** and **b** are quite different, but after normalization, their normalized hue histograms show their color is similar. However, color information is not sufficient to distinguish between different vehicles with similar color (e.g., **c**'s color histograms are similar to **a**'s and **b**'s), so texture information is also required.

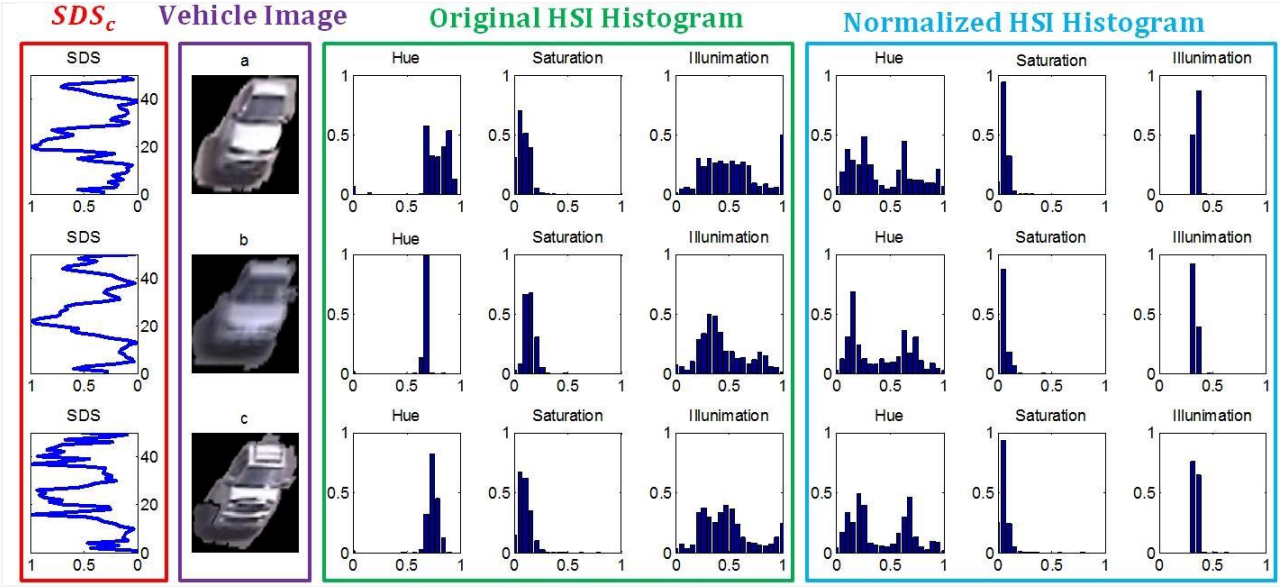

FIGURE 4-3 Vehicle images and their Standard Deviation Signature (SDS), original HSI histograms and normalized HSI histograms
a and b are identical while c is different.

4.2.3 Texture Feature

Classical texture descriptors (e.g., HOG, LBP) work poorly in low resolution vehicle images. We therefore propose a standard deviation based texture descriptor. As shown in Figure 4-3, vehicle **a** has no sunroof but vehicle **c** has. This difference can be described by the standard deviation in the roof regions of the vehicles. Mathematically, the Standard Deviation Signature (SDS) is a one-dimensional vector with the m_{th} dimension equaling the standard deviation of the foreground pixels in the m_{th} row or column of V_{U_i}. Row SDS of U_i is denoted as $T_{U_i}^{SDS_r}$ while column SDS is denoted as $T_{U_i}^{SDS_c}$. Thus, the m_{th} dimension of $T_{U_i}^{SDS_r}$ is defined as

$$T_{U_i}^{SDS_r} = \left(\frac{1}{cols - 1} \sum_{n=1}^{cols} \left(V_{U_i}(m,n) - \frac{1}{cols} \sum_{n=1}^{cols} V_{U_i}(m,n) \right)^2 \right)^{\frac{1}{2}} \qquad (4-1)$$

where $V_{U_i}(m,n)$ is the grayscale pixel value in row m and column n of V_{U_i} and $cols$ is the column number of foreground area. $T_{U_i}^{SDS_c}$ can be calculated in a similar way but in the column direction.

The red box in Figure 3 shows $T_{U_i}^{SDS_c}$ for each of the three vehicles. It is clear that the signatures of **a** and **b** are similar, while the signature of **c** is much rougher because **c** involves more textural differences.

4.2.4 Feature Distance

The feature sets F_{U_i} and F_{D_j} are just the set of all features extracted from U_i and D_j, respectively

$$F_{U_i} = \left\{S_{U_i}, C_{U_i}^H, C_{U_i}^S, C_{U_i}^I, C_{U_i}^{NH}, T_{U_i}^{SDS_r}, T_{U_i}^{SDS_c}, V_{U_i}\right\} \quad (4-2)$$

$$F_{D_j} = \left\{S_{D_j}, C_{D_j}^H, C_{D_j}^S, C_{D_j}^I, C_{D_j}^{NH}, T_{D_j}^{SDS_r}, T_{D_j}^{SDS_c}, V_{U_i}\right\} \quad (4-3)$$

where the raw vehicle images V_{U_i} and V_{D_j} are used to calculate the template distance. Thus, the feature distance describing the similarity of vehicle pair (U_i, D_j) is denoted as

$$\mathrm{DIS}(U_i, D_j) = \left[DIS_S, DIS_{C^H}, DIS_{C^S}, DIS_{C^I}, DIS_{C^{NH}}, DIS_{T^{SDS_r}}, DIS_{T^{SDS_c}}, \mathrm{DIS}_{Temp}\right] \quad (4-4)$$

Each dimension of $\mathrm{DIS}(U_i, D_j)$ is the distance of the corresponding feature of $F_{U_i}$and F_{D_j}. Based on the properties of size, color and texture features, different distance metrics are used in the feature distance vector.

The size distance DIS_S of a vehicle pair (U_i, D_j) is defined as

$$DIS_S = \frac{S_{U_i}}{S_{D_j}} \quad (4-5)$$

The color distance DIS_C of a vehicle pair (U_i, D_j) is defined as

$$\mathrm{DIS}_C = 1 - \left(1 - \frac{\sum_{\mathrm{k}=0}^{20}\left(\mathrm{C}_{U_i}(\mathrm{k}) \times C_{D_j}(\mathrm{k})\right)^{\frac{1}{2}}}{20\left(\mu\left(\mathrm{C}_{U_i}\right) \times \mu\left(\mathrm{C}_{\mathrm{D}_j}\right)\right)^{\frac{1}{2}}}\right)^{\frac{1}{2}} \quad (4-6)$$

where k is the k_{th} dimension of the histograms and $\mu(*)$ is the arithmetic mean function. Equation 4-6 is applied to DIS_{C^H}, DIS_{C^S}, DIS_{C^I} and $DIS_{C^{NH}}$.

The length of the Standard Deviation Signature of a vehicle pair may not be the same, but they can be normalized by linear interpolation. The texture distance DIS_T of (U_i, D_j) is defined as their covariance

$$DIS_T = \frac{\mu\left(T_{U_i} T_{D_j}\right) - \mu(T_{U_i})\mu(T_{D_j})}{v(T_{U_i})^{\frac{1}{2}} v\left(T_{D_j}\right)^{\frac{1}{2}}} \qquad (4-7)$$

where $v(*)$ is the variance function. Equation 4-7 is applied to both $DIS_{T^{SDS_r}}$ and $DIS_{T^{SDS_c}}$.

Besides the feature distances described above, a template distance is also adopted based on the grayscale pixel subtraction of V_{U_i} and V_{D_j}. The binary images L_{U_i} and L_{D_j} are obtained with foreground pixels equaling 1 and background pixels equaling 0. Then the maximal value $B(U_i, D_j)$ of two-dimensional cross correlation between L_{U_i} and L_{D_j} is calculated as

$$\mathrm{B}(U_i, D_j) = \max_{(\mathrm{k,l})} \sum_{\mathrm{m}=0}^{\mathrm{M}-1} \sum_{\mathrm{n}=0}^{\mathrm{N}-1} \mathrm{L}_{U_i}(\mathrm{m,n}) L_{D_j}(\mathrm{m}-\mathrm{k}, \mathrm{n}-\mathrm{l}) \qquad (4-8)$$

where M and N are the length and width of each of the binary images, separately. If $(\mathrm{k}_{\max}, \mathrm{l}_{\max})$ can maximize Equation 4-8, then the template distance of (U_i, D_j) is defined as

$$\mathrm{DIS}_{Temp} = \frac{\sum_{\mathrm{m}=1}^{\mathrm{M}} \sum_{\mathrm{n}=1}^{\mathrm{N}} \left| V_{U_i}(\mathrm{m,n}) - V_{D_j}(\mathrm{m}-\mathrm{k}_{\max}, \mathrm{n}-\mathrm{l}_{\max}) \right|^2}{255 * 255 * \mathrm{B}(U_i, D_j)} \qquad (4-9)$$

$\mathrm{DIS}(U_i, D_j)$ describes the similarity relationship between a vehicle pair (U_i, D_j) and serves as the input for SVM, which will be discussed in the next section.

4.3 Vehicle Matching

As noted in Section 4.2, Feature Extraction, two problems need to be solved: classification and mapping. This section presents the details showing how the two problems are solved by using the Support Vector Machine (SVM) and linear programming techniques.

4.3.1 SVM-Based Classification

SVM has been successfully applied to solve a number of classification problems (Mukkamala & Sung, 2003; , Zhang et al, 2011). The primary objective of SVM is to find a gap between two categories (namely, positive and negative) and this gap should be as wide as possible. For a linear inseparable problem, SVM maps the original finite-dimensional space into a much higher-dimensional space, making the separation linear in that space and thus obtaining better classification results.

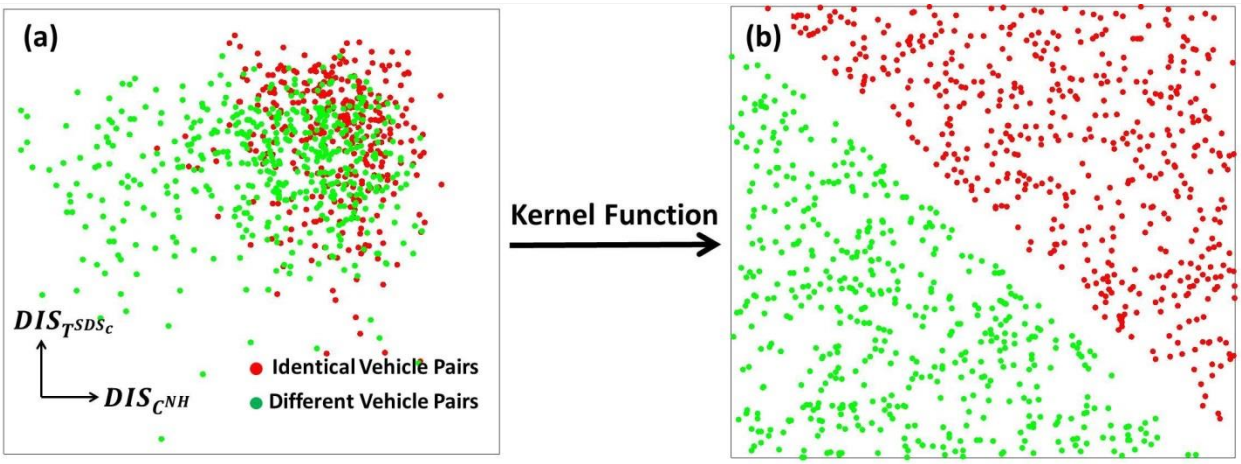

FIGURE 4-4 SVM for two category linear inseparable classification (a) Original feature space. (b) Higher feature space.

Scholkopf and Smola (2001) provide a full mathematical analysis of SVM; here, we will instead consider an example to illustrate how SVM works in practice. In the scatter plots shown in Figure 4-4, the X axis is $DIS_{C^{NH}}$ for a vehicle pair and the Y axis is $DIS_{T^{SDS_c}}$ for the same vehicle pair. We begin by randomly choosing 500 identical vehicle pairs (red points) and 500 different vehicle pairs (green points). In Figure 4-4 a, these are not linearly separable. However, after we map the original feature space onto a higher dimensional feature space with a kernel function, the two categories can be easily separated (Figure 4-4 b).

For a standard SVM framework, there are two stages: training and classification. In the training stage, we label the positive samples (identical pairs) as Arabic number 1 while negative samples (different pairs) are labelled as -1. An SVM classifier is trained based on $\mathrm{DIS}(U_i, D_j)$ and their labels. In the classification stage, for each pair of vehicles(U_i, D_j), the SVM classifier gives a confidence $\mathrm{Conf}(U_i, D_j)$, that describes the classification result. A value for $\mathrm{Conf}(U_i, D_j)$ that is larger than 0 means that (U_i, D_j) is matched, while a $\mathrm{Conf}(U_i, D_j)$ value that is less than 0

means that (U_i, D_j) is unmatched. Thus, the possibility that (U_i, D_j) are matched is proportional to $\mathrm{Conf}(U_i, D_j)$.

4.3.2 Linear-Programming-Based Mapping

$\mathrm{Conf}(U_i, D_j)$ describes how identical a vehicle pair is. However, it is possible for one upstream vehicle to be matched to more than one downstream vehicle. Mapping resolves this issue by formulating a global optimization problem that maximizes the overall confidence of all the matched vehicle pairs between two cameras by imposing several constraints. Mathematically, let $\mathrm{x}(\mathrm{U_i}, \mathrm{D_j})$ denote whether (U_i, D_j) is identical. If so, $\mathrm{x}(\mathrm{U_i}, \mathrm{D_j}) = 1$. If not, $\mathrm{x}(\mathrm{U_i}, \mathrm{D_j}) = 0$. Then, the maximization problem can be expressed as a standard linear program:

$$\max\Big(\sum_{\mathrm{U_i}}\sum_{\mathrm{D_j}} \mathrm{Conf}(\mathrm{U_i}, \mathrm{D_j})\mathrm{x}(\mathrm{U_i}, \mathrm{D_j}) + \sum_{\mathrm{U_i}} \mathrm{Conf}(\mathrm{U_i}, \mathrm{D_\varphi})\mathrm{x}(\mathrm{U_i}, \mathrm{D_\varphi}) + \sum_{\mathrm{D_j}} \mathrm{Conf}(\mathrm{U_\varphi}, \mathrm{D_j})\mathrm{x}(\mathrm{U_\varphi}, \mathrm{D_j})\Big) \quad (4-10)$$

Subject to

$$\mathrm{Conf}(\mathrm{U_i}, \mathrm{D_\varphi}) = \delta \text{ for all } \mathrm{U_i} \quad (4-11)$$

$$\mathrm{Conf}(\mathrm{U_\varphi}, \mathrm{D_j}) = \delta \text{ for all } \mathrm{D_j} \quad (4-12)$$

$$\sum_{\mathrm{U_i}} \mathrm{x}(\mathrm{U_i}, \mathrm{D_j}) + \mathrm{x}(\mathrm{U_\varphi}, \mathrm{D_j}) = 1 \text{ for all } \mathrm{D_j} \quad (4-13)$$

$$\sum_{D_j} \mathrm{x}(\mathrm{U_i}, \mathrm{D_j}) + \mathrm{x}(\mathrm{U_i}, \mathrm{D_\varphi}) = 1 \text{ for all } \mathrm{U_i} \quad (4-14)$$

$$\text{if } \mathrm{TM_{D_j}} \notin \left[\mathrm{TM_{U_i}} + \mathrm{TM_{min}}, \mathrm{TM_{U_i}} + \mathrm{TM_{max}}\right], \text{then } \mathrm{x}(\mathrm{U_i}, \mathrm{D_j}) = 0 \quad (4-15)$$

$$\mathrm{x}(\mathrm{U_i}, \mathrm{D_j}) \in \{0,1\}, \mathrm{x}(\mathrm{U_i}, \mathrm{D_\varphi}) \in \{0,1\}, \mathrm{x}(\mathrm{U_\varphi}, \mathrm{D_j}) \in \{0,1) \quad (4-16)$$

In Equations 4-11 and 4-12, δ is the confidence of void object mapping, and this is set to 0 because 0 is the decision boundary of confidence of matched and unmatched vehicle pairs. Equations 4-13 and 4-14 ensure a one-to-one mapping, that is, each vehicle in U can only be mapped to a single vehicle (including void objects) in D and vice versa. Note that U_φ and D_φ are not subject to this one-to-one mapping restriction.

The time constraint is also considered in Equation 4-15. The travel time for one vehicle moving from the upstream camera to the downstream camera under normal conditions is constrained. Let TM_{min} and TM_{max} denote the minimal and maximal time one vehicle needs to travel from the upstream camera to the downstream camera. $\left(TM_{U_i}, TM_{D_j}\right)$ is the timestamp denoting the time when (U_i, D_j) disappear from the upstream and downstream cameras, respectively. Thus, unreasonable travel times should be eliminated.

4.4 Results

The VRI algorithm was tested using two case studies.

- Case 1:
    - A 3.7-km section of a three-lane freeway with no entrances or exits (Figures 4-5(a) and (b)) from Camera W/O SIX FLAGS to Camera E/O PACIFIC.
    - The upstream location was recorded from 15:41:30 to 16:11:30 on May 26th, 2014; the downstream location was recorded from 15:42:30 to 16:12:30 on the same day.
- Case 2
    - A 1.7-km section of four-lane freeway with one exit (Figures 4-5(c) and (d)) from Camera N/O LINDBERGH to Camera REAVIS BARRACKS.
    - The upstream location was recorded from 15:20:00 to 15:40:00 on July 26th, 2014; the downstream location was recorded from 15:21:00 to 15:41:00 on the same day.

The frame rate of the videos was 12 frames per second (FPS), and the video resolution was 360*240 pixels. The average size of each vehicle was about 40*40 pixels. Illumination and viewpoint changes were involved in both cases to test the effectiveness of the proposed VRI algorithm.

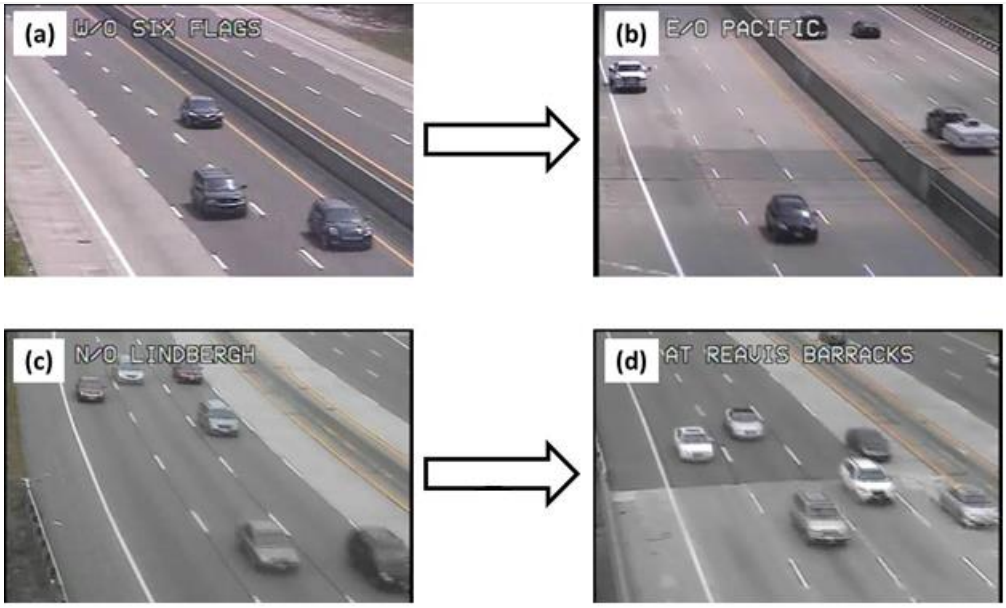

FIGURE 4-5 Screenshots of recorded videos
(a) Upstream frame in Case 1, (b) Downstream frame in Case 1, (c) Upstream frame in Case 2, and (d) Downstream frame in Case 2. Case 1 involves no entrances or exits while Case 2 has one exit.

The ground truth was obtained by manually detecting and re-identifying vehicles in the upstream and downstream videos. In Case 1, 776 vehicles were detected in the upstream video and 804 vehicles in the downstream video during the 30-min period, of which 713 pairs of vehicles were manually matched. In Case 2, 961 vehicles were detected in the upstream video and 775 vehicles in the downstream video during the 20-min period, of which 750 pairs of vehicles were manually matched. Copies of these videos were also recorded for training; 683 and 692 pairs of vehicles were manually matched for Cases 1 and 2 in the training stage, respectively.

4.4.1 Performance Metrics

Three metrics are utilized here to evaluate the performance of the VRI system:

$$\text{Precision} = \frac{TP}{TP + FP} \qquad (4-17)$$

$$\text{Recall} = \frac{TP}{TP + FN} \qquad (4-18)$$

$$\text{F-score} = 2 \cdot \frac{\text{precision}.\,\text{recall}}{\text{precision} + \text{recall}} \qquad (4-19)$$

where True Positives (TP) represent the number of correctly matched vehicle pairs. False Positives (FP) are the number of pairs of different vehicles mistakenly regarded as matched by the algorithms and False Negatives (FN) the number of identical vehicle pairs mistakenly regarded as different vehicles by the algorithms. Recall concerns the proportion of correctly matched vehicles among the ground truth sample, while precision focuses on the proportion of correctly matched vehicles among all vehicle pairs matched by the proposed VRI algorithm. The F-score is a comprehensive evaluation.

4.4.2 Quantitative Performance Evaluation

In Case 1, 492 pairs of vehicles were correctly matched while 239 pairs were deemed to be FP. Thus, the precision, recall and F-score for Case 1 are 67.31%, 69.00% and 68.14%, respectively. In Case 2, 430 pairs of vehicles were correctly matched while 337 pairs were deemed to be FP. Thus, the precision, recall and F-score of Case 2 are 56.06%, 57.33% and 56.69%, respectively. Sumalee et al. (2012) achieved 54.75% re-identification precision in videos with a much higher resolution of 764*563 pixels, thus the algorithm here outperforms their proposed probabilistic fusion method (Sumalee et al. , 2012).

Note that the performance for Case 2 was much lower than that for Case 1. This might be because there is a freeway exit between the two cameras in this case, so some vehicles in the upstream video will not appear in the downstream video, introducing noise when they are re-identified. To validate the analysis, we manually removed all the vehicles that exited before reaching the downstream camera, at which point the re-identification result improved to 70.82% in precision, 68.93% in recall and 69.86% in F-score. These results are comparable with those for Case 1. Placing surveillance cameras on the exit would thus enhance the algorithm's matching performance by making it possible to re-identify vehicles using three cameras (upstream, downstream and exit).

4.4.3 Comparison

To validate the effectiveness of the specific components in the proposed VRI algorithm, a series of comparisons were performed. The decrease in performance when one component is not considered indicates that this component makes a contribution to the VRI algorithm and the degree of the decrease can be considered to indicate the relative importance of that component.

Comparing the first two rows of Table 4-1 with the last row of Table 4-1 (the proposed VRI algorithm) clearly demonstrates that the operations of segmentation and warping applied to every vehicle image are helpful in improving the performance.

The next three rows in Table 4-1 indicate the relative importance of three features (size, color, texture). For example, in Case 2, the F-score decreases by 1.86%, 11.91% and 17.82% when the size, color and texture features, respectively, are not considered. This indicates that the texture feature is more important than the size and color features, which can be explained in several aspects. First, when vehicles are viewed from a long distance, their size difference is not obvious, thus it is not enough to distinguish one vehicle from others based on size. Second, in both Case 1 and Case 2, the colors of over 60% of the vehicles were either white or black, this limited color palette makes it harder to distinguish between the many vehicles with similar coloration. Third, the texture feature is sensitive to quite subtle differences between vehicles, such as whether the lights are on and whether the sunroof is open, which makes it well suited to the identification of individual vehicles.

The last three rows in Table 4-1 compare the classifier adopted in our paper with other classifiers implemented in previous work. Decision Tree is used in (Tawfik et al, 2004) while a Bayesian based classification model is utilized in (Sumalee et al., 2012; Cetin & Nichols, 2009). The results clearly show that our SVM outperforms other classifiers in the VRI classification problem.

Table 4-1 Algorithm Comparison (√: considered -:not considered DT: Decision Tree)

	Preprocessing		Feature			Classifier			Results for Case1			Results for Case 2		
	Segmentation	Warping	Size	Color	Texture	SVM	DT	Bayes	%Precision	%Recall	%F-score	%precision	%Recall	%F-score
Effect of omitting warping	√	–	√	√	√	√	–	–	62.88	64.38	63.62	54.68	56.13	55.39
Effect of omitting segmentation	–	√	√	√	√	√	–	–	60.94	61.71	61.32	54.12	53.47	53.79
Effect of omitting size	√	√	–	√	√	√	–	–	57.50	58.06	57.28	54.09	55.60	54.83
Effect of omitting color	√	√	√	–	√	√	–	–	57.99	60.03	58.99	44.11	45.47	44.78
Effect of omitting texture	√	√	√	√	–	√	–	–	36.02	37.59	36.79	38.29	39.47	38.87
Sumalee et al., 2012	√	√	√	√	√	–	√	–	29.88	25.95	27.82	30.40	27.60	28.93
Cetin & Nichols, 2009	√	√	√	√	√	–	–	√	45.37	47.41	46.36	41.94	43.33	42.62
Proposed VRI algorithm	√	√	√	√	√	√	–	–	**67.31**	**69.00**	**68.14**	**56.06**	**57.33**	**56.69**

4.4.4 Travel Time Estimation

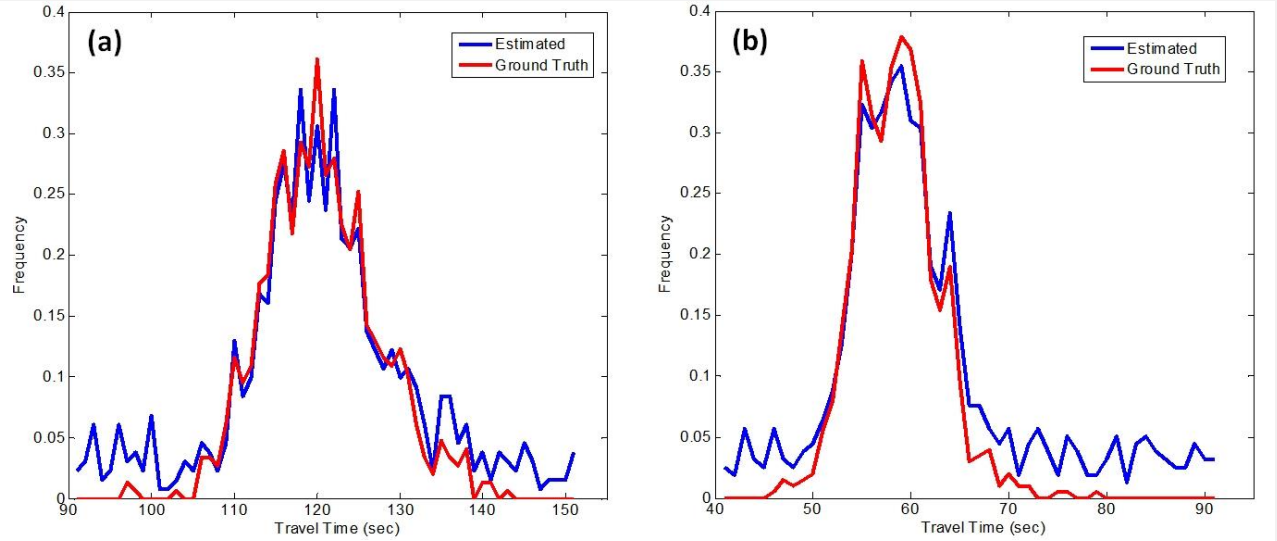

FIGURE 4-6 Comparison of the estimated and manually observed travel time distributions (a) Case 1 and (b) Case 2.

Travel time can be obtained by calculating the time differences between vehicle pairs in the upstream and downstream videos. Ground truth is obtained by manually matching vehicle pairs, while the estimated travel time distribution is obtained by TP and FP. Figures 4-6(a) and 4-6(b) show the travel time distributions for Cases 1 and 2, respectively. To verify the validity of the estimated travel time distributions, Root Mean Square Deviation (RMSD) is adopted as a performance metric here, which is calculated by

$$\text{RMSD} = \left(\frac{1}{K} \sum_{k=1}^{K} (X_k - X_k^*)^2 \right)^{\frac{1}{2}} \qquad (4-20)$$

where K is the number of bins of the time distribution, X_k is the estimated frequency of travel time and X_k^* is the ground truth of frequency. The RMSD for the estimated travel time distributions are 0.0270 and 0.0324 for Cases 1 and 2, respectively. These relatively small values for RMSD indicate that the results of the proposed VRI algorithm do indeed offer a reliable way to estimate the travel time distribution between the upstream and downstream cameras.

In addition to the estimation of travel time distribution, the average travel times can also be compared. Relative Error (RE) is adopted to measure the performance here, which is defined as

$$\mathrm{RE} = \frac{|\bar{Y} - \bar{Y}^*|}{\bar{Y}^*} \qquad (4-21)$$

where $\bar{Y}$ is the estimated average travel time while $\bar{Y}^*$ is the ground truth. The RE for Cases 1 and 2 are 0.27% and 0.66%, respectively, which also shows the accuracy of our travel time estimation.

Section 5 Development of a Prototype Freeway Travel Time Estimation System

To develop a network-wide travel time estimation system, three steps are required. First, a model of the entire network structure has to be constructed to enable the algorithm to estimate travel times along freeway corridors with turning junctions. Second, a more realistic model needs to be developed because the traditional instantaneous model may not be truly representative of true driving behaviors. The final step is to implement the proposed network structure and travel time estimation model in a computer-based system.

5.1 Network Development

5.1.1 Network Structure Overview

The traffic data provided by the TMC includes the spatial locations of individual traffic sensors. However, the connectivity (spatial relationship) information for consecutive sensors is not explicitly presented in the data. Without this connectivity information for each sensor and its neighbors, the travel time estimation system will not be able to determine where the study corridor "turns" at a freeway junction. For example, estimating travel time for the traffic coming from I-64 Westbound and heading to I-270 Southbound, the system has to know the sequence of sensors along the corridor "turns". To address this issue, a network structure needs to be built that includes each sensor's location and the connectivity between the sensors.

The form of the adjacency list (Cormen et al., 2009) has been specifically selected to represent the network structure in this project. Figure 5-1 shows a partial network structure and Table 5-1 lists details of the example nodes. Node *Nx* denotes the traffic sensors; *J1* denotes the interchange between I-64 and I-270; and link *Linkx* is the freeway link bounded by two consecutive sensors. In the figure, Link1, Link2, Link3, Link4 and Link5 are parts of I-64 Westbound; Link6, Link7, and Link8 are parts of I-270 Northbound; and Link9 and Link10 are parts of I-270 Southbound. The traffic flow can move from one link to another when the links are connected by a junction or a node. For example, in Figure 5-1 vehicles at Link2 can move to Link3, Link6 or Link9.

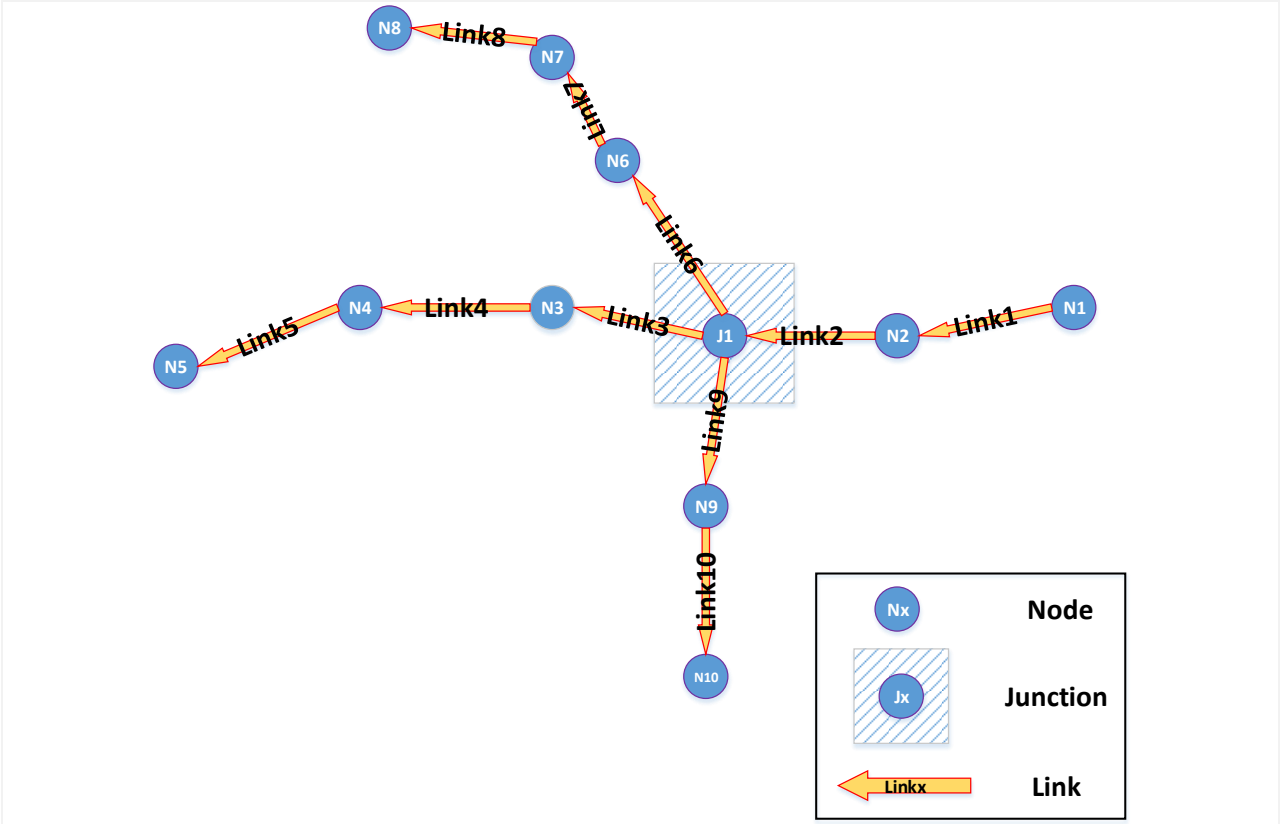

FIGURE 5-1Simplified network structure (partial display) for the I-64/I-270 junction

Table 5-1 Summary of Nodes

Node Name	Freeway	Cross Street	Sensor ID
N1	I-64	Spoede Road	MI064W027.4U
N2	I-64	Ballas Road	MI064W026.1U
N3	I-64	East Mason Road	MI064W025.2U
N4	I-64	Mason Road	MI064W024.2D
N5	I-64	Maryville Centre Drive	MI064W023.2D
N6	I-270	Rte AB-Ladue Road	MI270N013.6D
N7	I-270	Olive Blvd-Rte 340	MI270N014.8D
N8	I-270	Rte 340 Olive Blvd	MI270N015.4D
N9	I-270	Clayton Road	MI270S011.0D
N10	I-270	Rte 100-Manchester Road	MI270S010.0D
J1	I-270	I-64-Us40	MI270S012.4D

5.1.2 Node and Link Structure

Tables 5-2 and 5-3 show the definitions and examples of nodes and links on the network. A total of 462 nodes and 432 links have been manually created and stored in the database. A "fast search" mechanism has also been developed to ensure the node and link connectivity.

Table 5-2 Node Attributes

Attributes	Contents (example)	Description
ID	'MI170N000.3U'	A node represents a traffic sensor, the node ID is the same as the corresponding traffic sensor unique ID
Street Name	'I170'	Which freeway the traffic sensor is installed on
Direction	'North'	Which direction the traffic sensor is monitoring
Cross Street	SO Galleria Pkwy (MI170N000.3U)	Which street crosses the freeway near the traffic sensor
Cross Street (Short)	'SO Galleria Pkwy'	The shortened form of the name "Cross Street"
Absolute Mileage	0.4000	The mileage information configured in the traffic sensor
Lane Number	2	How many lanes the traffic sensor is monitoring
Upstream Traffic Sensor	'MI064W032.0U'	Which traffic sensor is upstream of a particular traffic sensor
Previous Link	429	Which link connects the "Upstream Traffic Sensor" with the traffic sensor
Downstream Traffic Sensor	'MI170N001.5U'	Which traffic sensor is downstream of a particular traffic sensor
Next Link	85	Which link connects the "Downstream Traffic Sensor" with the traffic sensor

Table 5-3 Link Table (Partial)

LinkID*	Upstream Traffic Sensor	Downstream Traffic Sensor	Link Length (miles)	Type
410	'MI070W223.6D'	'MI070W222.3D'	1.3	'link'
411	'MI070W222.3D'	'MI070W221.4D'	0.9	'link'
412	'MI070W221.4D'	'MI070W220.4D'	1	'link'
413	'MI070W220.4D'	'MI070W218.9D'	1.5	'link'
414	'MI070W218.9D'	'MI070W218.2D'	0.7	'link'
415	'MI070W218.2D'	'MI070W217.1D'	1.1	'link'
416	'MI070W217.1D'	'MI070W215.9D'	1.2	'link'
417	'MI070W215.9D'	'MI070W215.2D'	0.7	'link'

418	'MI070W215.2D'	'MI070W213.9D'	1.3	'link'
419	'MI070W213.9D'	'MI070W212.9D'	1	'link'
420	'MI070W212.9D'	'MI070W211.9D'	1.1	'link'
421	'MI070W211.9D'	'MI070W211.0D'	0.8	'link'
422	'MI070W211.0D'	'MI070W210.0D'	1	'link'
423	'MI070W210.0D'	'MI070W209.5D'	0.5	'link'
424	'MI070W209.5D'	'MI070W208.2D'	1.3	'link'
425	'MI070W208.2D'	'MI070W207.2D'	1	'link'
426	'MI070W207.2D'	'MI070W206.0D'	1.2	'link'
427	'MI070W206.0D'	'MI070W204.7D'	1.3	'link'
428	'MI070W204.7D'	'MI070W203.7D'	1	'link'
429	'MI064W032.0U'	'MI170N000.3U'	0.58	'Turning'
430	'MI170N007.2U'	'MI070W238.2D'	1.35	'Turning'
431	'MI170S000.3U'	'MI064E032.0U'	0.58	'Turning'
432	'MI064W026.1U'	'MI270S011.0D'	1.98	'Turning'

*: LinkID: Links on the network are assigned a unique ID
Upstream Traffic Sensor: the upstream traffic sensor for the link
Downstream Traffic Sensor: the downstream traffic sensor for the link
Link Length: the length of the link (unit = miles)
Type: "Link" indicates the link is either an individual freeway segment or contains a "Turning"

5.2 Car-Following-Model-Based Travel Time Estimation

An innovative travel time estimation method has been developed for this project. Unlike traditional freeway travel time estimation methods, the proposed method is based on a car-following model. Generally, car-following models are designed to ensure the fidelity of simulated vehicle movements in a microscopic traffic simulation environment. In contrast with this type of conventional application, the car-following model developed for this project estimates travel times in a real-world environment.

5.2.1 General Motors' Car-Following Model

A car-following model is usually used to measure the kinetic response of vehicles to the movement of the vehicles in front of them, taking into account the acceleration rate, current speed and the gaps between leading and following vehicles, etc. General Motors' car-following model (GM model), one of the most popular car-following models, was selected for the proposed travel time estimation model. The model is mathematically described in Equations 5-1 through 5-3. The initial inputs of the GM model include the initial relative positions, acceleration, and speeds of the leading and following vehicles. These parameters are updated at regular time

intervals using these equations. Here, 0.1 seconds was selected as the time interval so the kinetic response of the following vehicle will be estimated every 0.1 seconds.

$$v_n^t = v_n^{t-\Delta T} + a_n^{t-\Delta T} * \Delta T \qquad (5-1)$$

$$x_n^t = x_n^{t-\Delta T} + v_n^{t-\Delta T} * \Delta t + \frac{1}{2} a_n^{t-\Delta T} \Delta T^2 \qquad (5-2)$$

$$a_{n+1}^t = \left[\frac{\alpha_{l,m} (v_{n+1}^t)^m}{\left(x_n^{t-\Delta T} - x_{n+1}^{t-\Delta T}\right)^l} \right] * \left(v_n^{t-\Delta T} - v_{n+1}^{t-\Delta T}\right) \qquad (5-3)$$

Where: v_n^t is the speed of the n^{th} vehicle at time t

x_n^t is the traveling distance of the n^{th} vehicle at time t

a_n^t is the acceleration rate of the n^{th} vehicle at time t

ΔT is the calculation time step

l is a distance headway exponent that can take values in the range [-1, 4]

m is a speed exponent that can take values in the range [-2, 2]

$\alpha_{l,m}$ is a sensitivity coefficient

5.2.2 Virtual Leading and Following Vehicle

Generally, the GM model is used to estimate the kinetic responses of two physical vehicles in a simulation environment. In order to utilize the GM model to estimate real world travel times, the concept of virtual leading and following vehicles is utilized in the proposed model. The concept is demonstrated in Figure 5-2. Two functioning traffic sensors, Sa and Sb, that are installed along a freeway consistently report vehicle count, average speed and occupancy data throughout a time interval, T. The sensor S_b thus reports the speed information $sb_v^{T_i}$ at time interval T_i.

For the purposes of the model, Sb is treated as a virtual leading vehicle B. Virtual leading vehicle B has two main two kinetic characteristics, speed ($sb_v^{T_i}$) and acceleration rate ($sb_a^{T_i}$), in addition to its position. The virtual leading vehicle is deemed to be a fixed vehicle and the location of Sa is treated as the initial position of a virtual following vehicle A. The kinetic attributes of the virtual following vehicle A are represented as speed ($Sa_v^{T_i}$) and acceleration rate

($Sa_a^{T_i}$). In contrast with the fixed leading vehicle, the virtual following vehicle moves towards Sb. The initial gap, gap_{T_0}, between the virtual leading and following vehicles is constant, corresponding to the distance between the two sensors Sa and Sb. Table 5-4 lists the initial values of the two virtual vehicles at time 0. The gap between the leading and following vehicles (gap_{T_i}) will be reduced as the following vehicle approaches Sb. The travel time from Sa to Sb can be estimated by the time required for the following vehicle to reach Sb. The movement rules of the following vehicle comply with those imposed by the selected car-following model.

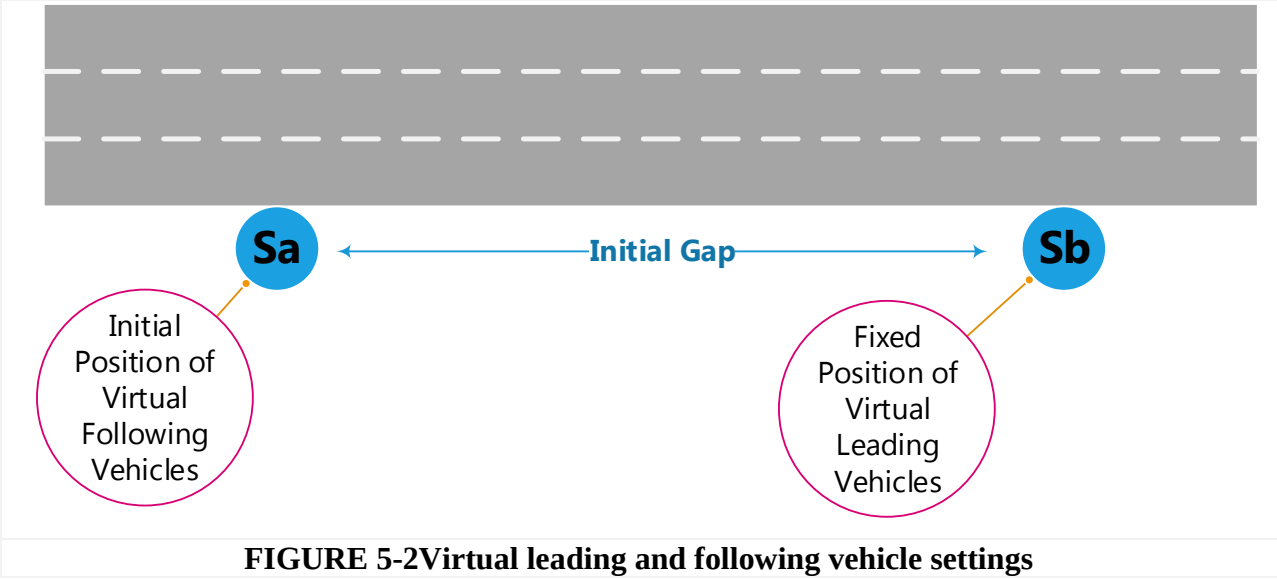

FIGURE 5-2Virtual leading and following vehicle settings

Table 5-4 Initial Values of the GM Model

	Time	Initial Speed	Initial Relative Position	Initial Accelerate Rate
Virtual Leading Vehicle (Sb)	T_0	$sb_v^{T_0}$	gap_{T_0}	0
Virtual Following Vehicle (Sa)	T_0	$sa_v^{T_0}$	0	0

5.2.3 Speed Change of Virtual Leading Vehicle

During each of the time intervals $T_0, T_1, T_2 \ldots, T_n$, a series of speed data $sb_v^{T_0}, sb_v^{T_1}, sb_v^{T_2} \ldots, sb_v^{T_n}$ can be acquired from the sensor Sb. Since traffic sensors report the data in discrete times, any changes in speed seen by Sb may not be fully represented. van Lint & van der Zijpp (2003) assumed that a linear relationship exists in two consecutive observed speed values, making it possible to transform the speed values into a piece-wise linear relationship in a

time domain. Similarly, for this research we also utilized a piece-wise linear relationship to map the speed from the discrete time domain to the continuous time domain. Equation 5-4 shows the mathematical transform applied.

$$sb_v^t = \frac{sb_v^{T_{i+1}} - sb_v^{T_i}}{T_{i+1} - T_i} * (t - T_i) + sb_v^{T_i} \ (T_i \le t \le T_{i+1}) \qquad (5-4)$$

The virtual leading vehicle speed should be initialized using Equation 5-4 from time 0 to T_n (assuming the travel time from Sa to Sb is smaller than or equal toT_n). With sb_v^t being known, sb_a^t then can be calculated using Equation 5-5.

$$sb_a^t = \frac{\partial sb_v^t}{\partial t} = \frac{sb_v^{T_{i+1}} - sb_v^{T_i}}{T_{i+1} - T_i} \ (T_i \le t \le T_{i+1}) \qquad (5-5)$$

The GM model can be executed given known sb_v^t and sb_a^t.

5.2.4 Parameter Selection

Three parameters in the GM model must be selected, namely 1) *t*he distance headway exponent, l; 2) the speed exponent m; and 3) a sensitivity coefficient $\alpha_{l,m}$. The parameter l was found to be critical for estimating freeway travel times because it represents the space headway information and is thus fairly likely to vary somewhat under different traffic conditions due to the changes in space headway. For example, the space headway between vehicles may be closer when the traffic is congested and lengthen when the traffic is flowing freely.

After testing various sets of parameters, two sets were empirically selected in order to reflect the traffic conditions typically encountered: 1) under free flow conditions: l = 1.2; m = 0.5; $\alpha_{l,m}$ = 8; and 2) under congested conditions: l = 0.75; m = 0.5; $\alpha_{l,m}$ = 8.

5.3 Implementation

A travel time estimation prototype system was developed using Matlab, a high-level technical computing language. The system consists of four modules:

1) & 2) Freeway Corridor Time Estimation (with and without a junction)

The travel times between any two given points on I-44, I-55, I-64, I-70, I-170 and I-270 (both directions) can be estimated based on time and dates. The results are output as

figures and numerical data. Speed heat maps can also be produced to investigate bottlenecks. Basically, this module handles corridors with and without a turning junction differently.

3) Data Assurance Report Production

The data quality issue (specifically, missing data) is critical for reporting accurate travel times. It was found that on some occasions the data is missing, thus affecting the accuracy of the travel time estimation. The data assurance report production module helps users understand and appreciate the implications of the quality of the results.

4) Traffic Volume Report Production

Traffic throughput will be significantly reduced due to special events, especially severe weather. This module helps users explain and deal with the percentage decrease in traffic volume.

Figure 5-3 shows the user interface of the new Travel Time Estimation System. The layout of the user interface consists of two main panels. The left panel provides the options of time periods. Two "Date Selection Modes" are provided: consecutive days and every weekday. The "Consecutive days" option allows users to select consecutive days for analysis, while the "Every weekday" option allows users to select the same weekday in consecutive weeks. For example, when a "start date" of "2013-09-24" is entered and "consecutive days" is set as 3, the resulting "consecutive days" would be set as "2013-09-24", "2013-09-25" and "2013-09-26"; while the results for "every weekday" for the same start date would be "2013-09-24", "2013-10-01" and "2013-10-08". The options of "Start Hour" and "End Hour" determine the times of day to be considered for the analysis, which also allows users to specify a particular time of interest. The right panel provides the travel time estimation functions for both individual freeways and corridors with a turning junction. The contents in the "Start Location" and "End Location" textboxes will change accordingly if the item in the "Freeways & Direction" listbox is re-selected.

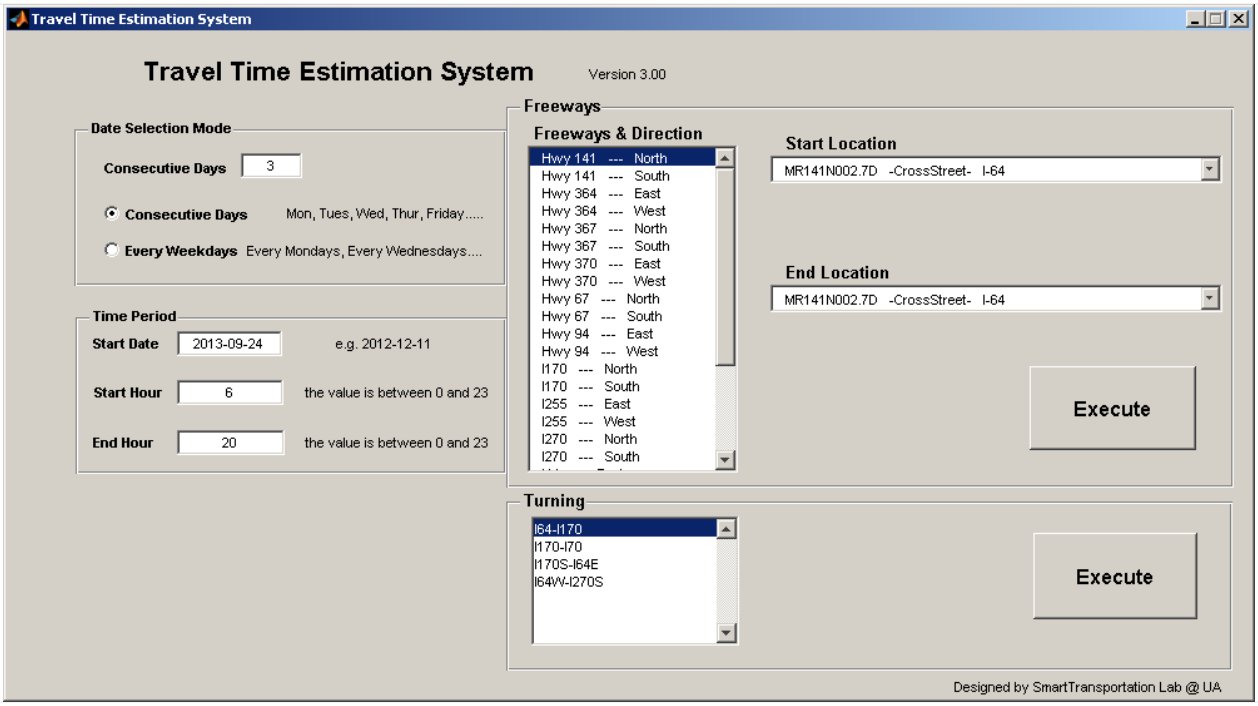

FIGURE 5-3 The Interface of the travel time estimation system

Figure 5-4 shows a screenshot of the message output during and after the travel time estimation procedure. The three major pieces of information it presents, link connectivity checking, travel time estimation and data assurance reporting, will be described in turn in the following sections.

```
Starting to check the connectivity of the links......
Result:
    The links are connected!
Checking the connectivity of the links is completed......

Starting to retrieve the data from remote database.....
    SELECT * FROM [2013_09_4Lane] where DetectorID = 'MI17ON005.0U' and (Date_Time between '24-S
    SELECT * FROM [2013_09_4Lane] where DetectorID = 'MI17ON005.0U' and (Date_Time between '25-S
    SELECT * FROM [2013_09_4Lane] where DetectorID = 'MI17ON005.0U' and (Date_Time between '26-S
    SELECT * FROM [2013_09_4Lane] where DetectorID = 'MI17ON006.2U' and (Date_Time between '24-S
    SELECT * FROM [2013_09_4Lane] where DetectorID = 'MI17ON006.2U' and (Date_Time between '25-S
    SELECT * FROM [2013_09_4Lane] where DetectorID = 'MI17ON006.2U' and (Date_Time between '26-S
    SELECT * FROM [2013_09_4Lane] where DetectorID = 'MI17ON007.2U' and (Date_Time between '24-S
    SELECT * FROM [2013_09_4Lane] where DetectorID = 'MI17ON007.2U' and (Date_Time between '25-S
    SELECT * FROM [2013_09_4Lane] where DetectorID = 'MI17ON007.2U' and (Date_Time between '26-S
    SELECT * FROM [2013_09_4Lane] where DetectorID = 'MIO7OW238.2D' and (Date_Time between '24-S
    SELECT * FROM [2013_09_4Lane] where DetectorID = 'MIO7OW238.2D' and (Date_Time between '25-S
    SELECT * FROM [2013_09_4Lane] where DetectorID = 'MIO7OW238.2D' and (Date_Time between '26-S
    SELECT * FROM [2013_09_4Lane] where DetectorID = 'MIO7OW236.6D' and (Date_Time between '24-S
    SELECT * FROM [2013_09_4Lane] where DetectorID = 'MIO7OW236.6D' and (Date_Time between '25-S
    SELECT * FROM [2013_09_4Lane] where DetectorID = 'MIO7OW236.6D' and (Date_Time between '26-S
    SELECT * FROM [2013_09_4Lane] where DetectorID = 'MIO7OW236.1D' and (Date_Time between '24-S
    SELECT * FROM [2013_09_4Lane] where DetectorID = 'MIO7OW236.1D' and (Date_Time between '25-S
    SELECT * FROM [2013_09_4Lane] where DetectorID = 'MIO7OW236.1D' and (Date_Time between '26-S
    SELECT * FROM [2013_09_3Lane] where DetectorID = 'MIO7OW235.OD' and (Date_Time between '24-S
    SELECT * FROM [2013_09_3Lane] where DetectorID = 'MIO7OW235.OD' and (Date_Time between '25-S
    SELECT * FROM [2013_09_3Lane] where DetectorID = 'MIO7OW235.OD' and (Date_Time between '26-S
Retrieving the data from remote database is completed......

Starting to check the data quality......
Results:
     [Time Period] 2013-09-24 from 06 to 20 [Data Missing Rate] 1.49 %
     [Time Period] 2013-09-25 from 06 to 20 [Data Missing Rate] 1.79 %
     [Time Period] 2013-09-26 from 06 to 20 [Data Missing Rate] 1.61 %
Checking the data quality is completed...... More information can be found here......
```

FIGURE 5-4 Screenshot of data processing summary

5.3.1 Travel Time Estimation

Before conducting the travel time estimation for a selected corridor, the system will execute "link connectivity checking" to ensure that the links on the corridor are logically connected. Figure 5-5 shows the message output related to checking link connectivity.

```
Starting to check the connectivity of the links......
Result:
    The links are connected!
Checking the connectivity of the links is completed......
```

(a) Log message output

```
Starting to check the connectivity of the links......
Result:
    The links are NOT connected!
Checking the connectivity of the links is completed......
```

(b) Error message output

FIGURE 5-5 Message output of checking link connectivity

5.3.2 Data Assurance Report Production

Once connectivity checking is successfully completed, the system reads the data from the database, arranges the data and then generates the travel time reports.

The function "Data Assurance Report" mainly focuses on investigating the data missing rate. Figure 5-6 (a) shows a data missing rate report for each day in an aggregate manner. The update frequency of the traffic data here is set as 30 seconds. However, due to wireless communication and time synchronization issues in the traffic sensors, the TMC occasionally fails to push the traffic data feed to the UA server. Figure 5-6 (b) shows the results of the data missing rate every five minutes.

```
Starting to check the data quality......
Results:
     [Time Period] 2013-09-24 from 06 to 20 [Data Missing Rate] 1.49 %
     [Time Period] 2013-09-25 from 06 to 20 [Data Missing Rate] 1.79 %
     [Time Period] 2013-09-26 from 06 to 20 [Data Missing Rate] 1.61 %
Checking the data quality is completed...... More information can be found here......
```

(a) The task of checking data missing rate

Web Browser - file:///C:/MySVN/MoDOTRealtime/MoDOT-PhaseI-Matlab/MatlabCode/Results/DataQuality.txt

DataQuality.txt

Location: file:///C:/MySVN/MoDOTRealtime/MoDOT-PhaseI-Matlab/MatlabCode/Results/DataQuality.txt

Pairs (Date & Time	Missing Rate)				
2013-09-24 06:00	0.000 %	2013-09-25 06:00	10.000 %	2013-09-26 06:00	0.000 %
2013-09-24 06:05	0.000 %	2013-09-25 06:05	0.000 %	2013-09-26 06:05	0.000 %
2013-09-24 06:10	0.000 %	2013-09-25 06:10	0.000 %	2013-09-26 06:10	0.000 %
2013-09-24 06:15	0.000 %	2013-09-25 06:15	0.000 %	2013-09-26 06:15	10.000 %
2013-09-24 06:20	10.000 %	2013-09-25 06:20	0.000 %	2013-09-26 06:20	0.000 %
2013-09-24 06:25	0.000 %	2013-09-25 06:25	0.000 %	2013-09-26 06:25	0.000 %
2013-09-24 06:30	0.000 %	2013-09-25 06:30	0.000 %	2013-09-26 06:30	0.000 %
2013-09-24 06:35	0.000 %	2013-09-25 06:35	10.000 %	2013-09-26 06:35	0.000 %
2013-09-24 06:40	0.000 %	2013-09-25 06:40	0.000 %	2013-09-26 06:40	0.000 %
2013-09-24 06:45	0.000 %	2013-09-25 06:45	0.000 %	2013-09-26 06:45	0.000 %
2013-09-24 06:50	0.000 %	2013-09-25 06:50	0.000 %	2013-09-26 06:50	10.000 %
2013-09-24 06:55	10.000 %	2013-09-25 06:55	0.000 %	2013-09-26 06:55	0.000 %
2013-09-24 07:00	0.000 %	2013-09-25 07:00	0.000 %	2013-09-26 07:00	0.000 %
2013-09-24 07:05	0.000 %	2013-09-25 07:05	10.000 %	2013-09-26 07:05	0.000 %
2013-09-24 07:10	0.000 %	2013-09-25 07:10	0.000 %	2013-09-26 07:10	0.000 %
2013-09-24 07:15	0.000 %	2013-09-25 07:15	0.000 %	2013-09-26 07:15	0.000 %
2013-09-24 07:20	0.000 %	2013-09-25 07:20	0.000 %	2013-09-26 07:20	0.000 %
2013-09-24 07:25	0.000 %	2013-09-25 07:25	0.000 %	2013-09-26 07:25	10.000 %
2013-09-24 07:30	10.000 %	2013-09-25 07:30	0.000 %	2013-09-26 07:30	0.000 %
2013-09-24 07:35	0.000 %	2013-09-25 07:35	0.000 %	2013-09-26 07:35	0.000 %
2013-09-24 07:40	0.000 %	2013-09-25 07:40	0.000 %	2013-09-26 07:40	0.000 %
2013-09-24 07:45	0.000 %	2013-09-25 07:45	10.000 %	2013-09-26 07:45	0.000 %

(b) The detailed report of data missing as shown in a web browser

FIGURE 5-6 Output of the data quality assurance module

5.3.3 Traffic Volume Report Production

In addition to travel time, traffic volume also plays an important role in measuring the performance of transportation systems from the perspective of vehicle throughput. This module was developed as a result of a suggestion by the MoDOT staff at Gateway Guide. The traffic volume report module is designed to assist traffic engineers charged with evaluating the impact

of special events such as weather or incidents on traffic throughput. Traffic volume is defined as the number of vehicles that pass a given point on a freeway section during a specified time period. Examples will be provided in Section 7.3 Case Study #3: Impact of Severe Weather Event on Traffic Volume.

Section 6 Model Verification

This section focuses on the verification of two types of travel time estimation: 1) freeway corridors with a turning junction and 2) freeway corridors without turning junctions. The objective is to verify whether the travel time estimation model can capture the delay at a junction.

6.1 Measures of Accuracy

Two measures of accuracy, namely the Mean Absolute Error (MAE) and Mean Absolute Percentage Error (MAPE), were selected to verify the model application for corridors including junctions. MAE provides an overview of all the errors and shows the gaps between the estimated travel times and the ground truth travel times. MAPE, showing the error as a percentage, is a scale independent measure of accuracy. Equations 6-1 and 6-2 show the definitions of the two measures.

$$MAE = \frac{1}{n}\sum_{i=1}^{n}|g_i - e_i| \qquad (6-1)$$

$$MAPE = \frac{1}{n}\sum_{i=1}^{n}\frac{|g_i - e_i|}{e_i} \qquad (6-2)$$

Where: g_i is the ground truth travel time at a time i; and

e_i is the estimated travel time at a time i.

6.2 Freeway Corridor with a Turning Junction

6.2.1 Data Description

Here, the model verification mainly focuses on the application of the travel time instantaneous model on corridors including a junction. As described in Section 3, the ground truth data was collected through video-based vehicle matching. The two corridors selected for the verification process were: 1) I-170 southbound ~ I-64 eastbound; 2) I-64 westbound ~ I-270 southbound. The video data collection time period focused on the weekday afternoon rush hours. Streaming videos were recorded to collect the travel time ground truth by matching identical vehicles. Note that the views shown by the video cameras were occasionally changed by the MoDOT staff in

the TMC as part of their regular freeway monitoring schedule. Table 6-1 provides an overview of ground truth video data source information.

Table 6-1Video Data Collection for Vision-Based Ground Truth Data Extraction

Corridor	Time Periods	Locations
I-170S – I-64E SO Galleria Pkwy (MI170S000.3U) →WO S Hanley Rd (MI064E032.0U) (0.58 miles)	1) 4:30 pm ~ 6:30 pm, March, 17,2014 2) 4:30 pm ~ 6:30 pm, March, 19,2014 3) 4:30 pm ~ 5:45 pm, March, 25,2014 4) 4:30 pm ~ 6:30 pm, April, 23, 2014	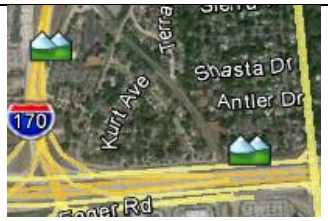
I64W – I270S Ballas Rd (MI064W026.1U) →I-64-Us40 (MI270S012.4D) →SO Clayton Road (MI270S011.0D) (1.98 miles)	1) 4:00 pm ~ 5:00 pm, March, 14, 2014 2) 4:00 pm ~ 6:00 pm, March, 19, 2014 3) 4:00 pm ~ 6:00 pm, March, 25, 2014 4) 4:15 pm ~ 6:00 pm, April, 23, 2014 5) 4:00 pm ~ 5:00 pm, April, 24, 2014	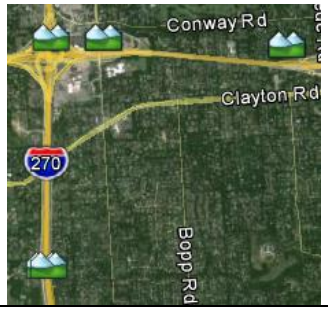

The vehicles were matched for 5 minute time segments. At least 10 samples of identical vehicles were matched during each 5-minute interval. The median value of the travel time was used to represent the ground truth travel time. Accordingly, the travel times estimated by the traffic sensor data were aggregated at the same (5-minute) time intervals for comparison purposes. Table 6-2 shows examples of vehicle-matching-based travel times collected from 4:00 pm to 5:00 pm on March, 14, 2014.

Table 6-2 Examples of Vehicle-Matching-Based Travel Times

Time Interval*	Vehicle-matching-based Travel Times (seconds)													Median (seconds)
4:00 pm - 4:05 pm	126	128	129	134	127	134	132	136	157	132				126
4:05 pm - 4:10 pm	136	135	131	129	123	123	123	127	130	130	127	130	129	132.5
4:10 pm - 4:15 pm	130	133	128	130	124	135	137	133	136	138	140	141	133	131.5
4:15 pm - 4:20 pm	141	139	143	133	140	140	141	143	140	153	140	153	151	146
4:20 pm - 4:25 pm	150	156	159	150	151	150	147	145	152	148	156	152	155	152.5
4:25 pm– 4:30 pm	147	148	153	152	151	150	155	137	126	140	140	138		147
4:30 pm– 4:35 pm	129	131	129	126	132	132	123	125	123	134	130	125	125	127
4:35 pm– 4:40 pm	143	135	125	135	138	124	135	141	132	129				143
4:40 pm– 4:45 pm	125	125	133	133	138	124	135	141	132	129				125
4:45 pm– 4:50 pm	131	130	133	127	125	125	128	134	131	134				131
4:50 pm– 4:55 pm	122	120	127	112	120	122	134	134	129	125				122
4:55 pm– 5:00 pm	127	129	134	133	136	130	125	127	134	129				127

6.2.2 Results

Table 6-3 lists the values of MAE and MAPE based on the ground truth and estimated travel times. Most of the MAPE values are greater than 10%, probably because the two corridors are relatively short (0.58 miles and 1.98 miles, respectively) so the values of MAE are relatively large. These results indicate that the estimated travel times obtained using the traffic sensor data were not capable of effectively representing the travel times along the corridors.

Table 6-3 Quantitative Comparison Between Vehicle-match-based and Estimated Travel Times

Corridors	Date & Time	MAE (seconds)	MAPE (%)
Corridor 1:	4:30 pm ~ 6:30 pm, March, 17,2014	8.70	23.76%
I170S – I64E (0.58 miles)	4:30 pm ~ 6:30 pm, March, 19,2014	34.03	88.11%
SO Galleria Parkway → WO S Hanley Road	4:30 pm ~ 5:45 pm, March, 25,2014	10.76	29.26%
	4:30 pm ~ 6:30 pm, April, 23,2014	44.88	112.48%
Corridor 2:	4:00 pm ~ 5:00 pm, March, 14, 2014	15.14	10.21%
I64W – I270S (1.98 miles)	4:00 pm ~ 6:00 pm, March, 19, 2014	16.08	13.71%
	4:00 pm ~ 6:00 pm, March, 25, 2014	8.57	7.00%
Ballas Road → I-64-Us40 → SO Clayton Road	4:15 pm ~ 6:00 pm, April, 23, 2014	55.23	40.51%
	4:00 pm ~ 5:00 pm, April, 24, 2014	15.20	11.22%

6.2.3 Discussion

Figure 6-1 shows the comparisons between the ground truth and estimated travel times on different days. Figures 6-1 (a) and (b) show the results for the corridor from I-170 southbound to I-64 eastbound on March 17 and March 25, 2014, respectively. Figures 6-1 (c) and (d) show the results for the corridor from I-64 westbound to I-270 southbound on March 19 and April 23, 2014, respectively.

As the graphs show, the estimated travel time (the dashed lines in Figure 6-1) were "flat" during the study times. This indicates that the proposed travel time estimation method failed to capture the traffic fluctuations typically experienced during rush hours. As everyone travelling these routes is all too aware, congestion occurs regularly along the two study corridors during the study time period. The video evidence also indicated congestion. The potential cause of the ineffective estimation results could be too few sensors on the turning junction. This lack of sufficient sensors along the turning junction has two consequences:

1) An inability to capture vehicle speed variation along the turning junction due to the lack of sensors.

Interchanges usually consist of uphill or downhill segments. Travelers tend to slow down when driving uphill segments, but their speed tends to increase when driving the downhill segments. Moreover, due to the geometric design of interchanges, traveling speeds usually decrease when vehicles are on curved segments. Therefore, the vehicle speed variation tends to be greater than commonly encountered on straight freeway segments.

2) An inability to capture vehicle speed changes within merging/weaving areas where freeways and interchanges are connected.

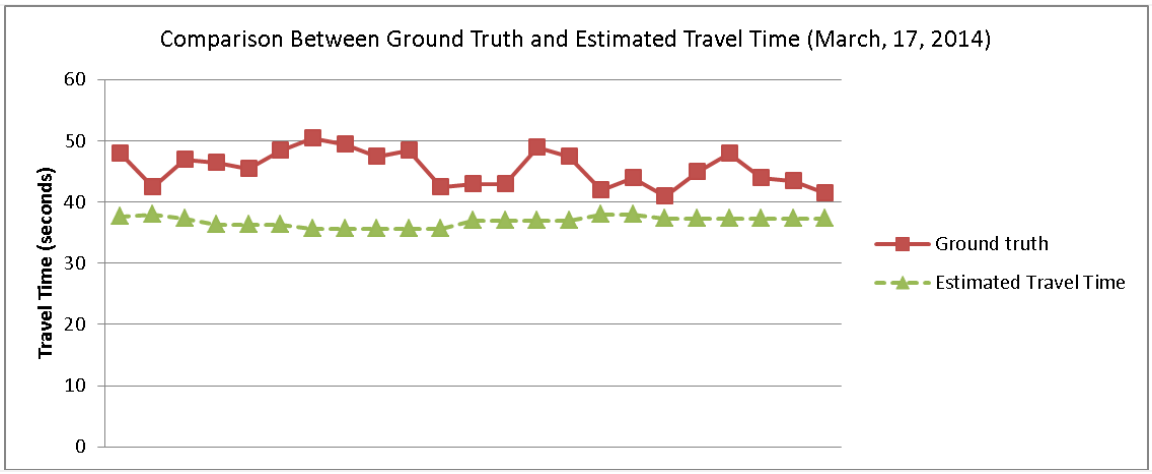

(a) Ground truth and estimated travel times comparison on March, 17, 2014
(from I-170 southbound to I-64 eastbound, 0.58 miles)

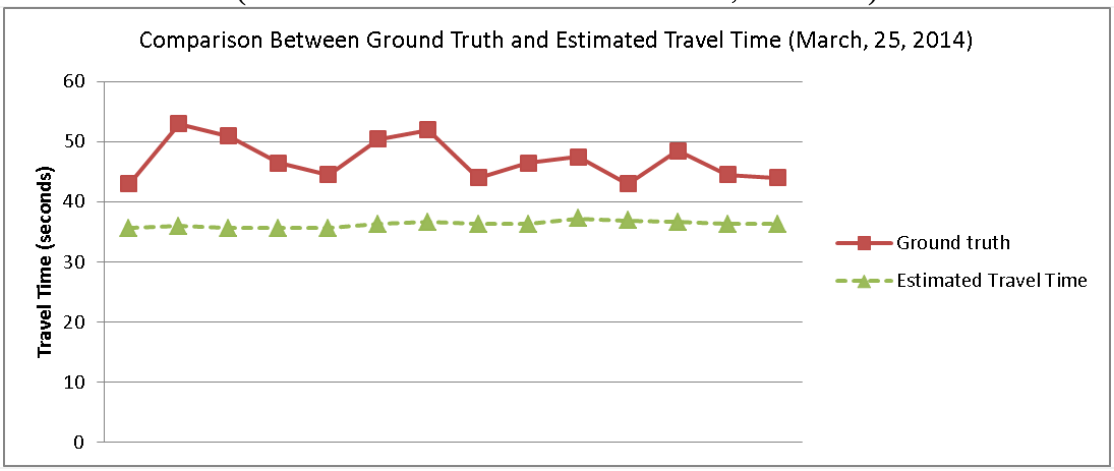

(b) Ground truth and estimated travel times comparison on March, 25, 2014
(from I-170 southbound to I-64 eastbound, 0.58 miles)

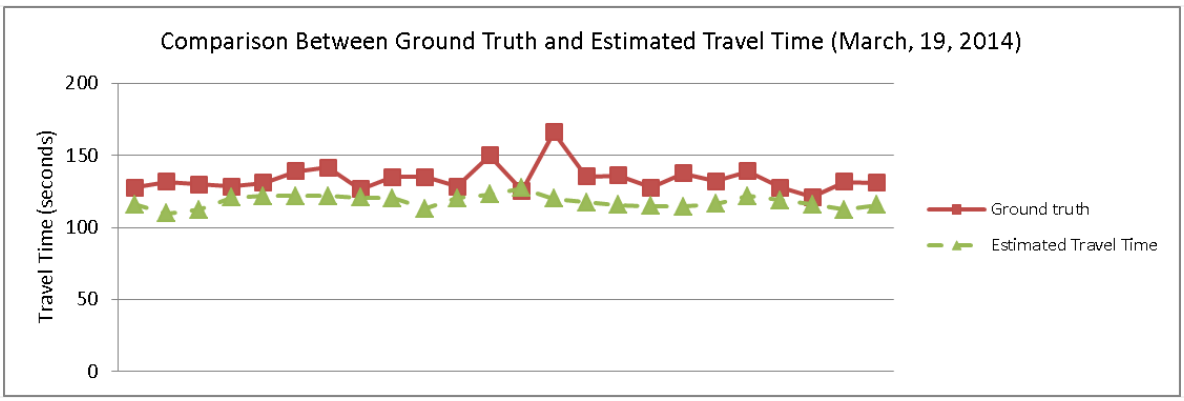

(c) Ground truth and estimated travel times comparison on March, 19, 2014
(from I-64 westbound to I-270 southbound, 1.98 miles)

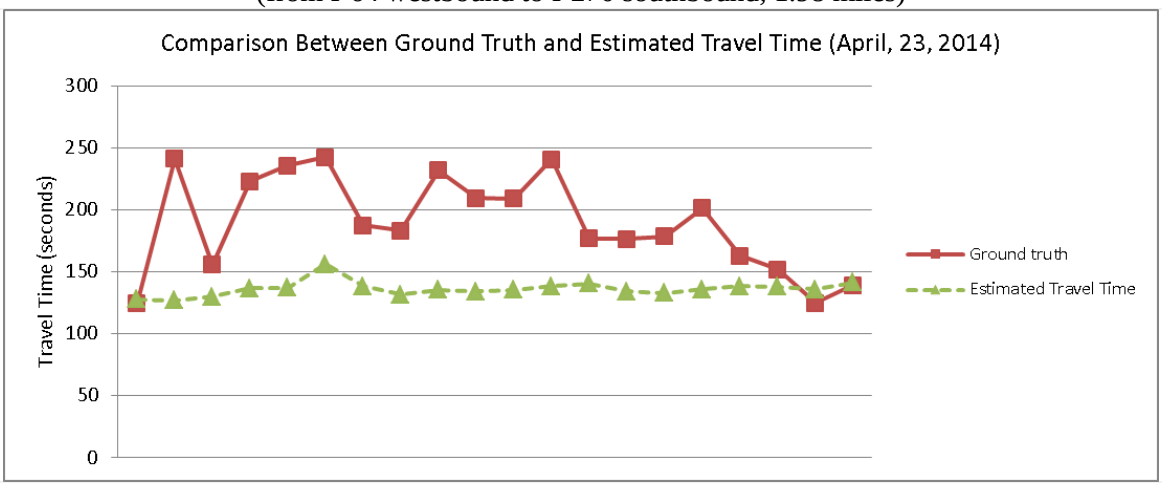

(d) Ground truth and estimated travel times comparison on April, 23, 2014
(from I-64 westbound to I-270 southbound, 1.98 miles)

FIGURE 6-1 Travel time dataset comparison

6.3 Freeway Corridor without a Turning Junction

In order to compare the results from freeway corridors with and without a turning junction, this section focuses on model verification for freeway corridors without a turning junction. This comparison is designed to ensure the proposed method can also be used in regular corridors.

6.3.1 Data Description

Four freeway corridors were selected for the model verification. Table 6-4 shows the detailed information for the study corridors. Both corridors are located on I-270. Corridor#1 is a 7.2 mile section of I-270 Southbound that is known to suffer from recurrent congestion on Tuesdays, Wednesday s and Thursdays. However, congestion is less severe on Fridays so Corridor#1 on Dec. 12, 2014, (a Friday) has been selected as the "free-flow" scenario in the verification

procedure. Corridor#2, which consistently suffers from traffic congestion on weekdays, was selected as the "congested" scenario.

Table 6-4 Study Corridors

Study Corridors	Time Period	Locations
Corridor#1: **I-270 Southbound** (7.2 miles) NO Dorsett Road @I270 → Rte D-Page Ave @I270 → NO Rte 340 Olive Blvd@I270 → Rte 340-Olive Blvd @I270 → Rte AB-Ladue Rd @I270 → I-64-Us40 @I270 → SO Clayton Road @I270	07:00 AM ~ 08:00 AM Dec. 12, 2014, Friday	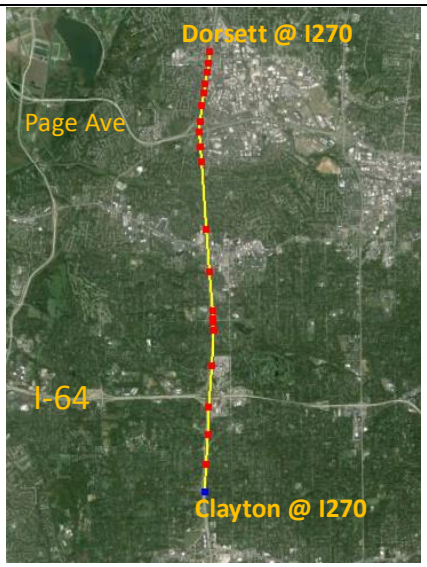
Corridor#2: **I-270 Northbound** (3.7 miles) Big Bend Road @I270 → Dougherty Ferry Rd@I270 → Rte 100-Manchester Rd @I270 → SO Clayton Road @I270	07:50 AM ~ 08:50 AM Dec., 16, 2014, Tuesday	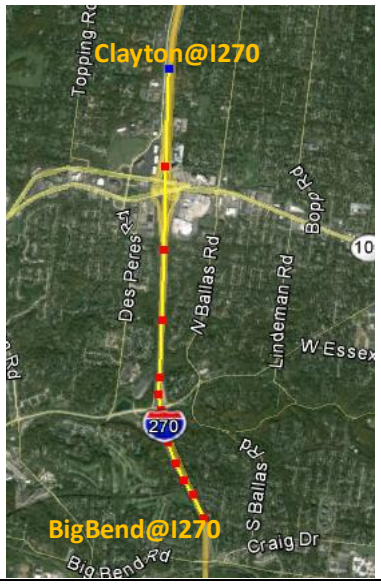

The ground truth travel times for the two selected freeway corridors were also collected using the proposed vehicle matching method presented in Section 4. Tables 6-5 and 6-6 show portions of the ground truth data used to verify the proposed travel time estimation model.

Table 6-5 Corridor#1, 7.2 miles (Partially Displayed)

Departure Time	Travel Time (seconds)	Departure Time	Travel Time (seconds)
12/12/2014 7:01:29	412	12/12/2014 7:04:49	454
12/12/2014 7:02:14	367	12/12/2014 7:05:44	412
12/12/2014 7:02:29	381	12/12/2014 7:05:37	428
12/12/2014 7:01:44	429	12/12/2014 7:05:55	423
12/12/2014 7:02:16	400	12/12/2014 7:05:59	438
12/12/2014 7:02:00	435	12/12/2014 7:06:19	433
12/12/2014 7:02:33	422	12/12/2014 7:06:35	427
12/12/2014 7:03:40	409	12/12/2014 7:06:32	441
12/12/2014 7:03:45	410	12/12/2014 7:07:06	418
12/12/2014 7:03:04	462	12/12/2014 7:05:57	497
12/12/2014 7:03:43	441	12/12/2014 7:07:29	405
12/12/2014 7:04:55	379	12/12/2014 7:06:38	458
12/12/2014 7:04:42	417	12/12/2014 7:07:00	437
12/12/2014 7:05:24	384	12/12/2014 7:06:10	487

Table 6-6 Corridor#2, 3.7 miles (Partially Displayed)

Departure Time	Travel Time (seconds)	Departure Time	Travel Time (seconds)
12/16/2014 7:48	588	12/16/2014 7:52	432
12/16/2014 7:49	577	12/16/2014 7:52	493
12/16/2014 7:49	527	12/16/2014 7:52	442
12/16/2014 7:49	557	12/16/2014 7:53	556
12/16/2014 7:50	519	12/16/2014 7:53	558
12/16/2014 7:50	542	12/16/2014 7:53	492
12/16/2014 7:50	466	12/16/2014 7:53	468
12/16/2014 7:50	452	12/16/2014 7:53	501
12/16/2014 7:50	537	12/16/2014 7:54	529
12/16/2014 7:51	549	12/16/2014 7:54	398
12/16/2014 7:51	481	12/16/2014 7:54	511
12/16/2014 7:51	501	12/16/2014 7:55	459
12/16/2014 7:51	485	12/16/2014 7:55	453
12/16/2014 7:52	451	12/16/2014 7:55	461

6.3.2 Results

Figure 6-2 shows the estimated travel times for Corridor#1 using the proposed travel time estimation method. Figure 6-2 (a) shows the estimated travel times with fluctuations over time. In order to clearly observe the trends in these travel times, a moving average method was applied to the original estimated travel time to smooth the estimated travel time. The smoothed travel

times are plotted in Figure 6-2 (b). Figure 6-2 (c) presents the comparison between the ground truth and estimated travel times graphically.

In order to quantify the differences between the ground truth and estimated travel times, the measures of accuracy listed in Section 6.1 were applied to the two data sets. Table 6-7 shows the quantitative comparison between the ground truth and estimated travel times. The MAE and MAPE values for Corridor#1 are 8.2 seconds and 1.88%, respectively. These low values indicate the high similarity between the ground truth and estimated travel times. The MAE and MAPE values for Corridor#2 are 35.7 seconds and 8.49%. Both of these results indicate that the estimated travel time adequately represents the ground truth travel times.

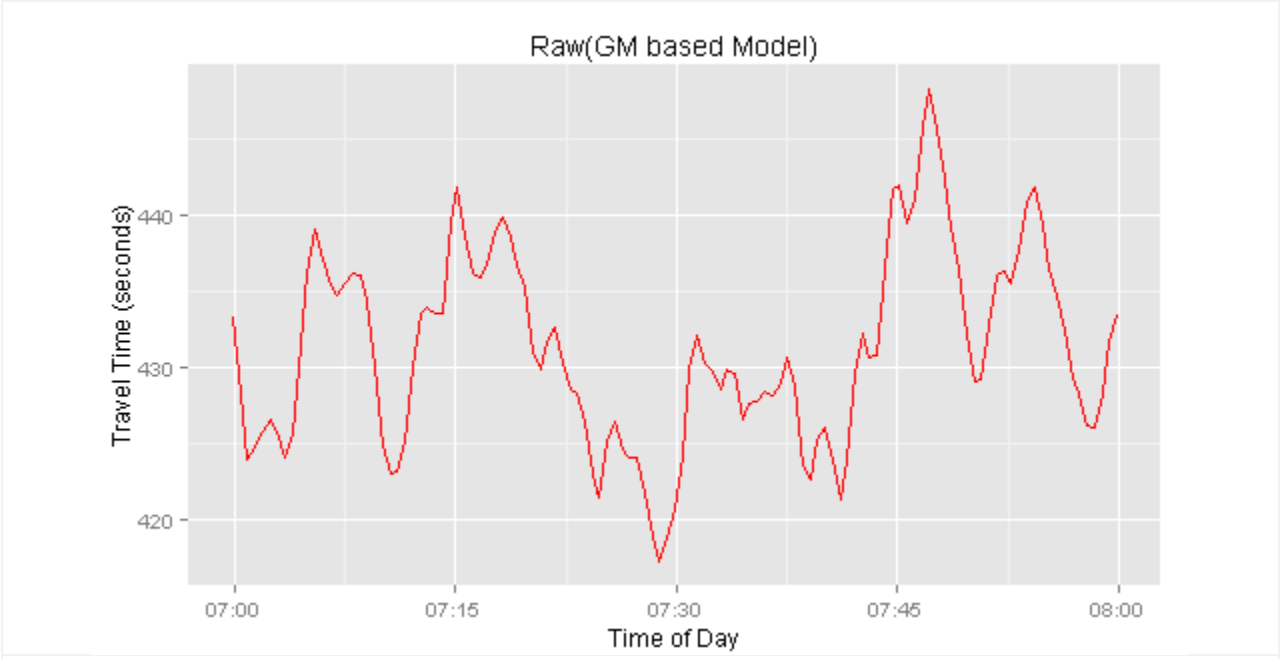

(a) Estimated travel time

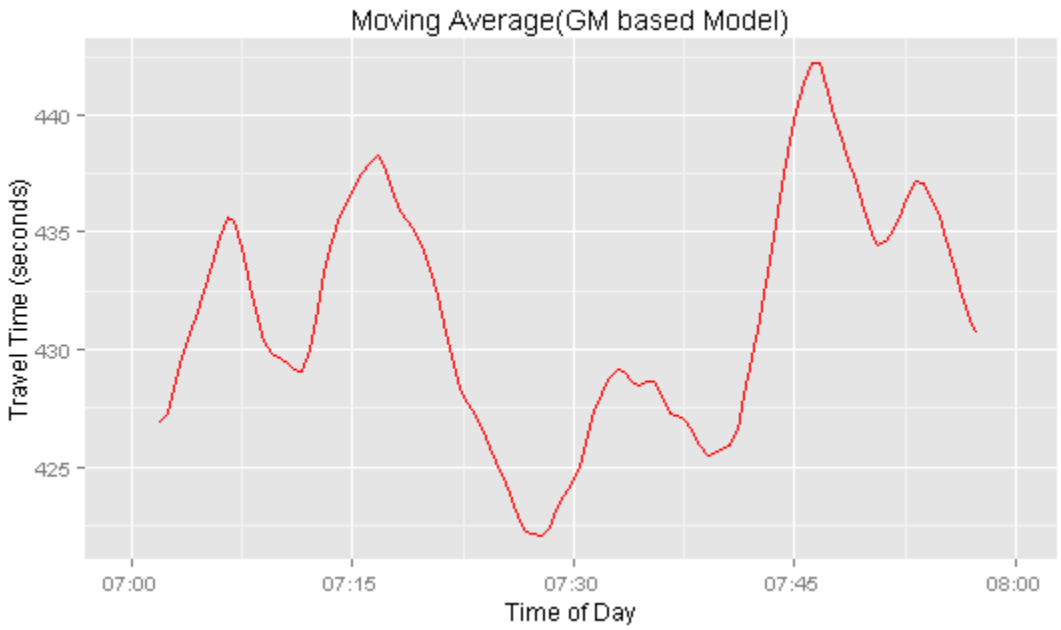

(b) Estimated travel time after applying moving average method

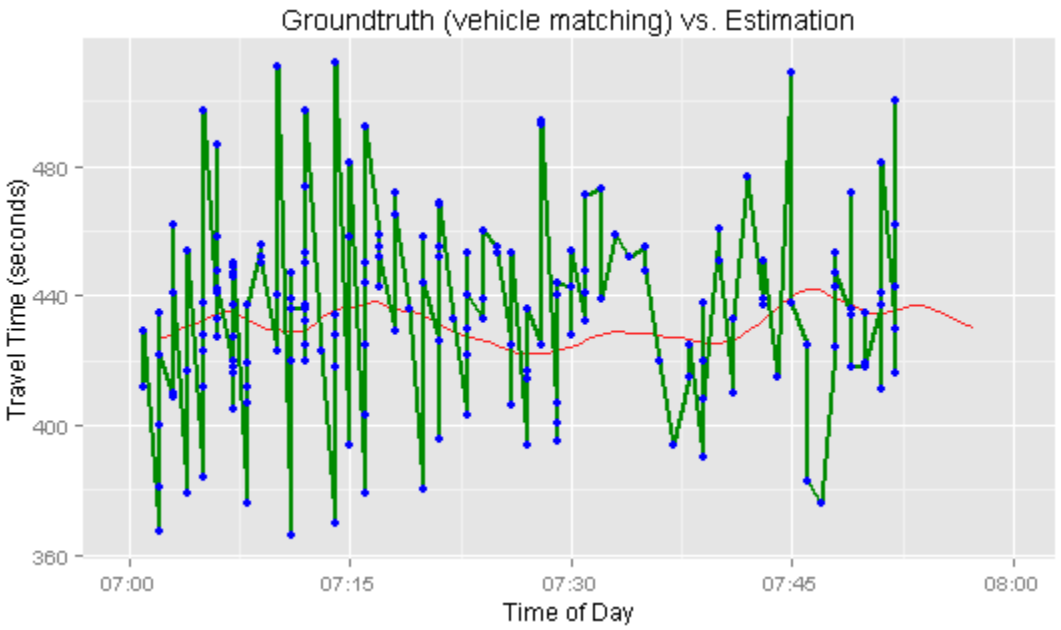

(c) Comparison between ground truth and estimated travel time

FIGURE 6-2 Travel time estimation for Corridor#1 (7 ~ 8 AM, Dec, 12, 2014, Friday)

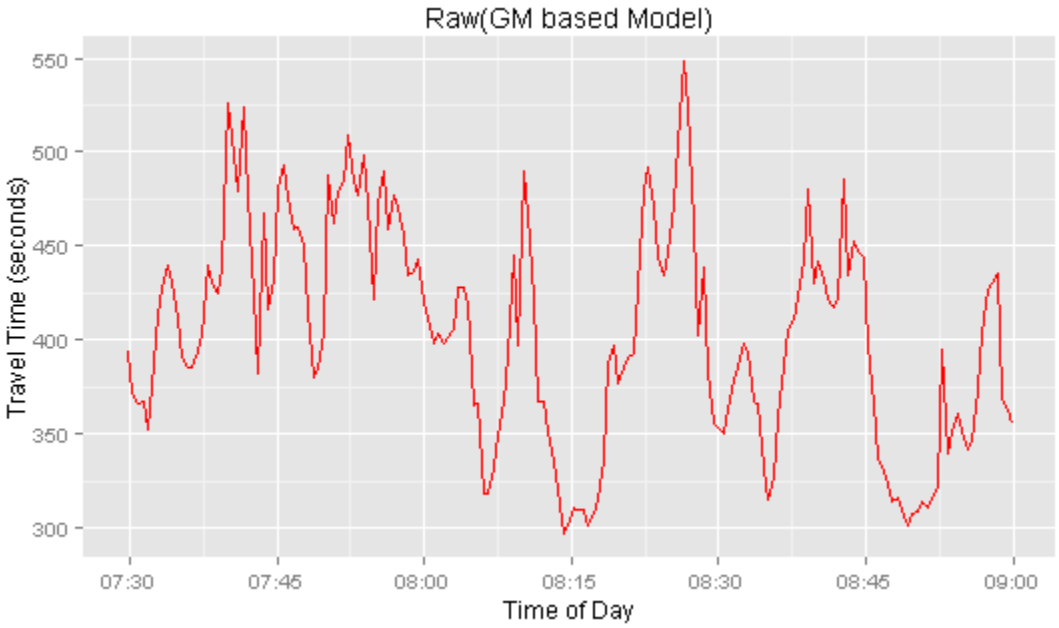

(a) Estimated travel time

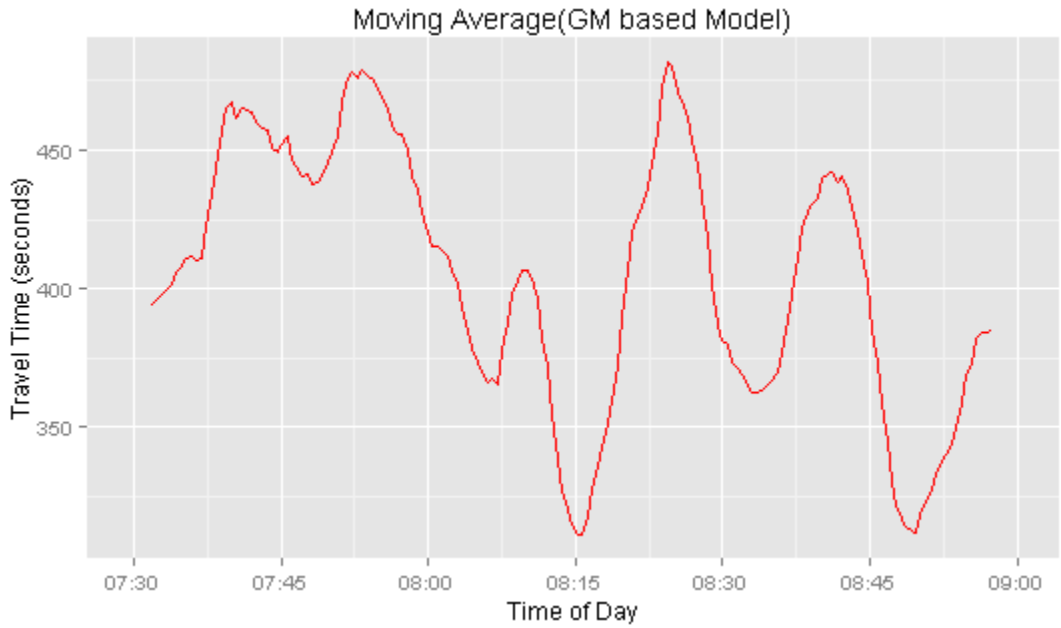

(b) Estimated travel time after applying moving average method

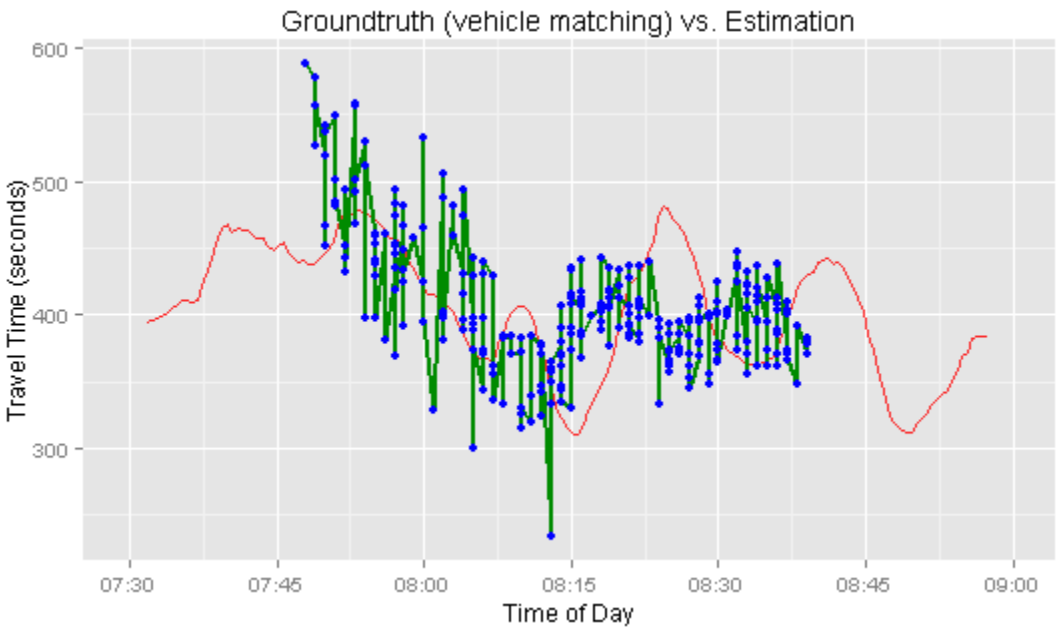

(c) Comparison between the ground truth and estimated travel time

FIGURE 6-3 Travel time estimation for Corridor#2 (7:50 ~ 8:50 AM, Dec, 16, 2014, Tuesday)

Table 6-7 Quantitative Comparison between the Ground Truth and Estimated Travel Times

Segments	Time Period	Length	MAE (seconds)	MAPE (%)
Corridor#1 (Free flow condition)	07:00 AM ~ 08:00 AM Dec. 12, 2014, Friday	7.2 miles	8.2	1.88
Corridor#2 (Congested condition)	07:50 AM ~ 08:50 AM Dec., 16, 2014, Tuesday	3.7 miles	35.7	8.49

6.3.3 Discussion

Figure 6-8 (c) and Figure 6-9 (c) show the graphical comparison between ground truth and estimated travel time. The findings of this comparison of the two travel times can be summarized as follows:

1) The trend in the estimated travel time provides a good visual match for the ground truth travel time trend.

In Phase I (Wu et al., 2013), the ground truth travel time was collected by only tracking heavy trucks, due to the low resolution of the available video feed. Theoretically, the ground truth travel time should thus be greater than the estimated travel time, because trucks usually move more slowly than passenger vehicles. The conclusion was that the estimated travel times

were underestimated. The ground truth travel times collected for this project were obtained by tracking both trucks and passenger vehicles. Therefore, the ground truth travel time can safely be treated as the true "ground truth travel time". Both of the trends shown in Figure 6-8 (c) and Figure 6-9 (c), as well as the quantitative comparison results listed in Table 6-7 confirm that the two data sets match.

2) The close match in the time lags between the estimated and the ground truth travel times

The time lag is less visible in Figure 6-8 (c), because the traffic along Corridor#2 during the study time period is moving under "free flow" conditions, with minimal fluctuations in the travel time. This is not the case for the "congested" traffic flow shown in Figure 6-9 (c), where an approximate 10 minute time lag can be observed.

6.4 Model Comparisons

This section compares the performance differences between the proposed model and previous travel time estimation models, specifically the instantaneous model and the time slice model (Li et al, 2006). Table 6-8 summarizes the details of the freeway corridor selected for this comparison.

Table 6-8 Study Corridors

Study Corridor	Time Period	Locations
Corridor#3: **I-270 Northbound** (1.8 miles) I-44 @I270 → Big Bend Road @I270	07:00 AM ~ 08:00 AM Dec, 17, 2014, Wednesday	

Figure 6-4 displays the results from the three travel time estimation models. Figure 6-4(a) shows the comparison between the ground truth and travel times estimated by the proposed GM car-following model, while Figures 6-4 (b) and (c) shows the travel times estimated by the instantaneous and time slice models, respectively.

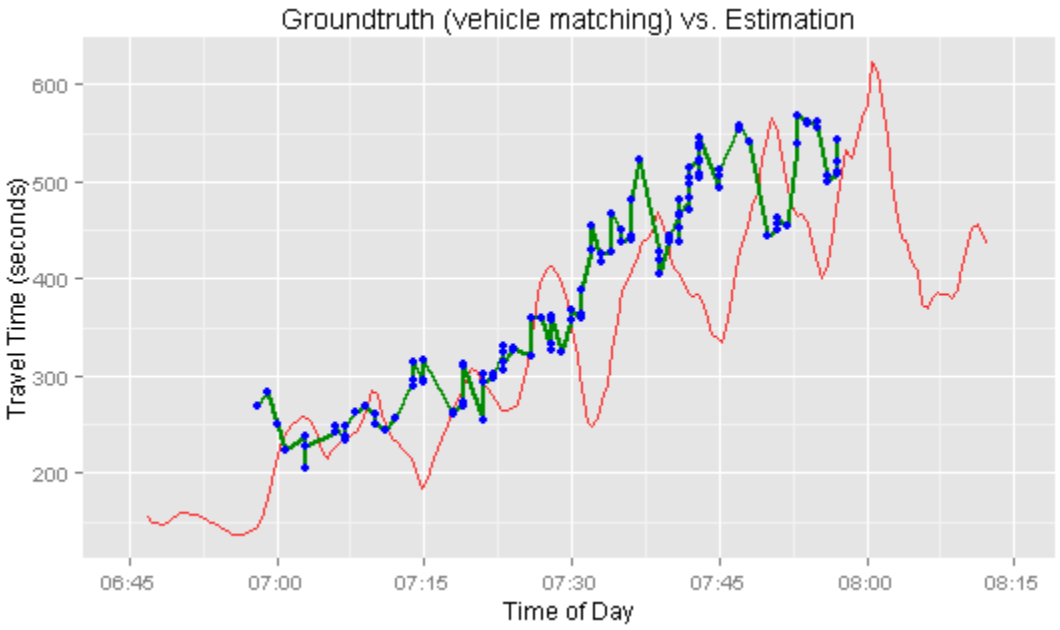

(a) Ground truth vs. estimated travel time (the proposed model)

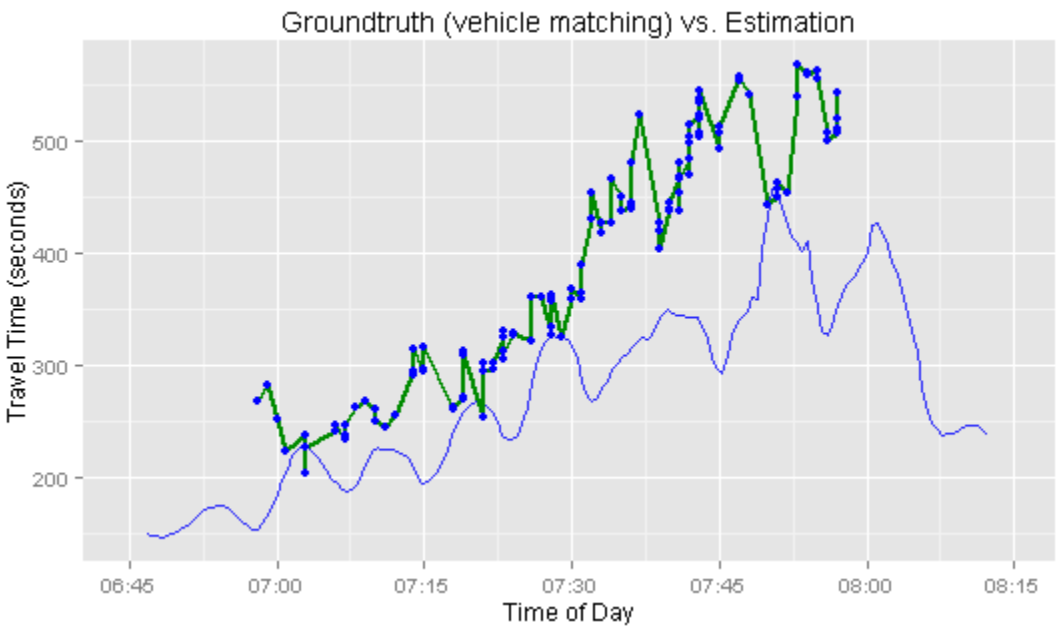

(b)Ground truth vs. estimated travel time (the instantaneous model)

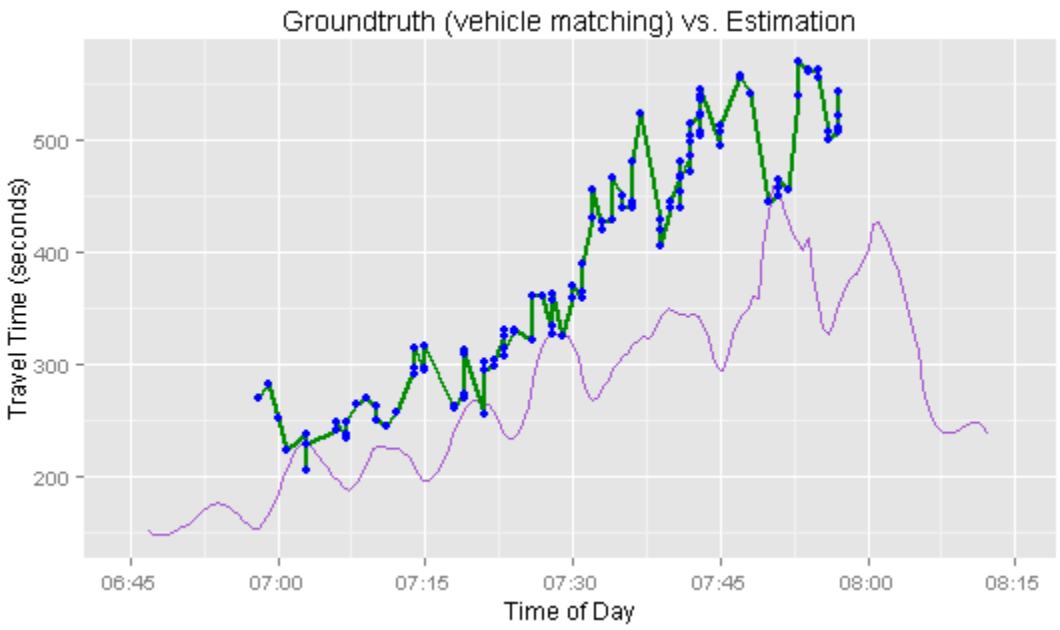

(c) Ground truth vs. estimated travel time (the time slice model)

FIGURE 6-4 Model comparisons

To facilitate the visual comparison of these models, Figure 6-5 provides an overview of all the travel time series produced by the proposed GM model, the instantaneous model, and time slice model on Rows 1, 2 and 3 respectively:

1) Column (a) shows the travel time series produced by each model;

2) Column (b) shows the smoothed travel times using the moving average method;

3) Column (c) shows the comparisons between the estimated and the ground truth travel times.

As Figure 6-4(a) shows, the estimated travel time exhibits much the same increasing trend as that in the ground truth travel time, with only minor differences. Figures 6-4 (b) and (c) show that the travel time profiles estimated by both instantaneous and time slice models also follow the same increasing trend as the ground truth travel time profile. However, the differences for these two models are relatively larger than that shown in Figure 6-4(a), which indicates that both the instantaneous and time slice models tend to underestimate travel times.

Some time lag was observed between the estimated and ground truth travel times, as shown in Figures 6-4 and 6-5. This time lag is present in not only the results of the proposed model but also in the results of the other two models. This might be because none of the models

are time-dependent travel time models, meaning that no speed is predicted along the corridor. These models estimate travel time only, based on the current conditions. On the other hand, the ground truth travel time data is time-dependent because the travel time is recorded when the identified vehicle actually finishes the trip along the corridor.

Table 6-9 shows a quantitative comparison of the results of all three models. Overall, the proposed model outperforms both the instantaneous and time slice models. In the cases of Corridors#2 and #3, the proposed GM method significantly outperforms the other two models, although in the case of Corridor#1, the proposed model is slightly (0.08%) less accurate than the other two models. Moreover, all the MAPEs are very small (less than 2%). These small differences are likely to be caused by random errors.

FIGURE 6-5 Overview of Model Comparisons

Table 6-9 Quantitative Comparison between the Ground Truth and Estimated Travel Times

Corridors	Time Period	Length		MAE (seconds)	MAPE (%)
Corridor#1 (Free flow condition)	07:00 AM ~ 08:00 AM Dec. 12, 2014, Friday	7.2 miles	Proposed model	8.2	1.88%
			Instantaneous model	8	1.81%
			Time Slice model	8	1.81%
Corridor #2 (Congested condition)	07:50 AM ~ 08:50 AM Dec., 16, 2014, Tuesday	3.7 miles	Proposed model	31	8.49%
			Instantaneous model	100	23.62%
			Time Slice model	100	23.62%
Corridor #3 (Congested condition)	07:00 AM ~ 08:00 AM Dec. 12, 2014, Friday	7.2 miles	Proposed model	63.7	17%
			Instantaneous model	105.7	26.4%
			Time Slice model	105.7	26.4%

Section 7 Case Studies

7.1 Case study #1: Performance Measurement on Major Routes

Now that the system has been expanded to cover all major freeway corridors in St. Louis for Phase 2, the project team has been able to apply the proposed travel time estimation model to all the major corridors in the St. Louis District, covering the stretches of I-44, I-55, I-64, I-70, I-255, I-170 and I-270 that fall within the Greater St. Louis area.

Figures 7-1 and 7-2 show the (average) travel time profiles and (average) speed heat maps on these five major corridors, including I-44 Westbound, I-55 Southbound, I-64 Westbound, I-70 Westbound, I-170 Southbound and I-270 Northbound, for the period from 6 am ~ 8 pm on Sept. 24, 25, and 26, 2013. The figures also show the daily travel time patterns for all the major freeway corridors in St. Louis.

Due to the efficiency of the prototype system, the research team was able to investigate some potential issues with the traffic sensor data. For example, several data quality issues have been identified during the course of this project. Figure 5-8(c) shows an example of the "Rte 94" sensor, which was consistently outputting a low speed value; the research team reported this issue to the St. Louis TMC for further investigation. Moreover, the research team has also been able to identify all the traffic sensors that require some attention (listed in Appendix I).

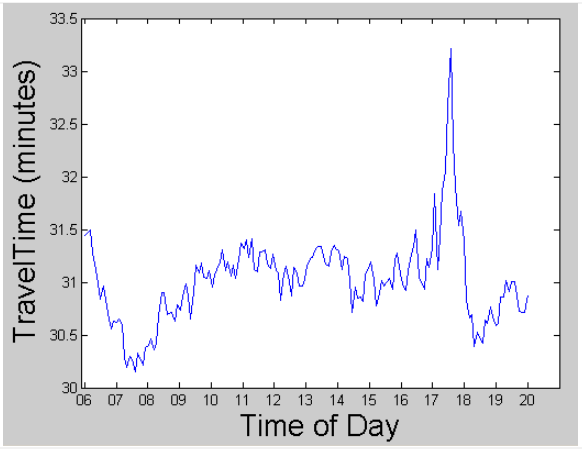

(a) Travel Time Profile (I-44 Westbound)

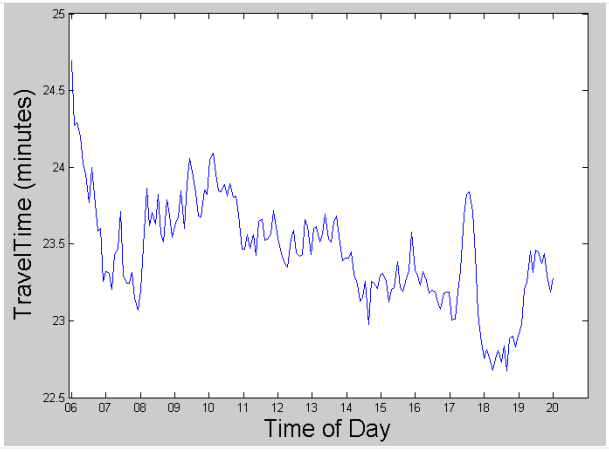

(b) Travel Time Profile (I-55 Southbound)

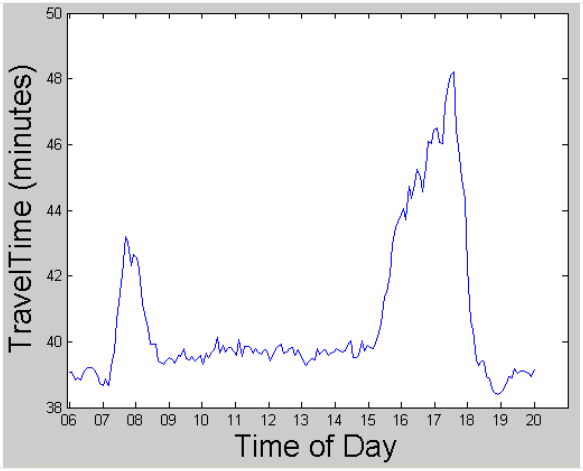

(c) Travel Time Profile (I-64 Westbound)

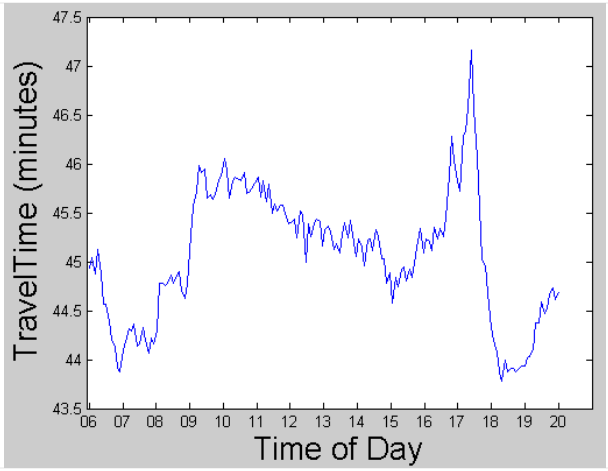

(d) Travel Time Profile (I-70 Westbound)

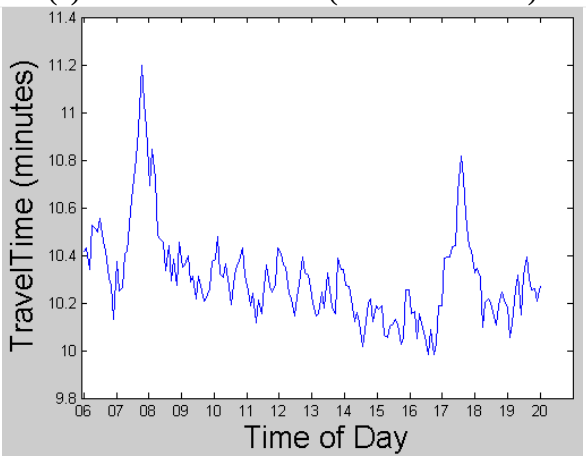

(e) Travel Time Profile (I-170 Southbound)

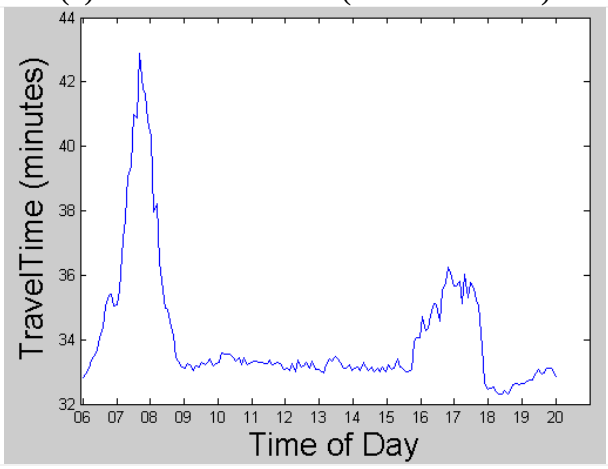

(f) Travel Time Profile (I-270 Northbound)

FIGURE 7-1 Travel time profiles for I-44, I-55, I-64, I-70, I-170 and I-270

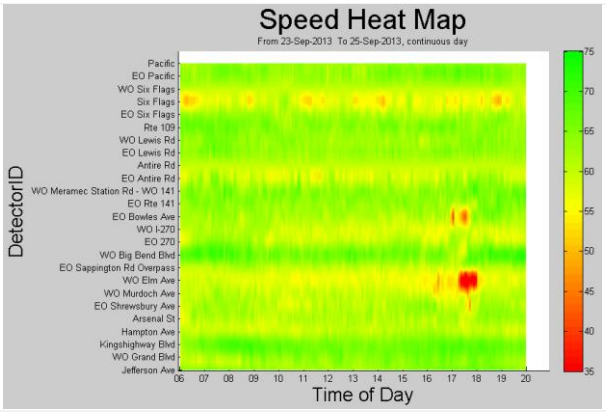

(a) Speed Heat Map (I-44 Westbound)

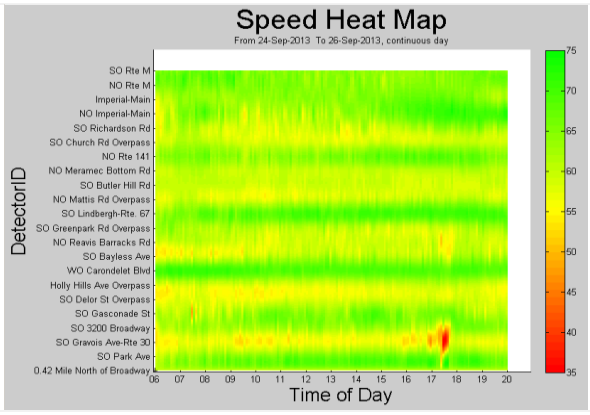

(b) Speed Heat Map (I-55 Southbound)

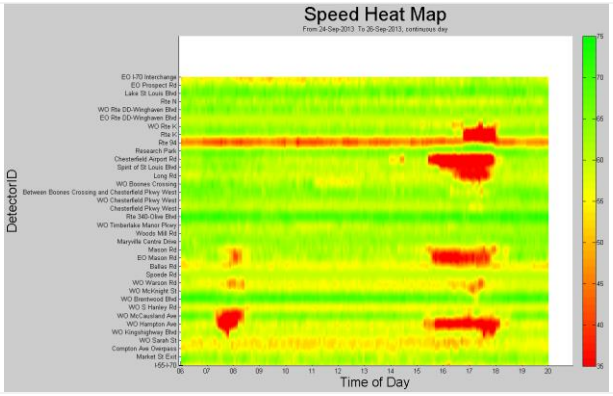

(c) Speed Heat Map (I-64 Westbound)

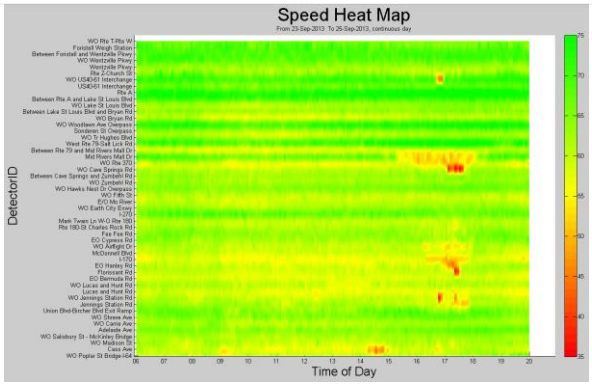

(d) Speed Heat Map (I-70 Westbound)

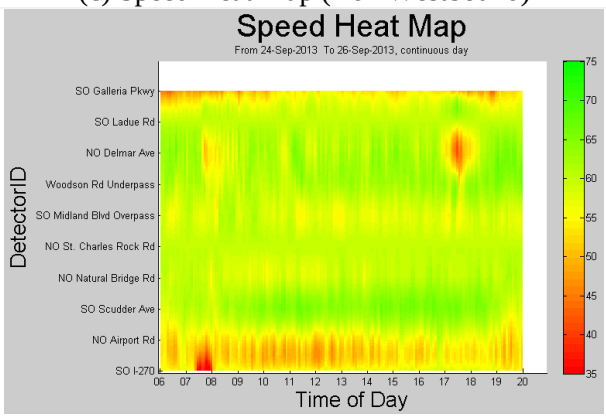

(e) Speed Heat Map (I-170 Southbound)

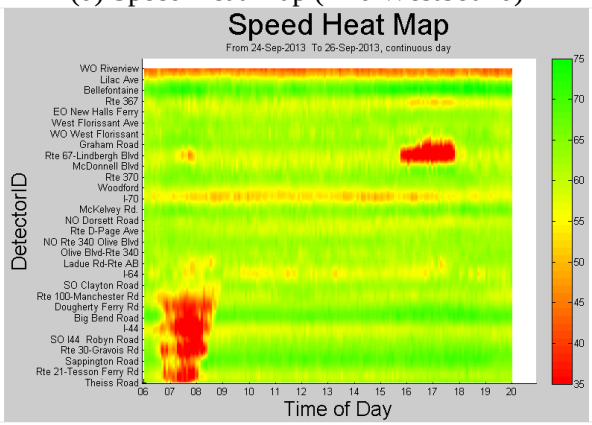

(f) Speed Heat Map (I-270 Northbound)

FIGURE 7-2 Speed heat maps for I-44, I-55, I-64, I-70, I-170 and I-270

7.2 Case study #2: Performance Measurement for a Freeway Corridor with a Turning Junction

According to the results in Section 6.2, the proposed model may not be able to fully capture the congestion at a freeway junction. Nevertheless, the model was able to estimate the travel time accurately on those freeway corridors without a turning junction. The results of the case study indicate that although the proposed model can indeed capture the congestion along the corridor the resulting travel times are likely to be underestimated. One potential solution is to add one more sensor between sensors to increase travel time estimation accuracy.

The two selected freeway corridors that include a junction are: Corridor 1: from I-64 Westbound to I-170 Northbound, and Corridor 2: from I-170 Northbound to I-70 Westbound, shown in Figures 7-3 (a) and (b), respectively. The travel time profiles and speed heat maps generated for the two segments are shown in Figures 7-3 (c) ~ (f). These results indicate that the proposed system is again capable of capturing the impact of congestion (vehicle delay), but as before, the estimated travel time is likely to be underestimated at freeway junctions due to the

limited number of traffic sensors. Therefore, it is reasonable to assume that the actual travel time will be higher than the estimated travel time shown in Figures 7-3 (c) and (d).

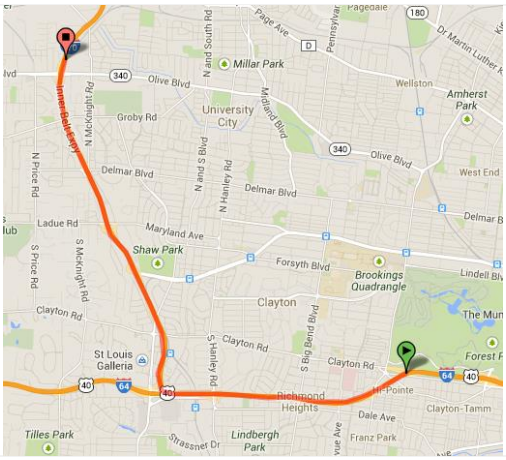

(a) Corridor-1 (from I-64WB to I-70NB)
(Total length: 6.68 miles)

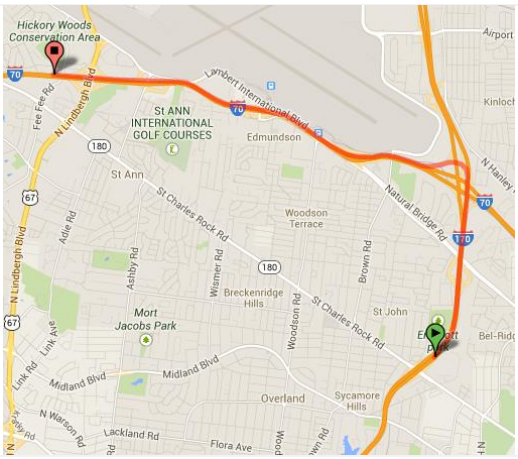

(b) Corridor-2 (from I-70NB to I-170WB)
(Total length: 6.75 miles)

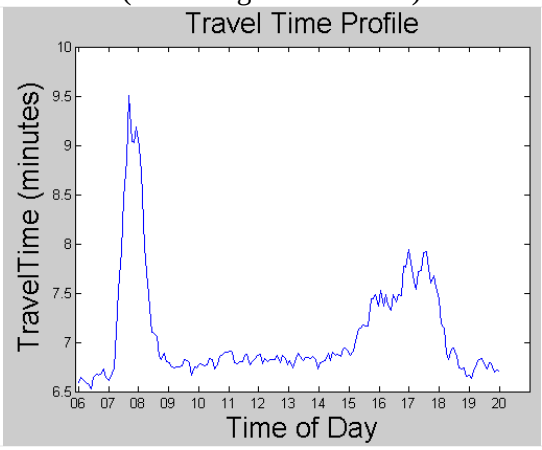

(c) Travel time for Segment 1

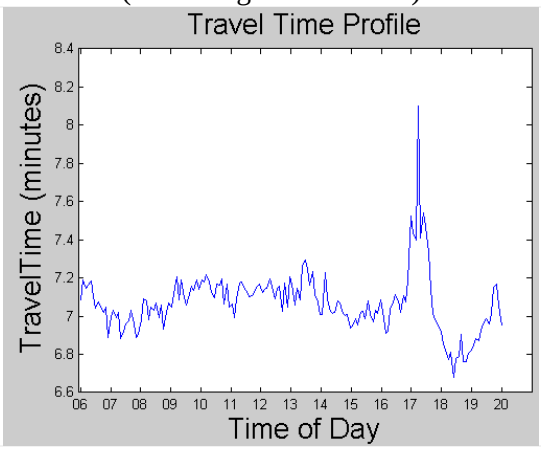

(d) Travel time for Segment 2

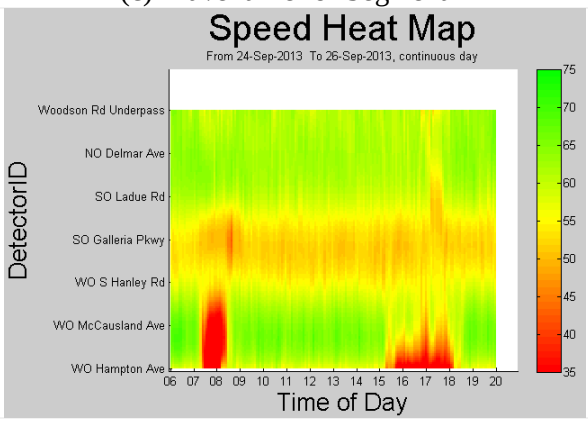

(e) Speed heat map for Corridor 1

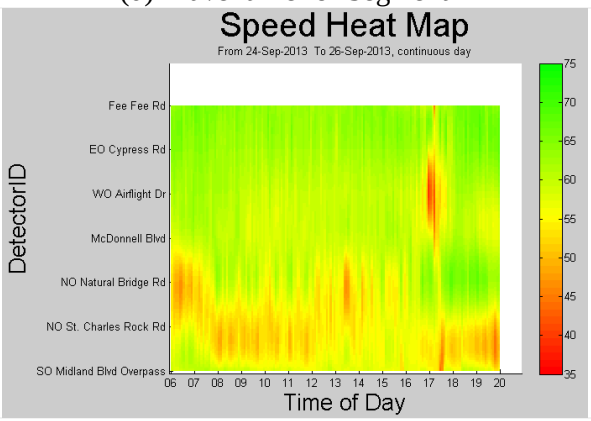

(f) Speed heat map for Corridor 2

FIGURE 7-3 Corridor travel time estimation (with a junction)

7.3 Case Study #3: Impact of Severe Weather Event on Traffic Volume

This case study is designed to evaluate the "Traffic Volume Report Production" module of the travel time prototype system. This module enables traffic engineers to query daily traffic volume more conveniently.

The Greater St. Louis area suffered from a major snowstorm on Jan 5th, 2014, followed by light snow events on Jan 6th and Jan 9th, 2014. Table 7-1 summarizes the weather conditions from Jan 5th to Jan 11th, 2014. The freeway performance was clearly impacted due to these weather events. In order to quantify the impact of a major snowstorm on the freeway system, especially the travel time and traffic volume on the freeway network, the project team used the proposed system to quantify the effect of the snowstorm on traffic volume. Two measures, Average Daily Traffic (ADT) and Daily Traffic (DT) were calculated using the traffic data collected at 10 traffic sensors along I-170 SB. The ADT information was then calculated based on all the data collected 24/7 throughout the entire month of September, 2013, when no significant weather-related events occurred and compared with the DT info calculated based on the data collected during the affected days, Jan 5th and Jan 6th, 2014.

Table 7-2 shows the impact of the snowstorm on traffic volume along the study corridor. Reductions of around 63.4% and 36.9% in traffic volume were observed on January 5th and 6th, 2014, respectively, compared to the ADT calculated for September, 2013.

Table 7-1 Weather Conditions (Jan. 5th, ~ Jan. 11th, 2014)

Date	Average Visibility (miles)	Weather Conditions	Graphical Representation
Jan 5th, 2014	0.2	Heavy Snow	
Jan 6th, 2014	10	Blowing Snow	
Jan 7th, 2014	10	Partly Cloudy	
Jan 8th, 2014	10	Mostly Cloudy	
Jan 9th, 2014	2.5	Light Snow	
Jan 10th, 2014	4	Light Rain	
Jan 11th, 2014	10	Mostly Cloudy	

Table 7-2 Impact of Snowstorm on Traffic Volume

Traffic Sensor Name and (ID)	Average Daily Traffic (September 2013)	Jan 5th, 2014 (Snowstorm Day)		Jan 6th, 2014	
		Daily Traffic (vehicles)	Volume Reduction*	Daily Traffic (vehicles)	Volume Reduction*
SO Galleria Pkwy (MI170S000.3U)	4494	3006	33.11%	3845	14.44%
SO Ladue Rd (MI170S001.5U)	29047	11757	59.52%	27834	4.18%
NO Delmar Ave (MI170S002.6U)	47411	12011	74.67%	25764	45.66%
Woodson Rd Underpass (MI170S003.8U)	48298	11989	75.18%	26397	45.35%
SO Midland Blvd Overpass (MI170S005.0U)	52617	15081	71.34%	30329	42.36%
NO St. Charles Rock Rd (MI170S006.2U)	27601	15940	42.25%	15793	42.78%
NO Natural Bridge Rd (MI170S007.2U)	52574	15793	69.96%	28990	44.86%
SO Scudder Ave (MI170S008.3U)	47759	17817	62.69%	40077	16.09%
NO Airport Rd (MI170S009.5U)	35916	11831	67.06%	23813	33.70%
SO I-270 (MI170S010.5U)	34210	7395	78.38%	14742	56.91%
Average			63.4%		36.9%

* The traffic volume reduction percentage is calculated by: $\frac{ADT - DT}{ADT} * 100\%$.

7.4 Case study #4: Travel Time Reliability Evaluation

Even though travel time is one of the most important freeway and arterial performance measures, travel time estimation might not truly represent road users' experiences on freeways. As part of the effort to address this discrepancy, travel time reliability has emerged as a new, potentially more representative, indicator of roadway performance, receiving a great deal of attention from both practitioners and researchers.

The major challenge facing travel time reliability studies is the need to collect a large volume of travel time data to create accurate travel time distributions. Due to the efficiency of the proposed travel time estimation prototype system, a huge amount of travel time data can be quickly calculated and generated. Given the ready availability of this real-life travel time data, Yang et al. (2014) took advantage of the travel time data generated in the proposed system and developed a new methodology to investigate travel time reliability issues. The non-parametric technique of kernel density estimation (KDE) was proposed to estimate the travel time distribution given a specific day of the week (DOW) and time of day (TOD). Figure 7-4 shows two study corridors on I-64 Westbound and Figure 7-5 shows the corresponding travel time distributions developed using our data. Due to the high efficiency of the travel time data generation, Yang et al. were able to generate accurate travel time distributions within an hour. Since travel time reliability is outside the scope of the present project, more details of this achievement can be found in Yang et al. (2014).

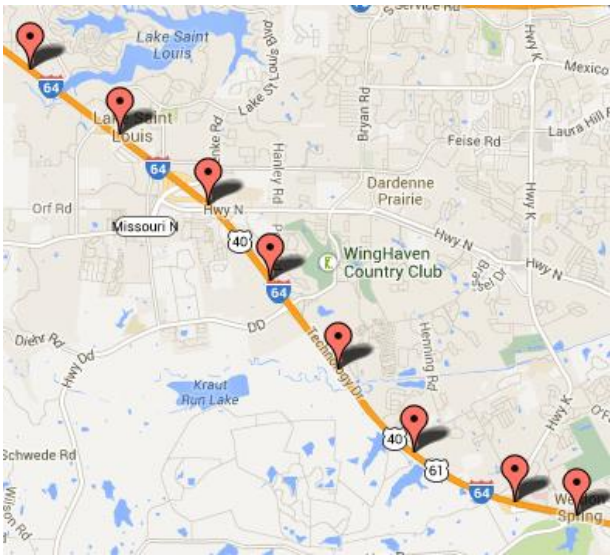

(a) Segment-1: I-64 westbound from Highway K to Prospect Road (8.02 miles) (b) Segment-2: I-64 westbound from Chesterfield Parkway to Research Park Drive (6.8 miles)

FIGURE 7-4 Study segments on I-64 Westbound (Yang et al., 2014)
(Background image has been retrieved from https://maps.google.com/).

Segment-1

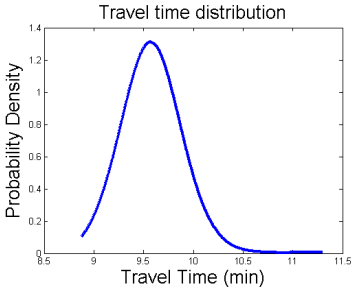

Mon., TOD = 9 a.m.
(1-a)

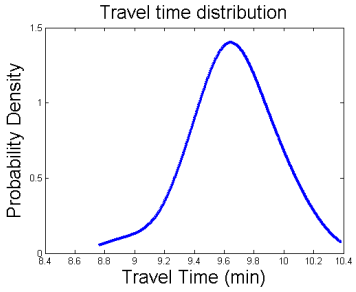

Tues., TOD = 9 a.m.
(1-b)

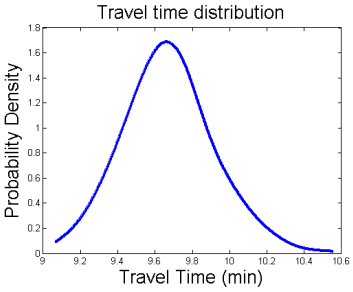

Wed., TOD = 9 a.m.
(1-c)

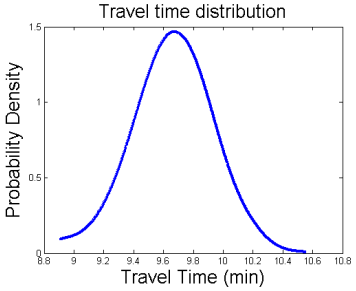

Thurs., TOD = 9 a.m.
(1-d)

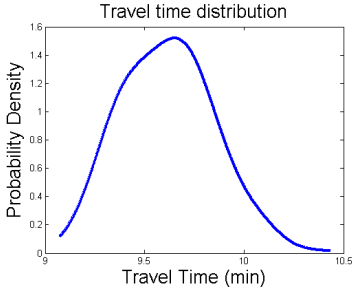

Fri., TOD = 9 a.m.
(1-e)

Segment-2

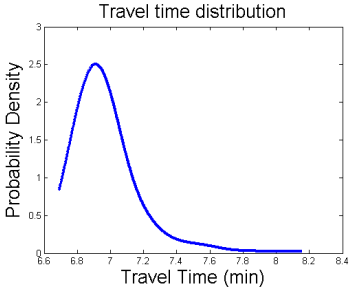

Mon., TOD = 9 a.m.
(2-a)

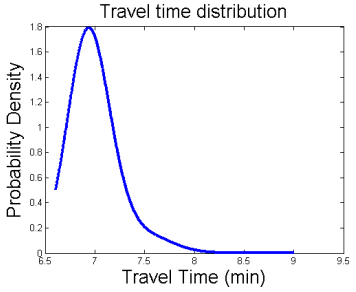

Tues., TOD = 9 a.m.
(2-b)

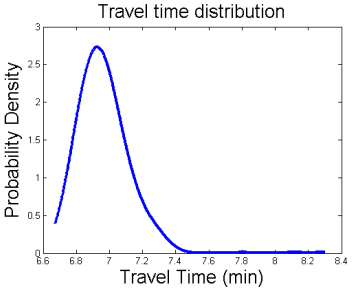

Wed., TOD = 9 a.m.
(2-c)

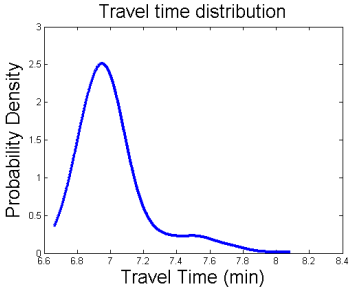

Thurs., TOD = 9 a.m.
(2-d)

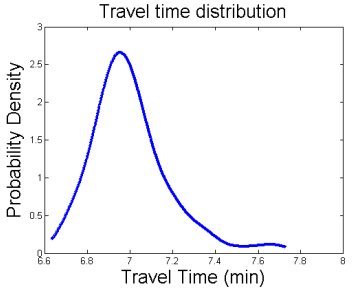

Fri., TOD = 9 a.m.
(2-e)

TOD = 9 a.m.

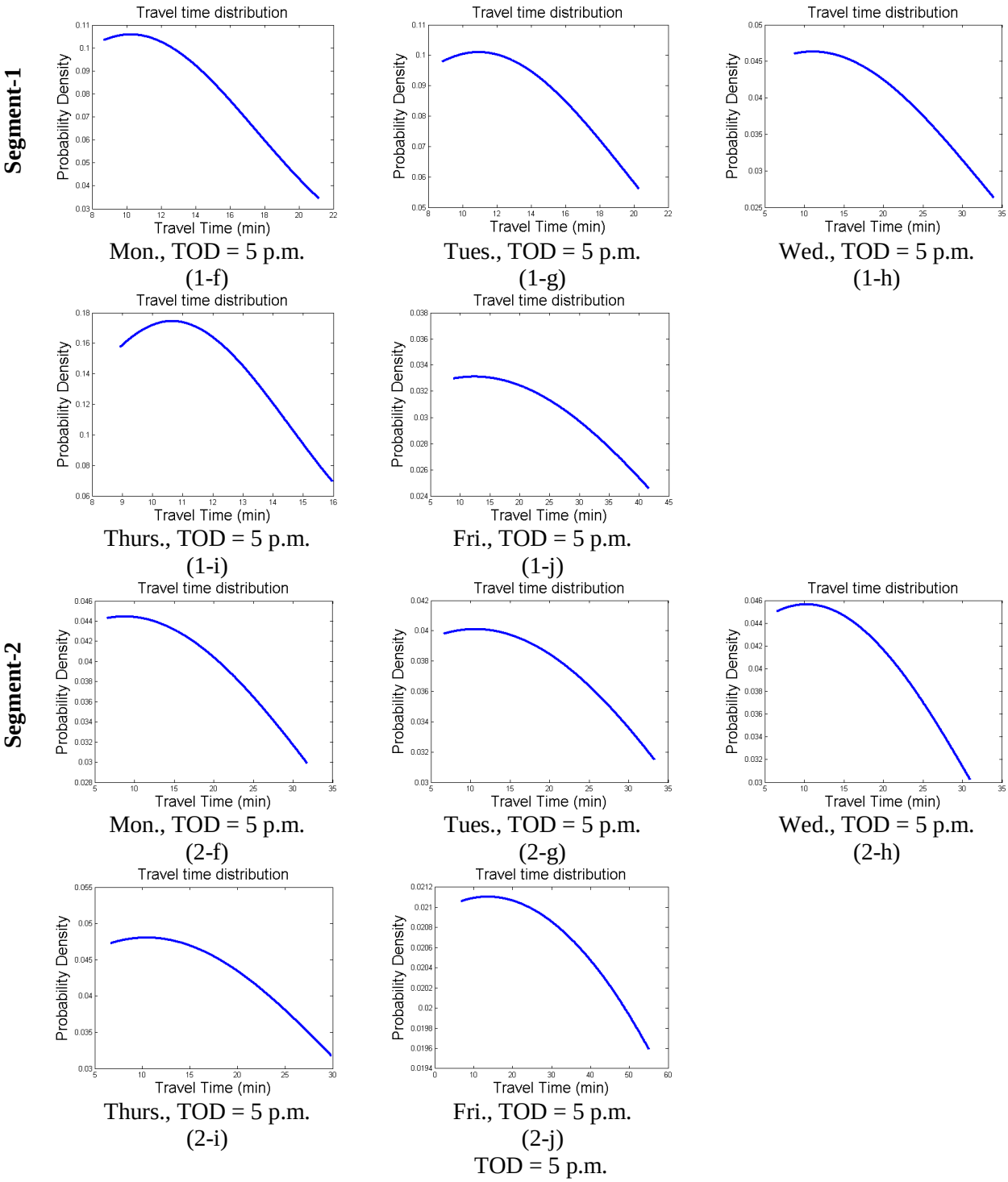

FIGURE 7-5 Travel time distributions estimated by KDE (Yang et al., 2014)

Section 8 Conclusions and Recommendations

8.1 Conclusions

The main goal of Phase II was to expand the functionality of the travel time estimation prototype system developed in Phase I to cover all the major freeways passing through St. Louis, MO (I-44, I-55, I-64, I-70, I-255, I-170 and I-270). The system is designed to facilitate processing the traffic data collected from existing traffic sensors. The new system has the potential to provide a highly useful freeway data analytics platform for the staff at Gateway Guide, the TMC in the MoDOT St. Louis District. The finished tasks of the project can be summarized as follows:

1) An innovative travel time estimation method based on a car-following model has been proposed by this project. The conventional travel time estimation models (i.e. the instantaneous model, and the time slice model) both suffer from significant difficulties in estimating accurate travel times in heavily congested traffic conditions. The verification procedure revealed that the proposed model was able to estimate more accurate travel times for congested conditions. It was mathematically proved that the proposed travel time estimation model outperforms the two earlier methods.
2) To facilitate ground truth travel time collection from traffic surveillance cameras, a new vision-based Vehicle Re-identification (VRI) algorithm has been proposed. The work was particularly challenging because of the low-resolution videos captured by the existing traffic surveillance cameras. The contribution of this work includes setting up a complete vehicle detection and feature extraction system that is capable of dealing with low quality vehicle images. By considering VRI as a classification and mapping problem, a Support Vector Machine (SVM) and linear programming were adopted to solve the vehicle matching problem. The approach was tested for two cases: one for a freeway segment with no entrances or exits and the other for a freeway segment with one exit. The re-identification F-scores for the two cases were found to be about 68% and 57%, respectively. The results are satisfying because the method would be able to provide sufficient samples for travel time verification. .
3) The newly developed travel time estimation method was then implemented in a prototype travel time estimation system which allows users to query point-to-point network travel times for specific times and dates. The system consists of four

modules: 1) travel time estimation for a freeway corridor with no turning junction, 2) travel time estimation for a stretch of freeway that includes a turning junction, 3) data assurance report production and 4) traffic volume report production.

4) Two case scenarios were selected for model verification consisting of a freeway corridor both with and without a turning junction. These scenarios must be treated differently because freeway junctions generally have far fewer sensors installed. As expected, the results showed that it remains fairly challenging to accurately estimate the true travel time at a freeway junction because variations in the traffic conditions cannot be easily captured by the upstream and downstream traffic sensors. In contrast, travel time estimation is fairly robust on a freeway corridor with no turning junction.
5) To demonstrate the effectiveness and efficiency of the proposed system, four case studies were conducted: 1) performance measurement on major routes, 2) performance measurement for a freeway corridor with a turning junction, 3) the impact of a severe weather event on traffic volume, and 4) travel time reliability evaluation.
6) The research team conducted comprehensive travel time analysis on all major freeways on February 26th, 2014. During the analysis process, 35 sensors were identified as "needing attention". The prototype system also proved to be a useful tool for investigating data quality.

8.2 Recommendations

The research team successfully achieved all the project objectives. It is hoped that the following suggestions will provide MoDOT with ideas to improve the accomplished work and potentially useful directions for future research:

- The research results showed that it was very challenging to accurately estimate travel time at freeway junctions. This is likely due to the almost total lack of sensors installed along the freeway junctions themselves (between two fixed traffic sensors), which made it difficult for the proposed model to estimate traffic between the two fixed sensors. There are three potential solutions that could improve the accuracy of travel time estimation at freeway junctions:

    - Install additional sensors at turning junctions
    - Use a different type of detector, e.g. Bluetooth detectors, to increase the data collection coverage
    - Use third party data (e.g. the HERE dataset) and data fusion approaches to increase accuracy

- The MoDOT is currently able to access the probe vehicle data provided by HERE. It is very likely that these results would be improved if this additional data source could be incorporated into the proposed method. In the meantime, it would be also interesting to compare the estimated travel time with that recorded in the probe vehicle dataset. Although the proposed vision-based Vehicle Re-identification (VRI) method provides satisfying results, the process of obtaining a training dataset is very time-consuming. Potential solutions could be: 1) VRI could be implemented by a high-performance computer language (e.g. C++); and/or 2) additional data classification methods could be selected for further testing to obtain a better balance between computation efficiency and matching rate.
- Besides installing additional sensors, the proposed travel time estimation model could be further calibrated to better estimate travel times in various future scenarios. Additional parameters, e.g. headway, traffic volume and vehicle classification could potentially be included in the model to increase estimation accuracy.
- At present, the proposed travel time estimation prototype system is more easily operated by a researcher than by a traffic engineer. Therefore, the prototype system still has room for improvement. In terms of system improvement, the following suggestions could be helpful:
    - Improve the user interface design to enhance the usability of the system.
    - Implement the system on a web-based platform instead of a standalone application so MoDOT staff can save their effort to pre-process the traffic data and maintain the research database.
- During the project, the research team found the dataset provided by the existing fixed sensors can not only be used for travel time estimation but also has the potential to open up new applications because in addition to speed and traffic volume, these fixed traffic

sensors also contain other useful information such as vehicle classification data. Moreover, the prototype system was designed to expand its functionality with minimal future effort. The list of preliminary ideas shown below can also be accomplished by the prototype system with only a relatively small additional effort in computer coding:

- Impact of heavy vehicles on travel time
- Investigate the relationship between traffic throughput and travel time for traffic control strategy development and congestion management
- Freeway Level of service monitoring based on the Highway Capacity Manual (HCM) method (TRB, 2010).
- Data-driven integrated corridor management
- Real-time/historical incident impact analysis
- Work zone analysis

- For "needing attention" sensors, potential solutions could be:
  - Collect feedback regularly from data users (e.g. MoDOT traffic studies staff, universities and research institutes)
  - Develop a data monitoring module in our database to consistently monitoring data qualify
  - Develop a software-based self-correction method to correct the erroneous data once the error is identified by the data monitoring module

References

Cetin, M., & A. P. Nichols. (2009). Improving the Accuracy of Vehicle Reidentification Algorithms by Solving the Assignment Problem. *In Transportation Research Record: Journal of the Transportation Research Board, No. 2129,Transportation Research Board of the National Academies, Washington, D.C., 2009,* pp. 1–8.

Cormen, T. H., Leiserson, C. E., Rivest, R. L., & Stein, C. (2009). *Introduction to Algorithms* (3rd ed., p. 1312). MIT Press.

Cortés, C. E., Lavanya, R., Oh, J., & Jayakrishnan, R. (2002). General-Purpose Methodology for Estimating Link Travel Time with Multiple-Point Detection of Traffic. *Transportation Research Record: Journal of the Transportation Research Board*, *1802*(2002), 181–189. doi:10.3141/1802-20

Dailey, D.(1993). Travel-time estimation using cross-correlation techniques. *Transportation Research Part B, 27*(2), 97–107.

Dailey, D. J. (1997). Travel Time Estimates Using a Series of Single Loop Volume and Occupancy Measurements. In *Transportation Research Board 76th Annual Meeting* (p. 14). doi:10.1.1.141.1613

Dalal, N, & Triggs, B. (2005). Histograms of Oriented Gradients for Human Detection, *In Computer Vision and Pattern Recognition, 2005*.

Felzenszwalb, P. F., & Huttenlocher, P. D. (2004). Efficient Graph-based Image Segmentation. *In International Journal of Computer Vision, 2004,* pp. 167-181.

Finlayson, G, & Xu, R. (2002). *Non-iterative Comprehensive Normalisation. In Conference on Colour in Graphics, Imaging, and Vision, 2002*.

Guo, Z, Zhang, L, & Zhang, D. (2010). A Completed Modeling of Local Binary Pattern Operator for Texture Classification, *In IEEE Transactions on Image Process, 2010,* pp. 1657–1663.

Hou, T, Wang, S., & Qin, H. (2009). Vehicle Matching and Recognition Under Large Variations of Pose and Illumination. *In Computer Vision and Pattern Recognition Workshops, 2009*, pp. 290–295.

Jiang, W.(2013). Vehicle Tracking with Non-overlapping Views for Multi-camera Surveillance System. *In High Performance Computing and Communications & 2013 IEEE International Conference on Embedded and Ubiquitous Computing, 2013*.

Kamijo, S., Kawahara, T. & Sakauchi, M. (2005). Vehicle Sequence Image Matching for Travel Time Measurement Between Intersections. *In IEEE International Conference on Systems Systems, Man and Cybernetics, 2005*, pp. 1359–1364.

Kanhere, N. K., S. T. Birchfield, W. A. Sarasua, and T. C. Whitney. (1993). Real-Time Detection and Tracking of Vehicle Base Fronts for Measuring Traffic Counts and Speeds on Highways. *In Transportation Research Record: Journal of the Transportation Research Board, No. 1993,Transportation Research Board of the National Academies, Washington, D.C., 2007,* pp. 155–164.

Lowe, D.G. (2004). Distinctive Image Features From Scale-invariant Keypoints. *In International journal of computer vision, 2004,* pp. 91-110.

Mukkamala, S., & Sung, H. A. (2003). Feature Selection for Intrusion Detection with Neural Networks and Support Vector Machines. *In Transportation Research Record: Journal of the Transportation Research Board, No. 1822, Transportation Research Board of the National Academies, Washington, D.C., 2003,* pp. 33-39.

Ni, D., & Wang, H. (2008). Trajectory Reconstruction for Travel Time Estimation. *Journal of Intelligent Transportation Systems*, *12*(3), 113–125. doi:10.1080/15472450802262307

Ozbay, S., & Ercelebi, E. (2005). Automatic Vehicle Identification by Plate Recognition. *In World Academy of Science, Engineering and Technology, 2005*, pp. 222-225.

Petty, F. K., Bickel, P., Ostland, M., Rice, J., Schoenberg, F., Jiang J., & Ritov, Y. (1998). Accurate estimation of travel times from single-loop detectors. *Transportation Research Part A: Policy and Practice*, *32*(1), 1–17. doi:10.1016/S0965-8564(97)00015-3

Scholkopf, B, & Smola, J. A. (2001). Learning with Kernels: Support Vector Machines, Regularization, Optimization, and Beyond, MIT press, 2001.

Stauffer, C, & W. Eric L. Grimson. (1999). Adaptive Background Mixture Models for Real-time Tracking. *In Computer Vision and Pattern Recognition*, 1999.

Sumalee, A., Wang, J., Jedwanna, K., & Suwansawat, S (2012). Probabilistic Fusion of Vehicle Features for Reidentification and Travel Time Estimation Using Video Image Data. *In Transportation Research Record: Journal of the Transportation Research Board, No. 2308, Transportation Research Board of the National Academies, Washington, D.C., 2012*, pp. 73-82.

Sun, C. C., Arr, G. S., Ramachandran, R. P., & Ritchie, S. G. (2004). Vehicle Reidentification Using Multidetector Fusion, *In IEEE Transactions on Intelligent Transportation Systems, 2004*, pp. 155–164.

Sun, L., Yang, J., & Mahmassani, H. (2008). Travel time estimation based on piecewise truncated quadratic speed trajectory. *Transportation Research Part A: Policy and Practice*, *42*(1), 173–186. doi:10.1016/j.tra.2007.08.004

Tawfik, A. Y., Abdulhai, B., Peng, A. & Tabib M. S.(2004). Using Decision Trees to Improve the Accuracy of Vehicle Signature Reidentification. *In Transportation Research Record:*

Journal of the Transportation Research Board, No. 1886, Transportation Research Board of the National Academies, Washington, D.C., 2004, pp. 24–33.

Torralba, A., Murphy, P. K., & Freeman, T. W. (2004). Sharing Features: Efficient Boosting Procedures for Multiclass Object Detection. *In Computer Vision and Pattern Recognition*, 2004.

van Lint, J. W. C., & van der Zijpp, N. J.(2003). Improving a Travel-Time Estimation Algorithm by Using Dual Loop Detectors. *Transportation Research Record: Journal of the Transportation Research Board, 1855*, 41–48.

Wang, Y., & Nihan, N. L. (2003). Can Single-Loop Detectors Do the Work of Dual-Loop Detectors ? *Journal of Transportation Engineering*, *129*(2), 169–176.

Wang, Y, Velipasalar, S., & Gursoy, C. M. (2011). Wide-area Multi-object Tracking with Non-overlapping Camera Views. *In International Conference on Multimedia and Expo, 2011*.

Wu, Y., Yang, S., & Abdoli, S. (2013). Freeway Travel Time Estimation Using Existing Fixed Traffic Sensors – Phase 1. Retrieved from: http://library.modot.mo.gov/RDT/reports/TR201311/cmr14-008.pdf

Yang, S, Malik, A & Wu, Y (2014). Travel Time Reliability using Hasofer Lind-Rackwitz Fiessler Algorithm and Kernel Density Estimation. *Accepted for publication in Transportation Research Record: Journal of the Transportation Research Board*.

Yin, Z., & Collins, R. (2009). Moving Object Localization in Thermal Imagery by Forward-backward Motion History Images. *In Augmented Vision Perception in Infrared, 2009*, pp.271-291.

Zhang, N, Zhang, Y., & Lu, H. (2011). Seasonal Autoregressive Integrated Moving Average and Support Vector Machine Models. *In Transportation Research Record: Journal of the Transportation Research Board, No. 2215, Transportation Research Board of the National Academies, Washington, D.C., 2011*, pp. 85-92.

Appendix

Appendix I - Traffic sensors identified as needing attention in St Louis

<table>
<tr><th>Freeway</th><th>Direction</th><th>Detector ID</th><th>Screenshot</th></tr>
<tr><td rowspan="4">I-64</td><td rowspan="3">Eastbound</td><td>MI064E017.0D</td><td>
<table>
<tr><th>Date_Time</th><th>DetectorID</th><th>Lane_Speed_1</th><th>Lane_Speed_2</th><th>Lane_Speed_3</th></tr>
<tr><td>2013-09-10 09:24:34.000</td><td>MI064E017.0D</td><td>66</td><td>56</td><td>37</td></tr>
<tr><td>2013-09-10 09:25:04.000</td><td>MI064E017.0D</td><td>66</td><td>55</td><td>37</td></tr>
<tr><td>2013-09-10 09:25:35.000</td><td>MI064E017.0D</td><td>66</td><td>58</td><td>35</td></tr>
<tr><td>2013-09-10 09:26:05.000</td><td>MI064E017.0D</td><td>66</td><td>60</td><td>38</td></tr>
<tr><td>2013-09-10 09:26:36.000</td><td>MI064E017.0D</td><td>67</td><td>62</td><td>40</td></tr>
<tr><td>2013-09-10 09:27:07.000</td><td>MI064E017.0D</td><td>68</td><td>62</td><td>40</td></tr>
<tr><td>2013-09-10 09:27:37.000</td><td>MI064E017.0D</td><td>68</td><td>60</td><td>40</td></tr>
<tr><td>2013-09-10 09:28:08.000</td><td>MI064E017.0D</td><td>66</td><td>59</td><td>37</td></tr>
<tr><td>2013-09-10 09:28:38.000</td><td>MI064E017.0D</td><td>66</td><td>62</td><td>37</td></tr>
<tr><td>2013-09-10 09:29:09.000</td><td>MI064E017.0D</td><td>68</td><td>60</td><td>37</td></tr>
<tr><td>2013-09-10 09:29:40.000</td><td>MI064E017.0D</td><td>68</td><td>63</td><td>37</td></tr>
</table>
</td></tr>
<tr><td>MI064E024.2D</td><td>
<table>
<tr><th>Date_Time</th><th>DetectorID</th><th>Lane_Speed_1</th><th>Lane_Speed_2</th><th>Lane_Speed_3</th></tr>
<tr><td>2013-09-10 09:00:08.000</td><td>MI064E024.2D</td><td>63</td><td>60</td><td>99</td></tr>
<tr><td>2013-09-10 09:00:39.000</td><td>MI064E024.2D</td><td>63</td><td>58</td><td>99</td></tr>
<tr><td>2013-09-10 09:01:10.000</td><td>MI064E024.2D</td><td>59</td><td>57</td><td>99</td></tr>
<tr><td>2013-09-10 09:01:40.000</td><td>MI064E024.2D</td><td>62</td><td>60</td><td>99</td></tr>
<tr><td>2013-09-10 09:02:10.000</td><td>MI064E024.2D</td><td>65</td><td>58</td><td>99</td></tr>
<tr><td>2013-09-10 09:02:40.000</td><td>MI064E024.2D</td><td>61</td><td>58</td><td>99</td></tr>
<tr><td>2013-09-10 09:03:11.000</td><td>MI064E024.2D</td><td>68</td><td>62</td><td>99</td></tr>
<tr><td>2013-09-10 09:03:42.000</td><td>MI064E024.2D</td><td>72</td><td>63</td><td>99</td></tr>
<tr><td>2013-09-10 09:04:12.000</td><td>MI064E024.2D</td><td>72</td><td>61</td><td>99</td></tr>
<tr><td>2013-09-10 09:04:43.000</td><td>MI064E024.2D</td><td>76</td><td>63</td><td>99</td></tr>
</table>
</td></tr>
<tr><td>MI064E028.6U</td><td>
<table>
<tr><th>Date_Time</th><th>DetectorID</th><th>Lane_Speed_1</th><th>Lane_Speed_2</th><th>Lane_Speed_3</th><th>Lane_Speed_4</th></tr>
<tr><td>2013-09-10 09:00:08.000</td><td>MI064E028.6U</td><td>43</td><td>65</td><td>54</td><td>0</td></tr>
<tr><td>2013-09-10 09:00:39.000</td><td>MI064E028.6U</td><td>43</td><td>65</td><td>54</td><td>0</td></tr>
<tr><td>2013-09-10 09:01:10.000</td><td>MI064E028.6U</td><td>42</td><td>65</td><td>57</td><td>0</td></tr>
<tr><td>2013-09-10 09:01:40.000</td><td>MI064E028.6U</td><td>42</td><td>65</td><td>57</td><td>0</td></tr>
<tr><td>2013-09-10 09:02:10.000</td><td>MI064E028.6U</td><td>40</td><td>65</td><td>47</td><td>0</td></tr>
<tr><td>2013-09-10 09:02:40.000</td><td>MI064E028.6U</td><td>40</td><td>65</td><td>47</td><td>0</td></tr>
<tr><td>2013-09-10 09:03:11.000</td><td>MI064E028.6U</td><td>41</td><td>55</td><td>45</td><td>0</td></tr>
<tr><td>2013-09-10 09:03:42.000</td><td>MI064E028.6U</td><td>41</td><td>55</td><td>45</td><td>0</td></tr>
<tr><td>2013-09-10 09:04:12.000</td><td>MI064E028.6U</td><td>44</td><td>55</td><td>46</td><td>0</td></tr>
<tr><td>2013-09-10 09:04:43.000</td><td>MI064E028.6U</td><td>44</td><td>55</td><td>46</td><td>0</td></tr>
<tr><td>2013-09-10 09:05:13.000</td><td>MI064E028.6U</td><td>42</td><td>50</td><td>47</td><td>0</td></tr>
<tr><td>2013-09-10 09:05:43.000</td><td>MI064E028.6U</td><td>42</td><td>50</td><td>47</td><td>0</td></tr>
</table>
</td></tr>
<tr><td>MI064E029.7U</td><td>
<table>
<tr><th>Date_Time</th><th>DetectorID</th><th>Lane_Speed_1</th><th>Lane_Speed_2</th><th>Lane_Speed_3</th><th>Lane_Speed_4</th></tr>
<tr><td>2013-09-10 09:00:08.000</td><td>MI064E029.7U</td><td>51</td><td>62</td><td>57</td><td>0</td></tr>
<tr><td>2013-09-10 09:00:39.000</td><td>MI064E029.7U</td><td>51</td><td>62</td><td>57</td><td>0</td></tr>
<tr><td>2013-09-10 09:01:10.000</td><td>MI064E029.7U</td><td>48</td><td>64</td><td>54</td><td>0</td></tr>
<tr><td>2013-09-10 09:01:40.000</td><td>MI064E029.7U</td><td>48</td><td>64</td><td>54</td><td>0</td></tr>
<tr><td>2013-09-10 09:02:10.000</td><td>MI064E029.7U</td><td>48</td><td>66</td><td>56</td><td>0</td></tr>
<tr><td>2013-09-10 09:02:40.000</td><td>MI064E029.7U</td><td>48</td><td>66</td><td>56</td><td>0</td></tr>
<tr><td>2013-09-10 09:03:11.000</td><td>MI064E029.7U</td><td>46</td><td>66</td><td>57</td><td>0</td></tr>
<tr><td>2013-09-10 09:03:42.000</td><td>MI064E029.7U</td><td>46</td><td>66</td><td>57</td><td>0</td></tr>
<tr><td>2013-09-10 09:04:12.000</td><td>MI064E029.7U</td><td>45</td><td>66</td><td>63</td><td>0</td></tr>
<tr><td>2013-09-10 09:04:43.000</td><td>MI064E029.7U</td><td>45</td><td>66</td><td>63</td><td>0</td></tr>
<tr><td>2013-09-10 09:05:13.000</td><td>MI064E029.7U</td><td>45</td><td>61</td><td>57</td><td>0</td></tr>
</table>
</td></tr>
<tr><td>Westbound</td><td>MI064W010.0D</td><td>
<table>
<tr><th>Date_Time</th><th>DetectorID</th><th>Lane_Speed_1</th><th>Lane_Speed_2</th><th>Lane_Speed_3</th></tr>
<tr><td>2013-09-10 09:00:08.000</td><td>MI064W010.0D</td><td>0</td><td>94</td><td>33</td></tr>
<tr><td>2013-09-10 09:00:39.000</td><td>MI064W010.0D</td><td>42</td><td>94</td><td>33</td></tr>
<tr><td>2013-09-10 09:01:10.000</td><td>MI064W010.0D</td><td>42</td><td>94</td><td>33</td></tr>
<tr><td>2013-09-10 09:01:40.000</td><td>MI064W010.0D</td><td>42</td><td>97</td><td>33</td></tr>
<tr><td>2013-09-10 09:02:10.000</td><td>MI064W010.0D</td><td>40</td><td>99</td><td>33</td></tr>
<tr><td>2013-09-10 09:02:40.000</td><td>MI064W010.0D</td><td>40</td><td>93</td><td>33</td></tr>
<tr><td>2013-09-10 09:03:11.000</td><td>MI064W010.0D</td><td>0</td><td>91</td><td>33</td></tr>
<tr><td>2013-09-10 09:03:42.000</td><td>MI064W010.0D</td><td>38</td><td>91</td><td>34</td></tr>
<tr><td>2013-09-10 09:04:12.000</td><td>MI064W010.0D</td><td>40</td><td>91</td><td>34</td></tr>
<tr><td>2013-09-10 09:04:43.000</td><td>MI064W010.0D</td><td>40</td><td>91</td><td>34</td></tr>
<tr><td>2013-09-10 09:05:13.000</td><td>MI064W010.0D</td><td>40</td><td>91</td><td>34</td></tr>
<tr><td>2013-09-10 09:05:43.000</td><td>MI064W010.0D</td><td>40</td><td>90</td><td>34</td></tr>
</table>
</td></tr>
</table>

MI064W012.8D

Date_Time	DetectorID	Lane_Speed_1	Lane_Speed_2	Lane_Speed_3
2013-09-10 09:00:08.000	MI064W012.8D	62	63	45
2013-09-10 09:00:39.000	MI064W012.8D	64	73	45
2013-09-10 09:01:10.000	MI064W012.8D	66	58	45
2013-09-10 09:01:40.000	MI064W012.8D	62	60	45
2013-09-10 09:02:10.000	MI064W012.8D	65	63	45
2013-09-10 09:02:40.000	MI064W012.8D	60	67	42
2013-09-10 09:03:11.000	MI064W012.8D	60	68	42
2013-09-10 09:03:42.000	MI064W012.8D	61	68	40
2013-09-10 09:04:12.000	MI064W012.8D	59	66	40
2013-09-10 09:04:43.000	MI064W012.8D	60	68	42
2013-09-10 09:05:13.000	MI064W012.8D	60	66	0
2013-09-10 09:05:43.000	MI064W012.8D	62	64	40
2013-09-10 09:06:14.000	MI064W012.8D	0	66	0

MI064W015.1D

Date_Time	DetectorID	Lane_Speed_1	Lane_Speed_2	Lane_Speed_3
2013-09-10 09:00:08.000	MI064W015.1D	57	66	37
2013-09-10 09:00:39.000	MI064W015.1D	60	71	36
2013-09-10 09:01:10.000	MI064W015.1D	60	63	36
2013-09-10 09:01:40.000	MI064W015.1D	57	61	36
2013-09-10 09:02:10.000	MI064W015.1D	58	66	34
2013-09-10 09:02:40.000	MI064W015.1D	58	63	34
2013-09-10 09:03:11.000	MI064W015.1D	0	68	33
2013-09-10 09:03:42.000	MI064W015.1D	0	62	32
2013-09-10 09:04:12.000	MI064W015.1D	60	66	32
2013-09-10 09:04:43.000	MI064W015.1D	60	67	32
2013-09-10 09:05:13.000	MI064W015.1D	60	66	0

MI064W015.9D

Date_Time	DetectorID	Lane_Speed_1	Lane_Speed_2	Lane_Speed_3
2013-09-10 09:00:08.000	MI064W015.9D	68	62	42
2013-09-10 09:00:39.000	MI064W015.9D	71	65	42
2013-09-10 09:01:10.000	MI064W015.9D	70	64	42
2013-09-10 09:01:40.000	MI064W015.9D	69	66	40
2013-09-10 09:02:10.000	MI064W015.9D	71	63	39
2013-09-10 09:02:40.000	MI064W015.9D	71	62	39
2013-09-10 09:03:11.000	MI064W015.9D	73	65	38
2013-09-10 09:03:42.000	MI064W015.9D	75	71	35
2013-09-10 09:04:12.000	MI064W015.9D	76	61	35
2013-09-10 09:04:43.000	MI064W015.9D	76	62	40
2013-09-10 09:05:13.000	MI064W015.9D	75	70	40
2013-09-10 09:05:43.000	MI064W015.9D	75	68	40

MI064W038.3U

Date_Time	DetectorID	Lane_Speed_1	Lane_Speed_2	Lane_Speed_3
2013-09-10 09:00:08.000	MI064W038.3U	43	61	53
2013-09-10 09:00:39.000	MI064W038.3U	43	61	53
2013-09-10 09:01:10.000	MI064W038.3U	40	57	58
2013-09-10 09:01:40.000	MI064W038.3U	40	57	58
2013-09-10 09:02:10.000	MI064W038.3U	40	60	48
2013-09-10 09:02:40.000	MI064W038.3U	40	60	48
2013-09-10 09:03:11.000	MI064W038.3U	43	57	49
2013-09-10 09:03:42.000	MI064W038.3U	43	57	49
2013-09-10 09:04:12.000	MI064W038.3U	41	63	47
2013-09-10 09:04:43.000	MI064W038.3U	41	63	47

I-70 — Eastbound

MI070E221.4D

Date_Time	DetectorID	Lane_Speed_1	Lane_Speed_2	Lane_Speed_3	Lane_Speed_4
2013-09-10 09:34:13.000	MI070E221.4D	65	41	49	59
2013-09-10 09:34:44.000	MI070E221.4D	65	42	48	59
2013-09-10 09:35:15.000	MI070E221.4D	65	40	50	60
2013-09-10 09:35:46.000	MI070E221.4D	66	40	47	60
2013-09-10 09:36:16.000	MI070E221.4D	66	39	51	56
2013-09-10 09:36:47.000	MI070E221.4D	66	39	48	62
2013-09-10 09:37:17.000	MI070E221.4D	66	39	47	57
2013-09-10 09:37:48.000	MI070E221.4D	69	42	50	58
2013-09-10 09:38:18.000	MI070E221.4D	71	40	53	62
2013-09-10 09:38:49.000	MI070E221.4D	73	42	53	60
2013-09-10 09:39:20.000	MI070E221.4D	73	45	51	60

MI070E227.2D

Date_Time	DetectorID	Lane_Speed_1	Lane_Speed_2	Lane_Speed_3
2013-09-10 09:41:22.000	MI070E227.2D	60	65	42
2013-09-10 09:41:52.000	MI070E227.2D	60	62	42
2013-09-10 09:42:23.000	MI070E227.2D	62	64	44
2013-09-10 09:42:54.000	MI070E227.2D	60	66	41
2013-09-10 09:43:24.000	MI070E227.2D	60	66	41
2013-09-10 09:43:55.000	MI070E227.2D	60	65	45
2013-09-10 09:44:25.000	MI070E227.2D	57	65	43
2013-09-10 09:44:56.000	MI070E227.2D	57	64	47
2013-09-10 09:45:26.000	MI070E227.2D	57	65	47
2013-09-10 09:45:57.000	MI070E227.2D	57	63	47
2013-09-10 09:46:27.000	MI070E227.2D	58	64	43
2013-09-10 09:46:58.000	MI070E227.2D	59	64	40

MI070E229.6D

Date_Time	DetectorID	Lane_Speed_1	Lane_Speed_2	Lane_Speed_3	Lane_Speed_4	Lane_Speed_5
2013-09-10 09:00:08.000	MI070E229.6D	62	57	66	57	-1
2013-09-10 09:00:39.000	MI070E229.6D	65	58	65	58	-1
2013-09-10 09:01:10.000	MI070E229.6D	68	54	68	59	-1
2013-09-10 09:01:40.000	MI070E229.6D	68	53	58	58	-1
2013-09-10 09:02:10.000	MI070E229.6D	65	57	60	57	-1
2013-09-10 09:02:40.000	MI070E229.6D	66	59	65	60	-1
2013-09-10 09:03:11.000	MI070E229.6D	64	60	57	59	-1
2013-09-10 09:03:42.000	MI070E229.6D	64	55	60	57	-1
2013-09-10 09:04:12.000	MI070E229.6D	60	54	67	58	-1
2013-09-10 09:04:43.000	MI070E229.6D	62	54	70	61	-1
2013-09-10 09:05:13.000	MI070E229.6D	63	49	68	60	-1

MI070E236.0D

Date_Time	DetectorID	Lane_Speed_1	Lane_Speed_2	Lane_Speed_3	Lane_Speed_4
2013-09-10 09:00:08.000	MI070E236.0D	59	61	67	-1
2013-09-10 09:00:39.000	MI070E236.0D	58	53	66	-1
2013-09-10 09:01:10.000	MI070E236.0D	57	51	60	-1
2013-09-10 09:01:40.000	MI070E236.0D	56	55	56	-1
2013-09-10 09:02:10.000	MI070E236.0D	57	52	57	-1
2013-09-10 09:02:40.000	MI070E236.0D	62	60	63	-1
2013-09-10 09:03:11.000	MI070E236.0D	66	50	66	-1
2013-09-10 09:03:42.000	MI070E236.0D	64	63	54	-1

MI070E238.2D

Date_Time	DetectorID	Lane_Speed_1	Lane_Speed_2	Lane_Speed_3	Lane_Speed_4
2013-09-10 09:00:08.000	MI070E238.2D	63	57	66	-1
2013-09-10 09:00:39.000	MI070E238.2D	63	53	68	-1
2013-09-10 09:01:10.000	MI070E238.2D	63	55	68	-1
2013-09-10 09:01:40.000	MI070E238.2D	63	55	68	-1
2013-09-10 09:02:10.000	MI070E238.2D	63	58	68	-1
2013-09-10 09:02:40.000	MI070E238.2D	65	60	65	-1
2013-09-10 09:03:11.000	MI070E238.2D	65	57	64	-1
2013-09-10 09:03:42.000	MI070E238.2D	65	57	62	-1

MI070E239.1D

Date_Time	DetectorID	Lane_Speed_1	Lane_Speed_2	Lane_Speed_3	Lane_Speed_4
2013-09-10 09:00:08.000	MI070E239.1D	53	48	73	75
2013-09-10 09:00:39.000	MI070E239.1D	55	48	73	75
2013-09-10 09:01:10.000	MI070E239.1D	56	49	71	75
2013-09-10 09:01:40.000	MI070E239.1D	57	51	75	75
2013-09-10 09:02:10.000	MI070E239.1D	55	53	78	76
2013-09-10 09:02:40.000	MI070E239.1D	55	57	75	76
2013-09-10 09:03:11.000	MI070E239.1D	55	55	75	76
2013-09-10 09:03:42.000	MI070E239.1D	55	57	76	76
2013-09-10 09:04:12.000	MI070E239.1D	54	55	75	75
2013-09-10 09:04:43.000	MI070E239.1D	53	54	73	75

Westbound

MI070W221.4D

Date_Time	DetectorID	Lane_Speed_1	Lane_Speed_2	Lane_Speed_3	Lane_Speed_4
2013-09-10 09:00:08.000	MI070W221.4D	65	60	55	0
2013-09-10 09:00:39.000	MI070W221.4D	65	62	57	0
2013-09-10 09:01:10.000	MI070W221.4D	64	60	52	0
2013-09-10 09:01:40.000	MI070W221.4D	64	58	52	0
2013-09-10 09:02:10.000	MI070W221.4D	65	62	55	0
2013-09-10 09:02:40.000	MI070W221.4D	65	60	53	0
2013-09-10 09:03:11.000	MI070W221.4D	0	57	57	0
2013-09-10 09:03:42.000	MI070W221.4D	65	58	58	0
2013-09-10 09:04:12.000	MI070W221.4D	65	60	58	0
2013-09-10 09:04:43.000	MI070W221.4D	62	54	50	0

MI070W233.8D

Date_Time	DetectorID	Lane_Speed_1	Lane_Speed_2	Lane_Speed_3	Lane_Speed_4
2013-09-10 09:00:08.000	MI070W233.8D	57	58	65	0
2013-09-10 09:00:39.000	MI070W233.8D	57	54	62	0
2013-09-10 09:01:10.000	MI070W233.8D	57	61	62	0
2013-09-10 09:01:40.000	MI070W233.8D	58	57	60	0
2013-09-10 09:02:10.000	MI070W233.8D	57	56	57	0
2013-09-10 09:02:40.000	MI070W233.8D	58	54	58	0
2013-09-10 09:03:11.000	MI070W233.8D	57	55	62	0
2013-09-10 09:03:42.000	MI070W233.8D	58	62	66	0
2013-09-10 09:04:12.000	MI070W233.8D	58	60	65	0

MI070W234.3D

Date_Time	DetectorID	Lane_Speed_1	Lane_Speed_2	Lane_Speed_3	Lane_Speed_4
2013-09-10 09:00:08.000	MI070W234.3D	68	55	58	-1
2013-09-10 09:00:39.000	MI070W234.3D	66	55	60	-1
2013-09-10 09:01:10.000	MI070W234.3D	68	55	53	-1
2013-09-10 09:01:40.000	MI070W234.3D	66	53	59	-1
2013-09-10 09:02:10.000	MI070W234.3D	71	59	60	-1
2013-09-10 09:02:40.000	MI070W234.3D	72	66	66	-1
2013-09-10 09:03:11.000	MI070W234.3D	73	63	67	-1
2013-09-10 09:03:42.000	MI070W234.3D	70	57	65	-1
2013-09-10 09:04:12.000	MI070W234.3D	67	58	66	-1
2013-09-10 09:04:43.000	MI070W234.3D	64	55	61	-1
2013-09-10 09:05:13.000	MI070W234.3D	68	55	62	-1
2013-09-10 09:05:43.000	MI070W234.3D	64	60	62	-1

MI070W236.1D

Date_Time	DetectorID	Lane_Speed_1	Lane_Speed_2	Lane_Speed_3	Lane_Speed_4
2013-09-10 09:00:08.000	MI070W236.1D	65	57	58	-1
2013-09-10 09:00:39.000	MI070W236.1D	64	54	61	-1
2013-09-10 09:01:10.000	MI070W236.1D	68	50	60	-1
2013-09-10 09:01:40.000	MI070W236.1D	68	48	57	-1
2013-09-10 09:02:10.000	MI070W236.1D	68	48	57	-1
2013-09-10 09:02:40.000	MI070W236.1D	66	47	60	-1
2013-09-10 09:03:11.000	MI070W236.1D	66	48	68	-1
2013-09-10 09:03:42.000	MI070W236.1D	68	48	68	-1
2013-09-10 09:04:12.000	MI070W236.1D	69	44	70	-1

MI070W236.6D

Date_Time	DetectorID	Lane_Speed_1	Lane_Speed_2	Lane_Speed_3	Lane_Speed_4
2013-09-10 09:00:08.000	MI070W236.6D	60	63	58	-1
2013-09-10 09:00:39.000	MI070W236.6D	63	62	59	-1
2013-09-10 09:01:10.000	MI070W236.6D	65	58	55	-1
2013-09-10 09:01:40.000	MI070W236.6D	63	58	57	-1
2013-09-10 09:02:10.000	MI070W236.6D	62	54	58	-1
2013-09-10 09:02:40.000	MI070W236.6D	57	52	57	-1
2013-09-10 09:03:11.000	MI070W236.6D	56	58	53	-1
2013-09-10 09:03:42.000	MI070W236.6D	60	61	54	-1
2013-09-10 09:04:12.000	MI070W236.6D	62	62	54	-1
2013-09-10 09:04:43.000	MI070W236.6D	62	60	50	-1

Freeway	Direction	Detector ID	Screenshot
I-44	**Eastbound**	MI044E257.7U	

Date_Time	DetectorID	Lane_Speed_1	Lane_Speed_2	Lane_Speed_3
2013-09-10 09:00:08.000	MI044E257.7U	0	57	55
2013-09-10 09:00:39.000	MI044E257.7U	0	57	55
2013-09-10 09:01:10.000	MI044E257.7U	0	54	55
2013-09-10 09:01:40.000	MI044E257.7U	0	54	55
2013-09-10 09:02:10.000	MI044E257.7U	0	53	54
2013-09-10 09:02:40.000	MI044E257.7U	0	53	54
2013-09-10 09:03:11.000	MI044E257.7U	0	50	53
2013-09-10 09:03:42.000	MI044E257.7U	0	50	53
2013-09-10 09:04:12.000	MI044E257.7U	0	48	52

MI044E262.0U

Date_Time	DetectorID	Lane_Speed_1	Lane_Speed_2	Lane_Speed_3
2013-09-10 09:00:08.000	MI044E262.0U	0	0	53
2013-09-10 09:00:39.000	MI044E262.0U	0	0	53
2013-09-10 09:01:10.000	MI044E262.0U	0	0	53
2013-09-10 09:01:40.000	MI044E262.0U	0	0	53
2013-09-10 09:02:10.000	MI044E262.0U	0	0	53
2013-09-10 09:02:40.000	MI044E262.0U	0	0	53
2013-09-10 09:03:11.000	MI044E262.0U	0	0	54
2013-09-10 09:03:42.000	MI044E262.0U	0	0	54
2013-09-10 09:04:12.000	MI044E262.0U	0	0	54
2013-09-10 09:04:43.000	MI044E262.0U	0	0	54
2013-09-10 09:05:13.000	MI044E262.0U	0	0	52

MI044E275.6U

Date_Time	DetectorID	Lane_Speed_1	Lane_Speed_2	Lane_Speed_3	Lane_Speed_4	Lane_Speed_5
2013-09-10 16:00:04.000	MI044E275.6U	46	65	64	68	66
2013-09-10 16:00:35.000	MI044E275.6U	46	65	64	68	66
2013-09-10 16:01:05.000	MI044E275.6U	48	64	66	68	68
2013-09-10 16:01:35.000	MI044E275.6U	48	64	66	68	68
2013-09-10 16:02:06.000	MI044E275.6U	48	63	64	66	69
2013-09-10 16:02:37.000	MI044E275.6U	48	63	64	66	69
2013-09-10 16:03:07.000	MI044E275.6U	50	67	62	66	68
2013-09-10 16:03:37.000	MI044E275.6U	50	67	62	66	68
2013-09-10 16:04:08.000	MI044E275.6U	47	68	63	65	68

MI044E289.5U

Date_Time	DetectorID	Lane_Speed_1	Lane_Speed_2	Lane_Speed_3
2013-09-10 16:51:20.000	MI044E289.5U	64	50	52
2013-09-10 16:51:50.000	MI044E289.5U	64	50	52
2013-09-10 16:52:21.000	MI044E289.5U	62	42	45
2013-09-10 16:52:52.000	MI044E289.5U	62	42	45
2013-09-10 16:53:22.000	MI044E289.5U	60	39	45
2013-09-10 16:53:52.000	MI044E289.5U	60	39	45
2013-09-10 16:54:23.000	MI044E289.5U	60	38	42
2013-09-10 16:54:53.000	MI044E289.5U	60	38	42
2013-09-10 16:55:24.000	MI044E289.5U	61	42	42
2013-09-10 16:55:54.000	MI044E289.5U	61	42	42
2013-09-10 16:56:25.000	MI044E289.5U	63	43	40
2013-09-10 16:56:55.000	MI044E289.5U	63	43	40

	Westbound	MI044W265.0U	

Date_Time	DetectorID	Lane_Speed_1	Lane_Speed_2	Lane_Speed_3
2013-09-10 16:00:04.000	MI044W265.0U	0	63	64
2013-09-10 16:00:35.000	MI044W265.0U	0	63	64
2013-09-10 16:01:05.000	MI044W265.0U	0	61	65
2013-09-10 16:01:35.000	MI044W265.0U	0	61	65
2013-09-10 16:02:06.000	MI044W265.0U	0	62	65
2013-09-10 16:02:37.000	MI044W265.0U	0	62	65
2013-09-10 16:03:07.000	MI044W265.0U	0	63	63
2013-09-10 16:03:37.000	MI044W265.0U	0	63	63
2013-09-10 16:04:08.000	MI044W265.0U	0	63	65

MI044W270.5U

Date_Time	DetectorID	Lane_Speed_1	Lane_Speed_2	Lane_Speed_3
2013-09-10 16:00:04.000	MI044W270.5U	77	58	55
2013-09-10 16:00:35.000	MI044W270.5U	77	58	55
2013-09-10 16:01:05.000	MI044W270.5U	77	55	57
2013-09-10 16:01:35.000	MI044W270.5U	77	55	57
2013-09-10 16:02:06.000	MI044W270.5U	73	55	53
2013-09-10 16:02:37.000	MI044W270.5U	73	55	53
2013-09-10 16:03:07.000	MI044W270.5U	74	56	54
2013-09-10 16:03:37.000	MI044W270.5U	74	56	54
2013-09-10 16:04:08.000	MI044W270.5U	75	58	52

MI044W277.3U

Date_Time	DetectorID	Lane_Speed_1	Lane_Speed_2	Lane_Speed_3	Lane_Speed_4
2013-09-10 16:25:57.000	MI044W277.3U	66	65	47	59
2013-09-10 16:26:28.000	MI044W277.3U	68	66	48	63
2013-09-10 16:26:58.000	MI044W277.3U	68	66	48	63
2013-09-10 16:27:28.000	MI044W277.3U	69	63	48	68
2013-09-10 16:27:59.000	MI044W277.3U	69	63	48	68
2013-09-10 16:28:29.000	MI044W277.3U	71	63	50	65
2013-09-10 16:29:00.000	MI044W277.3U	71	63	50	65
2013-09-10 16:29:31.000	MI044W277.3U	72	63	50	61
2013-09-10 16:30:02.000	MI044W277.3U	72	63	50	61
2013-09-10 16:30:32.000	MI044W277.3U	71	62	48	65
2013-09-10 16:31:02.000	MI044W277.3U	71	62	48	65
2013-09-10 16:31:33.000	MI044W277.3U	68	60	50	71
2013-09-10 16:32:04.000	MI044W277.3U	68	64	49	69

Freeway	Direction	Detector ID	Screenshot
I-55	**Northbound**	MI055N192.4U	
	Southbound	MI055S207.1U	

Date_Time	DetectorID	Lane_Speed_1	Lane_Speed_2	Lane_Speed_3	Lane_Speed_4	Lane_Speed_5
2013-09-10 16:00:04.000	MI055N192.4U	57	36	59	41	60
2013-09-10 16:00:35.000	MI055N192.4U	57	36	59	41	60
2013-09-10 16:01:05.000	MI055N192.4U	57	38	60	42	60
2013-09-10 16:01:35.000	MI055N192.4U	57	38	60	42	60
2013-09-10 16:02:06.000	MI055N192.4U	57	38	58	43	62
2013-09-10 16:02:37.000	MI055N192.4U	57	38	58	43	62
2013-09-10 16:03:07.000	MI055N192.4U	57	36	58	45	62
2013-09-10 16:03:37.000	MI055N192.4U	57	36	58	45	62
2013-09-10 16:04:08.000	MI055N192.4U	57	40	54	45	63
2013-09-10 16:04:38.000	MI055N192.4U	57	40	54	45	63

Date_Time	DetectorID	Lane_Speed_1	Lane_Speed_2	Lane_Speed_3	Lane_Speed_4
2013-09-10 16:00:04.000	MI055S207.1U	53	57	59	0
2013-09-10 16:00:35.000	MI055S207.1U	53	57	59	0
2013-09-10 16:01:05.000	MI055S207.1U	49	54	55	0
2013-09-10 16:01:35.000	MI055S207.1U	49	54	55	0
2013-09-10 16:02:06.000	MI055S207.1U	52	58	52	0
2013-09-10 16:02:37.000	MI055S207.1U	52	58	52	0
2013-09-10 16:03:07.000	MI055S207.1U	52	58	53	0
2013-09-10 16:03:37.000	MI055S207.1U	52	58	53	0
2013-09-10 16:04:08.000	MI055S207.1U	59	52	58	0
2013-09-10 16:04:38.000	MI055S207.1U	59	52	58	0
2013-09-10 16:05:09.000	MI055S207.1U	63	53	58	0

Freeway	Direction	Detector ID	Screenshot
I-270	**Northbound**	MI270N005.7D	

Date_Time	DetectorID	Lane_Speed_1	Lane_Speed_2	Lane_Speed_3	Lane_Speed_4
2013-09-10 16:00:04.000	MI270N005.7D	39	59	54	75
2013-09-10 16:00:35.000	MI270N005.7D	39	60	59	66
2013-09-10 16:01:05.000	MI270N005.7D	40	59	55	69
2013-09-10 16:01:35.000	MI270N005.7D	39	63	60	65
2013-09-10 16:02:06.000	MI270N005.7D	38	58	57	65
2013-09-10 16:02:37.000	MI270N005.7D	39	57	61	67
2013-09-10 16:03:07.000	MI270N005.7D	36	58	58	71
2013-09-10 16:03:37.000	MI270N005.7D	37	61	52	67
2013-09-10 16:04:08.000	MI270N005.7D	37	57	54	68

MI270N010.0D

Date_Time	DetectorID	Lane_Speed_1	Lane_Speed_2	Lane_Speed_3	Lane_Speed_4
2013-09-10 16:00:04.000	MI270N010.0D	84	62	58	53
2013-09-10 16:00:35.000	MI270N010.0D	83	55	58	58
2013-09-10 16:01:05.000	MI270N010.0D	76	52	59	58
2013-09-10 16:01:35.000	MI270N010.0D	76	54	63	57
2013-09-10 16:02:06.000	MI270N010.0D	78	57	62	53
2013-09-10 16:02:37.000	MI270N010.0D	80	63	61	49
2013-09-10 16:03:07.000	MI270N010.0D	81	66	59	56
2013-09-10 16:03:37.000	MI270N010.0D	81	68	54	53
2013-09-10 16:04:08.000	MI270N010.0D	0	67	53	55
2013-09-10 16:04:38.000	MI270N010.0D	80	66	60	52
2013-09-10 16:05:09.000	MI270N010.0D	83	64	60	46

MI270N012.4D

Date_Time	DetectorID	Lane_Speed_1	Lane_Speed_2	Lane_Speed_3	Lane_Speed_4
2013-09-10 16:00:04.000	MI270N012.4D	60	68	46	0
2013-09-10 16:00:35.000	MI270N012.4D	58	66	47	0
2013-09-10 16:01:05.000	MI270N012.4D	63	66	44	40
2013-09-10 16:01:35.000	MI270N012.4D	61	66	44	0
2013-09-10 16:02:06.000	MI270N012.4D	59	65	44	0
2013-09-10 16:02:37.000	MI270N012.4D	61	68	44	0
2013-09-10 16:03:07.000	MI270N012.4D	63	71	44	38
2013-09-10 16:03:37.000	MI270N012.4D	62	70	44	0
2013-09-10 16:04:08.000	MI270N012.4D	63	66	44	0
2013-09-10 16:04:38.000	MI270N012.4D	63	65	47	0
2013-09-10 16:05:09.000	MI270N012.4D	65	66	47	0

MI270N013.6D

Date_Time	DetectorID	Lane_Speed_1	Lane_Speed_2	Lane_Speed_3	Lane_Speed_4	Lane_Speed_5
2013-09-10 16:00:04.000	MI270N013.6D	76	55	60	61	0
2013-09-10 16:00:35.000	MI270N013.6D	76	53	62	60	0
2013-09-10 16:01:05.000	MI270N013.6D	76	54	58	60	0
2013-09-10 16:01:35.000	MI270N013.6D	76	52	56	59	0
2013-09-10 16:02:06.000	MI270N013.6D	76	50	60	63	0
2013-09-10 16:02:37.000	MI270N013.6D	76	54	61	63	0
2013-09-10 16:03:07.000	MI270N013.6D	76	50	62	62	0
2013-09-10 16:03:37.000	MI270N013.6D	71	54	58	63	0
2013-09-10 16:04:08.000	MI270N013.6D	73	53	58	65	0
2013-09-10 16:04:38.000	MI270N013.6D	73	53	60	68	0

MI270N020.0D

Date_Time	DetectorID	Lane_Speed_1	Lane_Speed_2	Lane_Speed_3	Lane_Speed_4
2013-09-10 16:16:49.000	MI270N020.0D	47	58	46	45
2013-09-10 16:17:20.000	MI270N020.0D	47	58	45	43
2013-09-10 16:17:50.000	MI270N020.0D	46	60	47	41
2013-09-10 16:18:20.000	MI270N020.0D	47	60	49	41
2013-09-10 16:18:51.000	MI270N020.0D	47	60	55	38
2013-09-10 16:19:21.000	MI270N020.0D	47	58	50	40
2013-09-10 16:19:52.000	MI270N020.0D	47	59	49	40
2013-09-10 16:20:22.000	MI270N020.0D	46	60	47	42
2013-09-10 16:20:53.000	MI270N020.0D	46	62	48	43
2013-09-10 16:21:24.000	MI270N020.0D	46	63	50	43

Freeway	Direction	Detector ID	Screenshot
I-170	**Northbound**	MI170N001.5U	

Date_Time	DetectorID	Lane_Speed_1	Lane_Speed_2	Lane_Speed_3
2013-09-10 16:41:11.000	MI170N001.5U	57	55	39
2013-09-10 16:41:42.000	MI170N001.5U	57	55	39
2013-09-10 16:42:12.000	MI170N001.5U	56	57	50
2013-09-10 16:42:43.000	MI170N001.5U	56	57	50
2013-09-10 16:43:13.000	MI170N001.5U	53	60	50
2013-09-10 16:43:43.000	MI170N001.5U	53	60	50
2013-09-10 16:44:13.000	MI170N001.5U	65	60	51
2013-09-10 16:44:44.000	MI170N001.5U	65	60	51
2013-09-10 16:45:14.000	MI170N001.5U	60	53	38
2013-09-10 16:45:44.000	MI170N001.5U	60	53	38
2013-09-10 16:46:15.000	MI170N001.5U	53	37	22
2013-09-10 16:46:45.000	MI170N001.5U	53	37	22
2013-09-10 16:47:16.000	MI170N001.5U	57	48	37
2013-09-10 16:47:46.000	MI170N001.5U	57	48	37
2013-09-10 16:48:16.000	MI170N001.5U	53	64	51
2013-09-10 16:48:47.000	MI170N001.5U	53	64	51